8-AI

UPWARD MIGRATION OF GAS KICKS IN A SHUT-IN WELL

A Thesis

Submitted to the Graduate Faculty of the
Louisiana State University and
Agricultural and Mechanical College
in partial fulfillment of the
requirements for the degree of
Master of Science

in

The Department of Petroleum Engineering

by
Jeffrey Lawrence Mathews
B.S., Louisiana State University, 1979
May 1980

ACKNOWLEDGEMENT

The author extends his deepest thanks to Dr. Adam "Ted" Bourgoyne, Jr., Chairman of the Department of Petroleum Engineering at Louisiana State University, under whose careful guidance and supervision this work was completed.

The suggestions made by the other faculty members of the Petroleum Engineering Department are greatly appreciated. Thanks are extended to Jim Sykora, Logan Magruder, and Bill Flores, who always had the test well prepared for experimental runs.

The research was financed through funds made available by the United States Geological Survey, US Department of the Interior under contract number 14-08-0001-17225. Without their support, this work would not have been possible.

Finally, the author would like to express a special thanks and dedicate this work to his parents for their love and encouragement over the past years, and Diane Marcotte, his future wife, for her moral support and assistance in completing this work.

TABLE OF CONTENTS (continued)

LIST OF TABLES

LIST OF FIGURES

LIST OF FIGURES (continued)

ABSTRACT

In this study, various proposed methods for safely handling the upward migration of gas kicks in a shut-in well were evaluated experimentally, using a 6000 ft well. Nitrogen gas was injected in the well to simulate a gas kick. The methods evaluated include: (1) the periodic release of mud from the well annulus in step with observed changes in the surface drill pipe pressure and (2) the periodic release of mud while monitoring both changes in the casing pressure and volume of mud being released. The second procedure, sometimes referred to as the volumetric method, is most applicable to field situations in which a meaningful drill pipe pressure is not available. For example, the drill string may be off-bottom or out of the hole entirely, or the bit may be plugged. Variations in the volumetric method as described in the well control manuals of several major operators were included in the study and the bottom hole pressure responses obtained experimentally were compared. Parameters which were studied experimentally include (1) kick size, (2) viscosity of the mud and (3) variations in the initial shut-in pressure.

In presenting the proposed volumetric method, previous investigators made several simplifying assumptions. These include (1) the gas density is negligible, (2) the kick remains as a continuous slug occupying the entire annular cross-section and (3) once gas reaches the surface,

no gas is to be produced. It was found that the latter two assumptions were not valid and may cause significant deviations in expected well behavior. However, if properly modified, the volumetric method was found to give acceptable results.

An attempt was made to develop a mathematical model for predicting the behavior of a gas kick in a closed well. However, results obtained with the mathematical model did not give good agreement with the experimental data.

CHAPTER I

INTRODUCTION

A "blowout" may be defined as an uncontrolled flow of formation fluids from a well. As the easily accessible supplies of oil and gas are depleted, oil companies are forced to drill and explore in harsher and more dangerous environments where the risk is even greater that a blowout could occur. Surface blowouts are extremely dangerous and can result not only in the loss of the well but also rig equipment and even human lives. Extensive environmental damage may also occur. Blowouts are extremely expensive and oil companies spend annually hundreds of millions of dollars to fight surface blowouts. Another type of blowout, the underground blowout (discussed later), is much more common and may be as costly to the oil companies as surface blowouts.

Various procedures are available for safe removal of formation fluids once they enter the well. All well control procedures rely on the use of the drilling fluid, or "mud" as it is commonly called. The drilling fluid exerts a pressure in the wellbore in excess of the pore pressure of any formations that are exposed in the uncased portion of the well. The cased portion of the wellbore has a string of pipe, known as casing, cemented to the formations over the interval the pipe is set to protect these formations. Thus, the uncased portion of the well is the open

hole below the bottom casing string.

During the drilling of a well in a new area, a formation may be penetrated which has an unexpected pore pressure greater than the hydrostatic pressure of the column of mud in the wellbore. When this happens fluid from the formation enters the wellbore displacing or "kicking" drilling fluid from the well. This formation fluid is commonly referred to as a "kick." A kick may also be taken at a point higher in the well due to a decrease in the pressure exerted by the mud. One such occurrence is when the drill string is pulled out of the hole too fast, resulting in a "swabbing" effect. The swabbing action in effect pulls the formation fluids into the wellbore.

The well must be monitored constantly at the surface to detect when a kick has occurred. One indication of a kick is an increase in the volume of mud in the mud tanks at the surface. This volume increase is due to the intruding formation fluids which push some of the mud out of the well.

Once a kick is detected the bit is raised off-bottom and the mud pumps used to circulate the mud are shut down. Then blowout preventers located on the wellhead at the surface are closed. These preventers seal the space between the surface casing and the drill string, effectively shutting in the well. The well is then allowed to stabilize, and the stabilized conditions usually indicate if the intruding fluid is liquid or gas. For the purpose of discussion only gas kicks will be presented here since they are the most dangerous and most difficult to control.

Normally the drilling fluid inside the drill string contains little or none of the kick fluids. For gas kicks the bottomhole pressure stabilizes to the formation pore pressure during shut-in conditions. Therefore, the pore pressure can be calculated by adding the shut-in drill pipe pressure at the surface to the hydrostatic pressure exerted by the mud in the drill string since the mud's density is known. Knowledge of this bottomhole pressure allows calculation of the mud density which would be required to "kill" the well, or exert a pressure which slightly exceeds the formation pore pressure.

The accepted procedure for removing the kick fluids from the well is to maintain a bottomhole pressure slightly greater than the formation pore pressure while circulating the kick from the well and pumping the heavier mud into the well. This pressure maintenance is accomplished by means of an adjustable surface choke which holds a backpressure on the drill pipe-casing annulus.

The aforementioned procedure is commonly referred to as the "Wait-and-Weight" method, in that the mud density is increased to the required "kill" value before it is circulated into the well. A second procedure, known as the "Driller's" method, circulates the kick out of the well before increasing the mud density. Thus, once the kick fluids are out of the well, the well is not "killed" until the mud density is increased to the required kill value and the mud is circulated throughout the well.

After the well has been shut in due to the presence of a kick, there may be a considerable lapse of time before the well control procedures explained above can be implemented. These delays may be caused by (1) time to increase the mud density to the desired kill weight or (2) mechanical problems, such as pump failure. If the formation fluids are predominantly gas, the large density difference between the gas and the drilling fluid will cause the gas to migrate up the hole during this shut-in period. As the gas migrates upward, wellbore pressures continually increase until such time that the pressure opposite the weakest formation exceeds that formation's fracture pressure, resulting in the breakdown of that formation and an underground blowout.

The fracture pressure of a formation is defined as the pressure exerted on the formation which will cause it to fracture or break down. This fracture pressure can also be stated in terms of an equivalent mud density such that a column of mud having that density would cause the formation to break down. If the formation does fracture, wellbore fluids flow into it and an underground blowout—i.e., an uncontrolled flow of fluids from the deeper, high pressure formation to the fractured shallower strata—occurrs.

Under normal conditions, the excessive pressures resulting from upward gas migration in a shut-in well can be alleviated by allowing the gas to expand by periodic bleeding of mud at the surface. The expansion is controlled by maintaining the drill pipe pressure at a value slightly in excess of its initial shut-in value through the use of

a surface choke. Since the pressure thus exerted on the "kicking" formation exceeds its pore pressure, additional fluids cannot enter the well. As the drill pipe pressure increases due to the upward gas migration, mud is bled from the annulus using the surface choke, giving the kick room to expand in the annulus and thereby reducing the kick's pressure.

However, certain conditions arise when a meaningful drill pipe pressure is not available. These situations include (1) the drill bit is plugged, shutting off pressure communication between the drill pipe and formation; and (2) the drill string could be off-bottom, causing the drill pipe and casing pressures to read the same until the kick has migrated above the bit. In addition, the drill string could be out of the hole entirely. For the second instance, the pipe could be stripped back to the bottom of the hole if proper precautions are taken, but this is time-consuming and significant gas migration will occur during the stripping operations. ("Stripping" refers to the replacement of the drill string back to well bottom while the well is shut in.)

To cope with the above situations where a meaningful drill pipe pressure is not available, the volumetric method of well control has been suggested by various authors[4,5,6,10,12] as an alternate method to handle upward gas migration. The volumetric method is based on observed changes in casing pressure and metered volumes of drilling fluid bled from the well. As presented the method is based on theoretical considerations

and without experimental verification. Simplifying assumptions made in developing the method include (1) the kick remains as a continuous slug occupying the entire annular cross-section, (2) the gas density is negligible and (3) once gas reaches the surface, no gas is to be produced.

The purpose of this study was to experimentally evaluate the proposed methods for safely handling the upward migration of gas kicks in a shut in well. Both the conventional and volumetric methods were included in the study. In addition, a secondary objective was to develop a mathematical model for predicting the behavior of a gas kick in a shut-in well.

CHAPTER II

LITERATURE REVIEW

A review of the literature was made concerning (1) methods for describing the behavior of gas in a static well annulus and (2) methods for safely handling the upward migration of gas kicks in a shut-in well.

2.1 Gas Behavior in the Well Annulus

During operations involving the removal of kick fluids from a well, an important parameter to keep track of is the change in bottomhole pressure with changes in the surface pressures. Referring to Figure 2.1, if the drill pipe pressure is available and essentially no kick fluids have displaced mud from the drill string, bottomhole pressure is given by

$$P_1 = PDP + 0.052\rho D \quad \text{.....(2.1)}$$

where P_1 = bottomhole pressure, psig

PDP = shut-in drill pipe pressure, psig

ρ = mud density, ppg

D = true vertical depth of well, feet

If drill pipe pressure data is not available, the calculation of bottomhole pressure becomes more difficult due to there being at least two different fluids in the annulus. For this type calculation the surface annular pressure is used. The problem arises as to how to treat the formation fluids and their effect on the annular pressure. For purposes

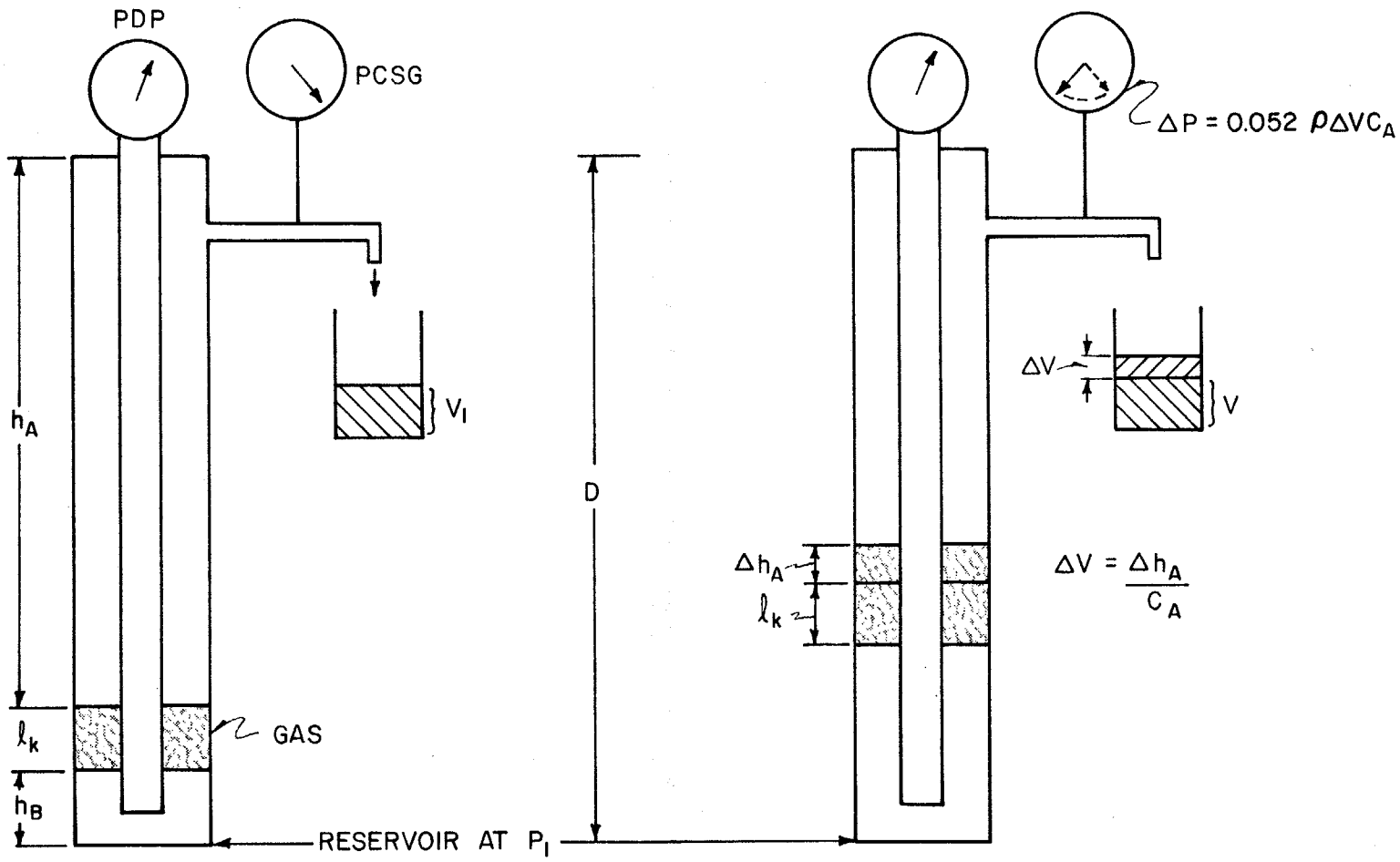

FIGURE 2.1 BASIC APPROACH TO PREDICTING WELL BEHAVIOR ASSUMING GAS REMAINS AS A SLUG

of discussion gas is assumed to be the intruding fluid.

2.1.1 Simplest Annular Model of a Kick

The simplest model of a gas kick is to assume the gas enters the well as a continuous slug and remains as such while it migrates up the hole (Figure 2.1). If it is also assumed that the gas has a negligible density, then the bottomhole pressure is given by

$$P_1 = PCSG + 0.052\rho(D - l_k) \quad \text{.....(2.2)}$$

where PCSG = shut-in annular (casing) pressure, psig

l_k = length of the kick zone, feet

The length of the kick zone is given by

$$l_k = GC_A \quad \text{.....(2.3)}$$

where G = initial pit gain due to kick, bbl

C_A = annular capacity in the region of the kick zone, ft/bbl

If the well remains shut in as the gas migrates up the wellbore, the pressure of the gas remains essentially constant. Referring to the real gas equation of state,

$$PV = znRT \quad \text{.....(2.4)}$$

where P = pressure, psia

V = volume, ft^3

z = gas compressibility factor

n = number of lb/moles of gas

R = universal gas constant, 10.73 psia-ft^3/lb-mole-^0R

T = temperature , ^{0}R

Since the well is shut in and the mud is assumed to be incompressible, it follows that the gas volume and total number of moles of gas remain constant. In addition, the temperature of the gas does not vary appreciably; and if it is assumed that the gas compressibility (z) factor is relatively constant, then as the gas migrates up the wellbore its pressure remains essentially constant at the pore pressure of the formation from which it came. Thus, excessive pressures within the well can develop as the gas migrates upward. From equation (2.2) it can be seen that the bottomhole pressure increases directly with increases in surface casing pressure which in turn increases due to the migration of the gas kick.

As discussed in Chapter 1, if the wellbore pressure opposite the weakest formation in the uncased portion of the hole exceeds that formation's fracture pressure an underground blowout could occur. The importance of this fracture pressure is shown in Figure 2.2. At initial shut-in conditions the equivalent density at the casing seat is well below the fracture density of 15 lb/gal. However, if the well remains shut in the gas retains its initial pressure as it migrates upward, resulting in increased wellbore pressures. At some point during the upward migration of the gas the pressure exerted on the weak formation exceeds the formation's fracture pressure, resulting in breakdown of that formation and a possible underground blowout.

To alleviate this buildup in wellbore pressure the gas

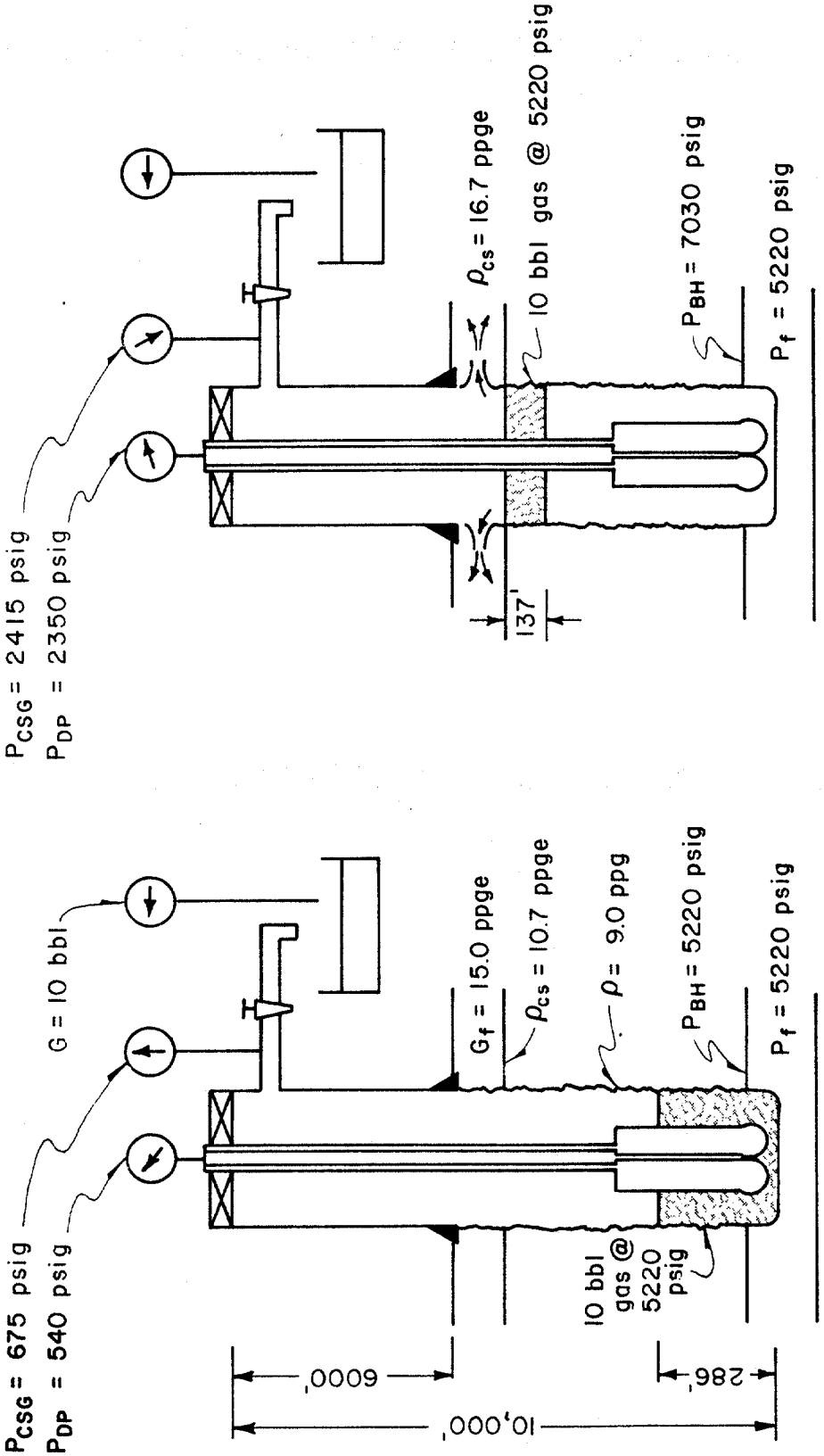

FIGURE 2.2 PROBLEM OF UPWARD GAS MIGRATION WITH WELL SHUT IN

is allowed to expand. Again referring to Figure 2.1, it can be seen that reduction of the bottomhole pressure is primarily related to a change in the length of the mud column in the annulus, assuming negligible gas density. Therefore, bottomhole pressure is given by:

$$P_1 = PCSG + 0.052\rho(h_A + h_B) \quad \text{.....(2.5)}$$

where P_1 = bottomhole pressure, psig

PCSG = shut-in casing pressure, psig

h_A = height of mud above gas, feet

h_B = height of mud below gas, feet

The height $(h_A + h_B)$ remains constant as long as the gas is not allowed to expand. The effect of gas expansion is to reduce the height of mud above the gas, and thus the total height $(h_A + h_B)$ reduces as well.

To maintain bottomhole pressure P_1, the casing pressure must be allowed to increase to a value (PCSG + ΔP) and held at this value until a volume of mud whose hydrostatic head in the well is equal to ΔP is bled. This may be stated as:

$$P_1 = (PCSG + \Delta P) + 0.052\rho(h_A + h_B) - 0.052\rho\Delta h_A \quad \text{.....(2.6)}$$

where Δh_A = reduction of height of mud above gas due to bleeding, feet

Combining equations (2.5) and (2.6),

$$\Delta P = 0.052\rho\Delta h_A \quad \text{.....(2.7)}$$

This equation relates surface casing pressure changes with

changes in the total length of the mud column in the annulus. This relationship will be dealt with in more detail later in this discussion.

2.1.2 Gas-Cut Mud Equations

On certain occasions the hydrostatic pressure exerted by a column of mud in the wellbore may be slightly less than the formation pore pressure at the given depth and/or the zone has a low permeability. In this case a slow feed-in of formation fluids may occur. If the fluid is gas, the drilling mud's density will be reduced due to dispersion of the gas into the mud, and the mud is said to be gas-cut. Another instance when a mud can become gas-cut is due to the gas released from rock cuttings which come from a formation containing gas.

Several authors[2,10,11,14,16] have attempted to derive equations which calculate the loss in mud hydrostatic pressure due to gas-cutting. These equations were designed for the cases discussed above; however, the equations may also be used when relatively small kicks are taken or if the kick is well-dispersed in the mud.

In 1938, M. W. Strong[14] derived an equation to estimate hydrostatic pressure loss due to gas cutting. However, in 1957, Robert White[16] discovered an error in Strong's equation. The corrected form presented by White is given by:

$$h = \frac{1}{D_m}\left[p_s + \frac{p_s\, n}{100 - n}\ln\left(\frac{p_h + p_s}{p_s}\right)\right] \quad \ldots\ldots\ldots\ldots (2.8)$$

where h = depth, ft

p_h = pressure at depth h due to mud column only, atm

D_m = hydrostatic gradient of uncut mud, atm/ft

p_s = pressure at well head, atm

n = percentage by volume of gas in mud at well head at pressure p_s

Bill Rehm[10] simplified the Strong-White equation to:

$$\Delta P = n \ln p_1 \quad \text{.....(2.9)}$$

where ΔP = reduction of bottomhole pressure due to gas-cut mud, atm

p_1 = bottomhole pressure, atm

$n = \frac{W_1 - W_2}{W_2}$ = surface gas-mud ratio

W_1 = original mud density, ppg

W_2 = gas-cut mud density, ppg

Bourgoyne[2] derived an equation for gas-mud mixtures using the real gas equation of state. The final integrated form is given by

$$P_2 - P_1 = a(D_2 - D_1) - b \ln \left(\frac{P_2}{P_1}\right) \quad \text{.....(2.10)}$$

where P_2 = pressure at bottom of interval, psia

P_1 = pressure at top of interval, psia

$a = 0.052\rho_f + 0.00693\, MN_V$

ρ_f = mud density, ppg

M = molecular weight of gas, lb/lb-mole

N_V = number of moles of gas per cubic foot of mud

D_2 = depth to top of interval, feet

D_1 = depth to bottom of interval, feet

$b = 10.73\ \bar{z}\ \bar{T}\ N_v$

$\bar{z}$ = average gas compressibility factor

$\bar{T}$ = average temperature of gas, ^0R

The major difference of Bourgoyne's equation is that gas density is not assumed negligible as it is in White's equation. The above equation does require a trial-and-error procedure to calculate the pressure change $(P_2 - P_1)$.

2.1.3 Volumetric Considerations

In section 2.1.1 an equation was derived which relates changes in bottomhole pressure to changes in the length of the mud column in the annulus during upward migration of the gas kick. This change of length of the mud column can be related to a change in the surface mud pit volume since the gas in the well has expanded by this amount. This type of calculation is referred to as a volumetric approach and is discussed by Rehm[10].

Again referring to Figure 2.1, the incremental increase in the length of the gas zone Δh_A [from equation (2.7)] is given by

$$\Delta h_A = \Delta V\ C_A \quad \text{.....(2.11)}$$

where ΔV = incremental change in surface mud pit volume, bbl

C_A = annular capacity in the region of the gas zone, ft/bbl

Combining equations (2.7) and (2.11) results in the basic equation for the volumetric method of well control:

$$\Delta P = 0.052\ \rho\ \Delta V\ C_A \quad \text{.....(2.12)}$$

This equation equates changes in the surface mud pit volume with changes in annular pressure and is the basic equation used by the various authors[4,5,6,10,12] who discuss the volumetric method for handling upward gas migration in a shut-in well when drill pipe pressure data is not available. This particular procedure of well control is discussed in section 2.2.2.

2.1.4 Gas Slip Velocity

Due to the large density difference between the gas and mud, the gas will slip past the mud and migrate up the annulus. The gas will occupy a certain fraction of the annulus cross-sectional area depending on the properties of the gas and mud.

In experiments conducted first by Rader[8] and then Ward[15] and Koederitz[7], the gas bubble was noticed to travel up one side of the annulus and liquid backflow occurred opposite the bubble (Figure 2.3). Based on their data and the results of Rader *et al*[9], a gas slip velocity correlation was developed for gas migrating up a static fluid column and is given by

$$\bar{V}_s = [0.16+0.092 \log_{10}(N_{RB})]\sqrt{\frac{(d_2+d_1)(\rho_f-\bar{\rho}_g)}{\rho_f}} \quad \text{.....(2.13)}$$

where $\bar{V}_s$ = average gas slip velocity, ft/sec

d_2 = outer diameter of annulus, inches

d_1 = inner diameter of annulus, inches

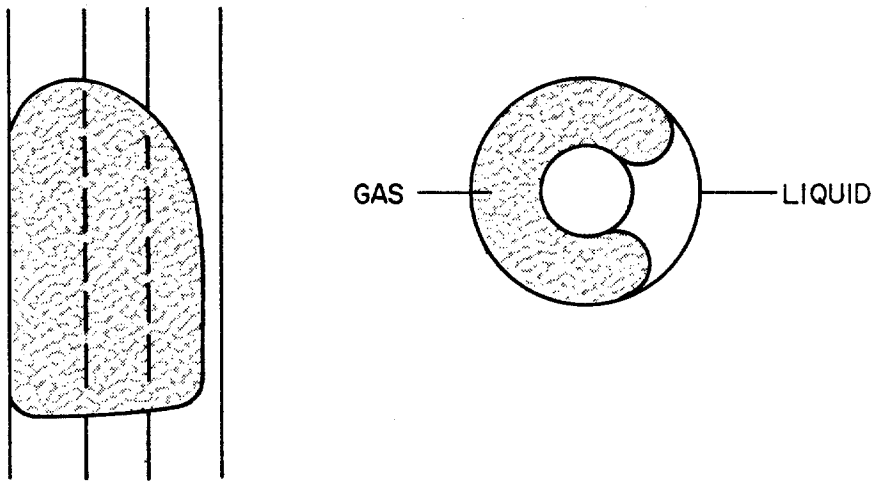

FIGURE 2.3 SHAPE OF BUBBLE AS IT RISES UP ANNULUS

$\bar{\rho}_g$ = average gas density, ppg

N_{RB} = Bubble Reynolds number

Bubble Reynolds number for non-Newtonian fluids is given by

$$N_{RB} = \frac{133,632\ \rho_f\ \bar{V}_s^{(2-n)}}{K} \left[\frac{0.0208}{2+1/n}\ (d_2-d_1)\right]^n \quad \ldots\ldots\ldots\ldots\ldots\ldots\ldots\ldots (2.14)$$

where n = flow behavior index of mud

K = consistency index of mud, eq. cp.

The use of this Bubble Reynolds number will give approximate results for use in the slip velocity equation which was determined empirically for Newtonian fluids. Also, the portion of equation (2.13) in brackets is valid up to a Bubble Reynolds number of 100,000. Above this value, a value of 0.62 is suggested for the portion in brackets.

The calculation of gas slip velocity is an iterative

procedure since slip velocity occurs in the log term of equation (2.13). Thus a value is assumed and a new value is calculated and used as the next trial value until the trial value essentially equals the calculated value.

Gas slip velocity has a strong influence on the pressure behavior of a shut-in well. The rate at which the gas migrates up the hole affects the rate of change of surface annular pressure. In addition, knowledge of the gas slip velocity allows calculation of the annular cross-sectional area that is occupied by the gas versus that occupied by the mud which is slipping below the gas zone.

Since the gas is migrating upwards in a closed system, the upward flow rate of the gas must equal the downward flow rate of the mud. Thus,

$$\bar{V}_s F_g = \bar{V}_{LB} (1-F_g) \quad \text{.....(2.15)}$$

where F_g = fraction of annulus cross-sectional area occupied by the gas

$\bar{V}_{LB}$ = average velocity of the mud in the liquid backflow region, ft/sec

Solving for the gas fraction gives

$$F_g = \frac{\bar{V}_{LB}}{\bar{V}_{LB} + \bar{V}_s} \quad \text{.....(2.16)}$$

Use of equation (2.16) to calculate gas fraction requires that the liquid backflow velocity be known. The following paragraphs discuss the derivation of this velocity.

Figure 2.4 illustrates a gas bubble in a tube and annulus. Liquid is flowing along the edges of the bubble due

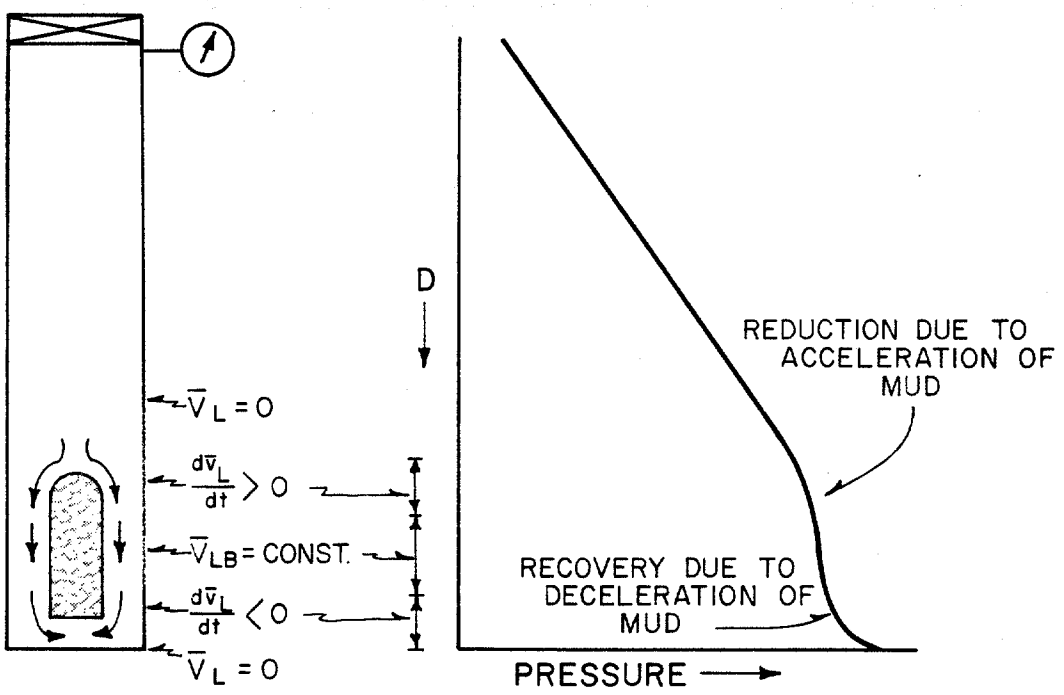

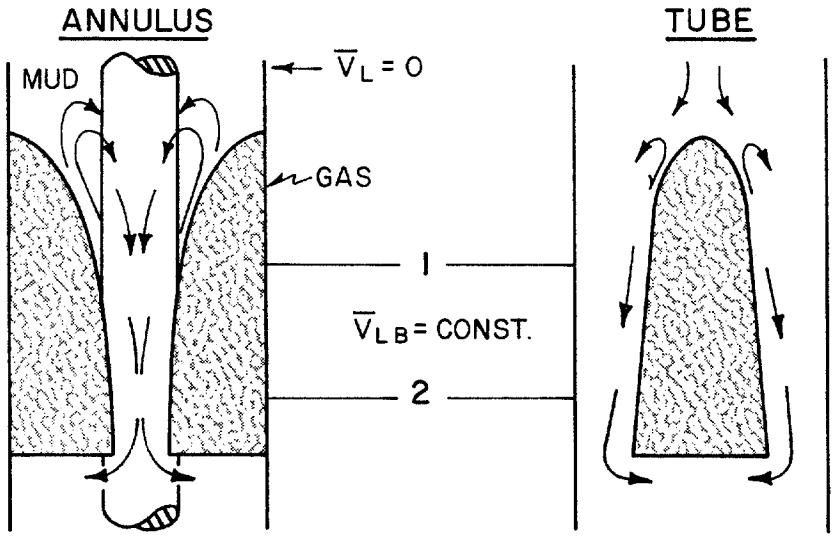

FIGURE 2.4 PRESSURE BEHAVIOR IN THE VICINITY OF A GAS KICK AND DERIVATION OF FRICTIONAL PRESSURE LOSS EQUATION

to the gas slipping upwards. Under steady-state conditions, the pressure change from point 1 to point 2 must be the same for both the liquid and the gas. Therefore,

$$p_2 = p_1 - \Delta p_f + 0.052\rho_f \Delta L \quad \text{(Liquid)} \quad \ldots\ldots\ldots\ldots\ldots (2.17a)$$

$$p_2 = p_1 + 0.052\bar{\rho}_g \Delta L \quad \text{(Gas)} \quad \ldots\ldots\ldots\ldots\ldots\ldots (2.17b)$$

where p_1, p_2 = pressures at points 1 and 2, psi

Δp_f = frictional pressure loss in liquid back-flow region, psi

ΔL = length from point 2 to point 1, feet

Note that frictional pressure loss within the gas is assumed negligible due to its low density and viscosity.

Solving for the frictional pressure gradient gives

$$\frac{\Delta p_f}{\Delta L} = 0.052(\rho_f - \bar{\rho}_g) \quad \ldots\ldots\ldots\ldots\ldots\ldots (2.18)$$

Therefore, the viscous pressure gradient in the liquid back-flow region depends only upon the density difference between the liquid and gas.

Using the Bingham plastic fluid model and slot flow equations, the frictional pressure gradient for a slot of width (d_2-d_1) is given by[2]

$$\frac{\Delta p_f}{\Delta L} = \frac{\mu_p \bar{V}_{LB}}{1000(d_2-d_1)^2} + \frac{T_y}{200(d_2-d_1)} \quad \text{(Laminar)} \quad \ldots\ldots\ldots (2.19a)$$

$$\frac{\Delta p_f}{\Delta L} = \frac{\rho_f^{0.75} \bar{V}_{LB}^{1.75} \mu_p^{0.25}}{1396(d_2-d_1)^{1.25}} \quad \text{(Turbulent)} \quad \ldots\ldots\ldots\ldots\ldots (2.19b)$$

where μ_p = plastic viscosity of liquid, cp

T_y = yield point of liquid, lb/100 ft^2

Equation (2.19b) assumes the Fanning friction factor is related to the liquid Reynolds number by[2]

$$f = \frac{0.0791}{N_{RL}^{0.25}} \quad \text{.....(2.20)}$$

Liquid Reynolds number is calculated from[2]

$$N_{RL} = \frac{757\ \rho_f \bar{V}_{LB}(d_2-d_1)}{\mu_p} \quad \text{.....(2.21)}$$

Combining equation (2.18) with equations (2.19a) and (2.19b) and solving for liquid backflow velocity gives

$$\bar{V}_{LB} = \frac{52(\rho_f-\bar{\rho}_g)(d_2-d_1)^2}{\mu_p} - \frac{5\ T_y(d_2-d_1)}{\mu_p} \quad \text{.....(2.22a) (Laminar)}$$

$$\bar{V}_{LB} = 11.564\left[\frac{(\rho_f-\bar{\rho}_g)^4(d_2-d_1)^5}{\rho_f{}^3\mu_p}\right]^{1/7} \quad \text{.....(2.22b) (Turbulent)}$$

Equation (2.22a) applies if the liquid backflow channel is in laminar flow and equation (2.22b) if the flow pattern is turbulent. Based on velocity-frictional pressure loss relationships, the smaller velocity calculated from equations (2.22a) and (2.22b) is the correct value. This value, combined with the slip velocity calculated from equation (2.13), will give a value for gas fraction [equation (2.16)]. However, the viscous effects of the gas-liquid interface are not considered in the above derivations. To correct for this, Figure 2.5 should be entered with the computed gas fraction, and the corrected gas fraction is read using the dashed line.

Two additional effects of gas slippage past the mud in a shut-in well are (1) pressure changes due to acceleration

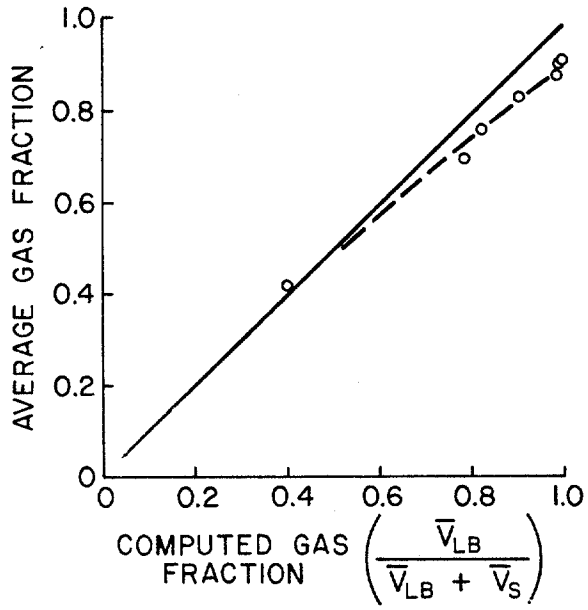

FIGURE 2.5 COMPARISON OF THEORETICAL AND OBSERVED GAS FRACTIONS (after Rader et al.[9])

of the initially static mud and (2) rate of change of surface casing pressure.

Pressure Changes Due to Acceleration Effects

Again consider Figure 2.4. Initially, the liquid above the gas bubble is static (zero velocity). However, as the bubble forces its way upward, the liquid undergoes an acceleration effect while slipping past the upper curved surface of the gas. This acceleration causes a decrease in the pressure exerted by the mud and is given by[2]

$$(\Delta p)_{acc} = 8.073 \times 10^{-4} \rho_f \bar{V}_{LB}^2 \quad \ldots\ldots\ldots\ldots (2.23)$$

where $(\Delta p)_{acc}$ = pressure loss associated with the acceleration of the liquid

This decrease in pressure can be seen in the plot of pressure versus depth (Figure 2.4).

In addition, after the liquid has slipped past the gas, it decelerates until its velocity becomes zero. Thus a pressure recovery occurs immediately below the bubble, and this pressure increase is calculated using equation (2.23).

Rate of Casing Pressure Change

Consider a large gas bubble of initial length, L_g, located at the bottom of a well. If the gas rises toward the surface as a slug during shut-in conditions, then the surface pressure is related to the mean gas pressure by

$$p_s = p_m - 0.052\bar{\rho}_g L_g/2 - 0.052\rho_f D \quad \text{.....(2.24)}$$

where p_s = surface pressure, psig

p_m = mean gas pressure (located at midpoint of gas slug), psig

D = depth to top of gas kick, feet

Therefore, the rate of pressure increase is given by

$$\frac{dp_s}{dt} = -0.052\rho_f \frac{dD}{dt} = 0.052\rho_f \bar{V}_s \quad \text{.....(2.25)}$$

This equation shows that the rate of surface pressure increase is constant since the gas is rising at a constant terminal velocity. However, this value of slip velocity does change during the volumetric method due to bleeding of mud from the surface and resulting expansion of the gas.

However, if the large bubble of gas breaks into slugs of average length L_{gs} separated by slugs of liquid of length L_{LS}, then the surface pressure is given by

$$p_s = p_m - 0.052\bar{\rho}_g \frac{L_g}{2} - 0.052\rho_f \frac{L_g}{2} \left(\frac{L_{LS}}{L_{gs}}\right) - 0.052\rho_f D \quad \text{.....(2.26)}$$

If S is defined as the ratio of the average liquid-slug length to the average gas-slug length, then the rate of change of casing pressure increase is given by

$$\frac{dp_s}{dt} = -0.052\rho_f \frac{L_g}{2} \left(\frac{dS}{dt}\right) - 0.052\rho_f \frac{dD}{dt} \quad \text{.....(2.27)}$$

The velocity of the first gas slug is (-dD/dt) which is $\bar{V}_s$, or

$$\frac{dp_s}{dt} = 0.052\rho_f \left(\bar{V}_s - \frac{L_g}{2} \frac{dS}{dt}\right) \quad \text{.....(2.28)}$$

Since (dS/dt) is greater than zero, the calculated rate of surface pressure change using equation (2.28) is less than the value using equation (2.25).

2.2 Methods for Handling Upward Gas Migration

The following sections discuss procedures which have been suggested for maintaining well control in the instances that normal kick removal operations—i.e., "Wait-and-Weight" or "Driller's" methods—cannot be implemented and are illustrated in Figure 2.6.

2.2.1 Conventional Drill Pipe Pressure Control

If a reliable drill pipe pressure is available during

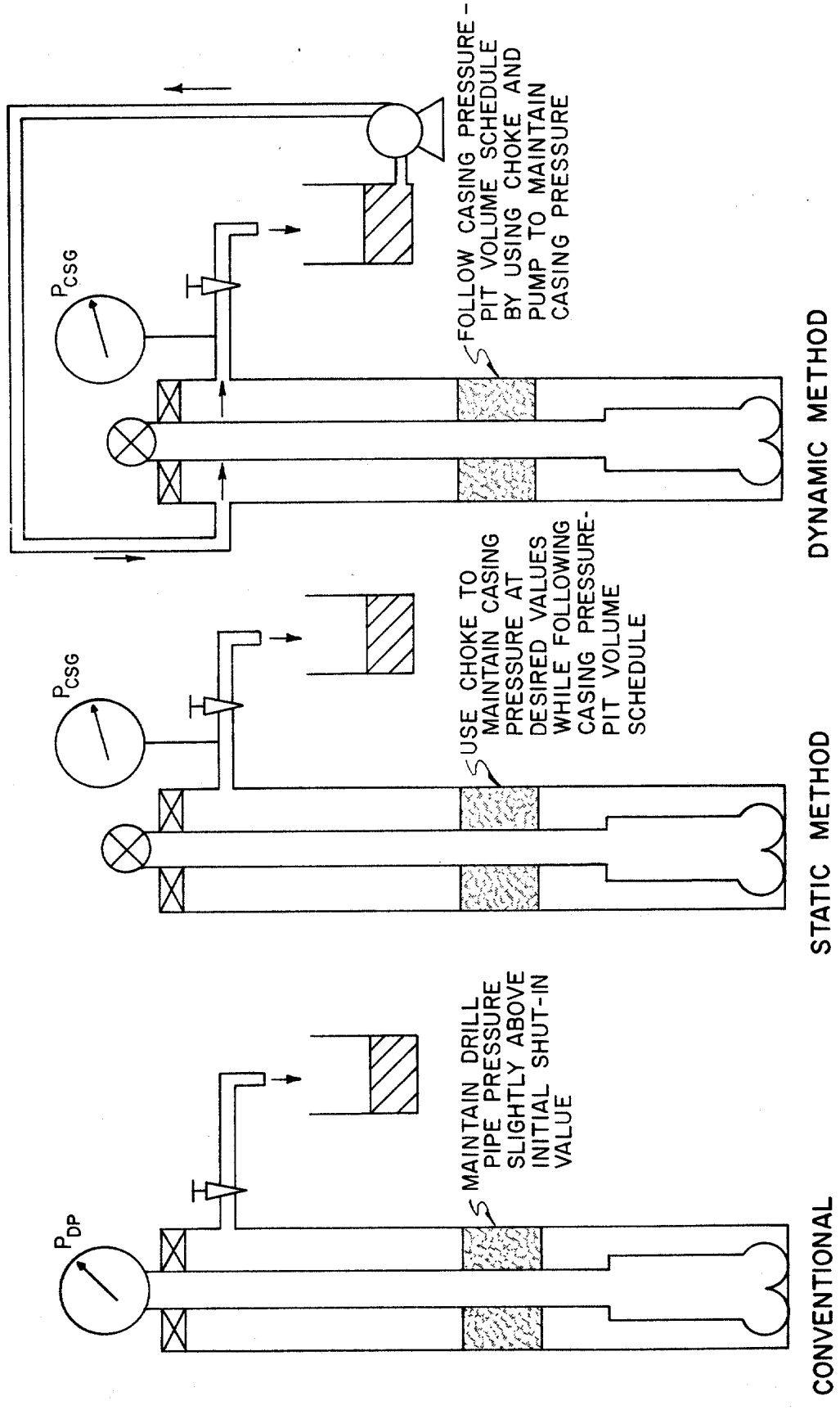

FIGURE 2.6 PROPOSED METHODS FOR SAFE HANDLING OF UPWARD MIGRATION OF GAS KICKS IN A SHUT-IN WELL

the shut-in period after a kick has been taken, the accepted practice is to maintain a bottomhole pressure slightly in excess of the formation pore pressure. Referring to equation (2.1), it can be seen that changes in the bottomhole pressure are directly related to changes in the surface shut-in drill pipe pressure. Therefore, drill pipe pressure is allowed to increase to a value slightly greater than its initial shut-in value, thus keeping bottomhole pressure above the formation pore pressure (Figure 2.6). Then the drill pipe pressure is maintained at this value by bleeding small increments of mud from the well using a hand-adjustable surface choke. It is important to stress that small volumes (i.e., about 0.5 bbl) should be bled rather than bleeding until the drill pipe pressure falls to the desired value. This is due to the amount of time required for pressure changes due to choke manipulation to be felt by the drill pipe pressure gauge. If excessive bleeding occurs, additional influx of formation fluid into the well may result.

Example Calculations

An example showing the approximate well behavior which would result when using the constant drill pipe pressure method is shown in Figures 2.7 and 2.8. The geometry of the LSU "B-7" test well is used. The drill pipe pressure is allowed to increase by 100 psi to a final value of 380 psig (schematic 1 on Figure 2.7). Then mud is bled from the well in small increments to maintain the drill pipe pressure constant at 380 psig. Schematics 2 and 3 of Figure 2.7 show the location of the kick at later times as well as the pit gain

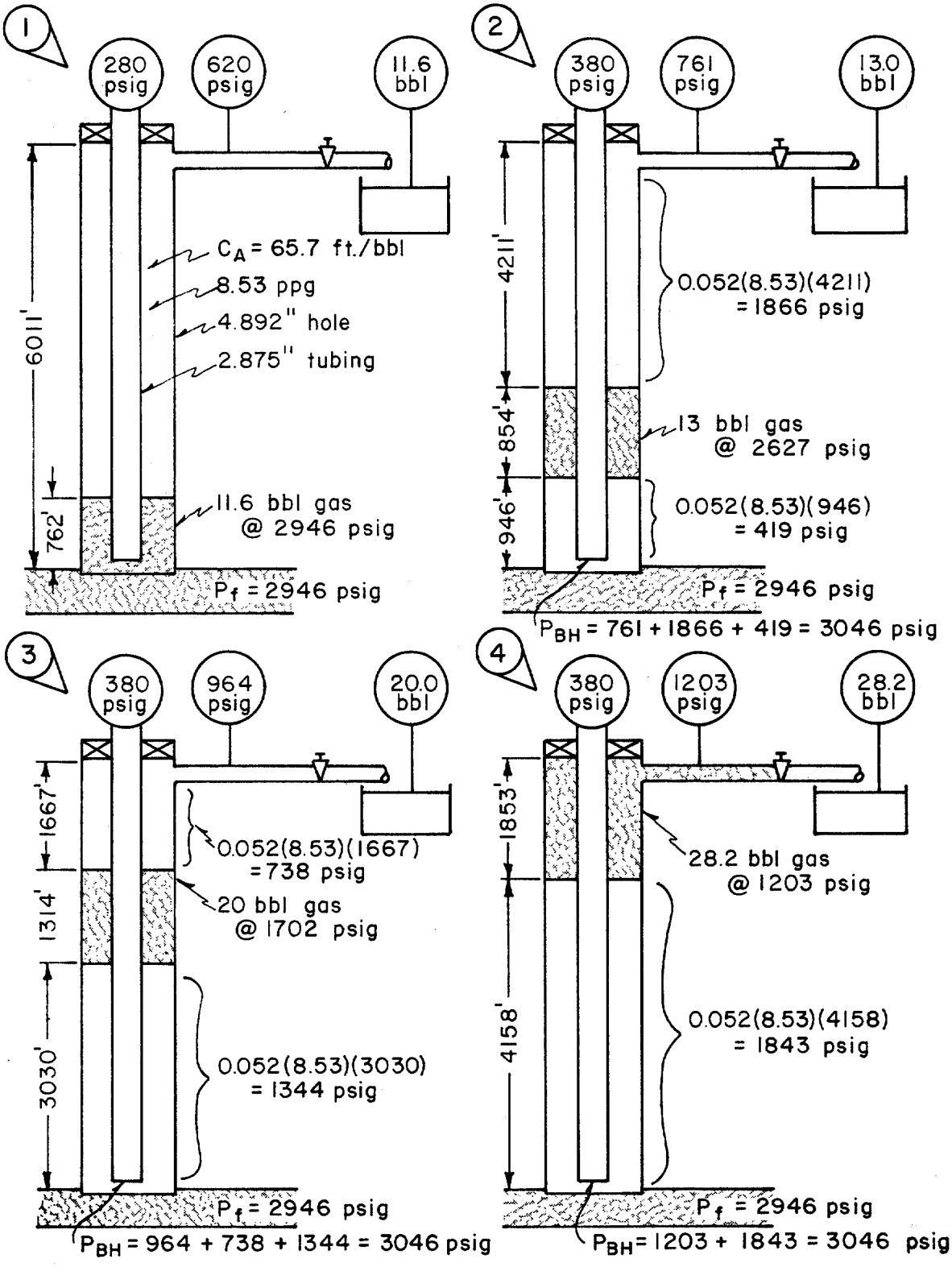

FIGURE 2.7 EXAMPLE ILLUSTRATING CONSTANT DRILL PIPE PRESSURE PROCEDURE

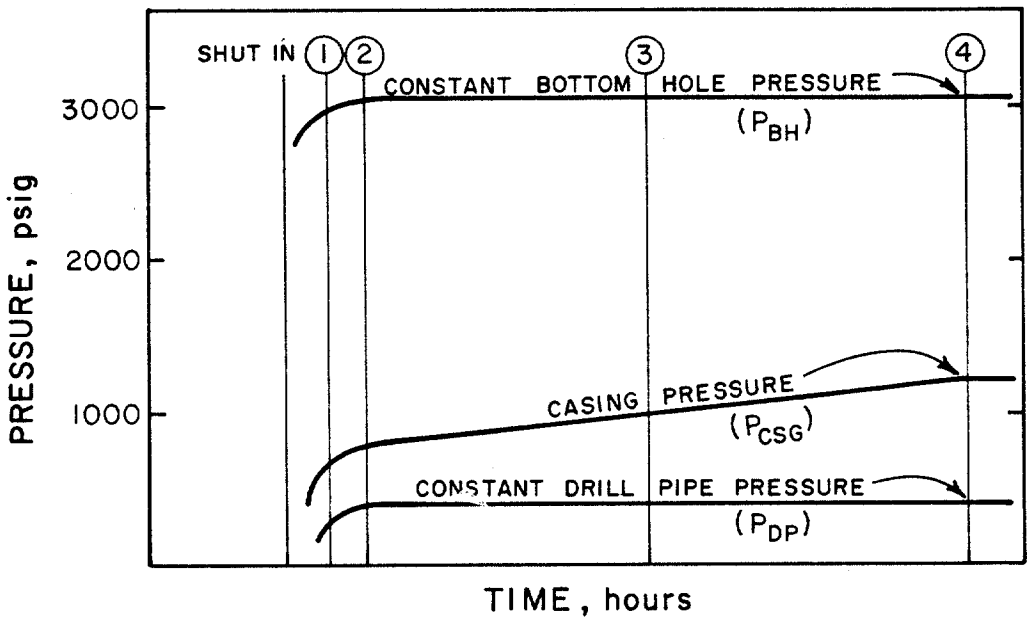

FIGURE 2.8 PRESSURE BEHAVIOR FOR GAS RISING IN A SHUT-IN WELL AT CONSTANT DRILL PIPE PRESSURE

due to bleeding mud and the value of casing pressure. As an illustration of the equations used for the example, the well conditions in schematic 3 are presented.

The ideal gas law for isothermal conditions states that the product of pressure and volume remains constant. Therefore,

$$P_f G = P_2 V_2 \quad \text{.....(2.29)}$$

where P_f = formation pore pressure, psia

G = initial pit gain, bbl

P_2 = pressure of the gas at later time, psia

V_2 = volume of the gas at later time, bbl

The formation pore pressure is calculated using equation (2.1) and the initial shut-in conditions:

$$P_f = 280 + 0.052(8.53)6011 = 2946 \text{ psig}$$

Then the gas pressure after a total gain of 20 bbls at the surface is given by equation (2.29):

$$P = (2946 + 15)(\frac{11.6}{20}) - 15 = 1702 \text{ psig}$$

Since the annular capacity of the well is 65.7 ft/bbl, the kick zone length is

$$l_k = 20(65.7) = 1314 \text{ feet}$$

The bottomhole pressure is 100 psi above the formation pore pressure due to the buildup of the drill pipe pressure. Thus the length of the mud column below the kick zone is

$$h_B = \frac{(2946 + 100) - 1702}{0.052(8.53)} = 3030 \text{ feet}$$

This results in a column of mud above the kick of 1667 feet. Finally, the surface casing pressure is given by equation (2.2):

$$PCSG = 3046 - 0.052(8.53)(6011 - 1314)$$

$$= 964 \text{ psig}$$

Schematic 4 of Figure 2.7 shows the well conditions once the gas reaches the surface. To calculate the final gas pressure and volume equations (2.2) and (2.29) are used along with the relation for gas zone length:

$$l_k = V_2 C_A = \left(\frac{P_f G}{P_2}\right) C_A \quad \ldots\ldots\ldots\ldots\ldots\ldots\ldots\ldots (2.30)$$

Since the final bottomhole pressure is 3046 psig (3061 psia) and the gas pressure equals the casing pressure at this point,

$$3061 = PCSG + 0.052(8.53)(6011 - l_k)$$

$$= PCSG + 0.052(8.53)\left[6011 - \frac{2961(11.6)65.7}{PCSG}\right]$$

or,

$$PCSG^2 - 397.42\ PCSG - 999{,}954.1 = 0$$

Use of the quadratic equation and the positive root gives PCSG = 1218 psia. The gas volume is

$$V_2 = \left(\frac{2961}{1218}\right)11.6 = 28.2 \text{ bbl}$$

and the gas zone length is 28.2(65.7) = 1853 feet.

It is interesting to note that the final value of casing pressure is the same as if the gas had been circulated to the surface using the "Driller's Method" of well control, maintaining a bottomhole pressure above formation pressure by 100 psi.

Certain conditions may arise, however, when a meaningful drill pipe pressure is not available. Such instances include (1) the drill bit could be plugged up, thus shutting off pressure communication between the drill pipe and formation; and (2) the drill string could be off-bottom or out of the hole entirely. It is in these instances that the volumetric method for handling upward migration of gas kicks in a shut-in well is recommended.

2.2.2 Volumetric Methods

The volumetric method of well control has been suggested by various authors[4,5,6,10,12] as a contingency plan to handle upward gas migration in a shut-in well when other procedures are not applicable. The procedure is as follows:

(1) Let the casing pressure build to 100 psi above the initial shut-in value to provide a margin for error.

(2) Allow the casing pressure to rise by a selected pressure increment—usually 50 psi is adequate.

(3) Bleed at constant casing pressure the volume of mud which would generate a hydrostatic pressure equal to the selected pressure increment.

Steps 2 and 3 are repeated each time the required volume of mud has been bled from the well. Also, once gas has reached the surface, the authors recommend no additional bleeding.

The procedure outlined above is usually recommended as a static procedure, in that no pumping of mud in any fashion occurs. A variation of this method, known as the dynamic method[12], is similar to the aforementioned procedure except that mud is pumped across the top of the annulus, and either the pump speed or choke setting is adjusted to control the casing pressure. As each increment of mud is bled from the well, the casing pressure is allowed to rise as before. Both methods are shown in Figure 2.6, and an example calculation of the volumetric method is outlined below.

Example Calculations

The annular geometry of the LSU "B-7" test well is used

for this example. Referring to Figure 2.9 and equation (2.12), the volume of mud needed to create a hydrostatic pressure of 50 psi in the well (the well has a constant annular capacity) is given by

$$\Delta V = \frac{\Delta P}{0.052 \rho C_A} = \frac{50}{0.052(8.53)65.7} \simeq 1.7 \text{ bbls}$$

The casing pressure is allowed to increase from 620 psig to 720 psig to give a 100 psi safety margin. Then the casing pressure is allowed to increase an additional 50 psi and then held constant at that value by periodic bleeding of mud from the annulus using a surface choke until 1.7 bbl of mud have been bled.

To find the location of the kick zone after the casing pressure is first built up to 770 psig, equation (2.29) is used. Since no bleeding has occurred, the gas volume stays constant as does the gas pressure.

The formation pore pressure is calculated based on initial conditions [equations (2.2) and (2.3) and Figure 2.9, schematic 1]:

$$p_f = 620 + 0.052(8.53)[6011 - 11.6(65.7)]$$
$$= 2946 \text{ psig}$$
$$\simeq 2961 \text{ psia}$$

The new bottomhole pressure after the 150 psi buildup (schematic 2) is equal to (2946 + 150) = 3096 psig. Therefore, a column of mud having a hydrostatic pressure of 150 psi lies between the gas kick and the formation, or

$$h_B = 150 \text{ psi}/[0.052(8.53)\text{psi/ft}] = 338 \text{ feet}$$

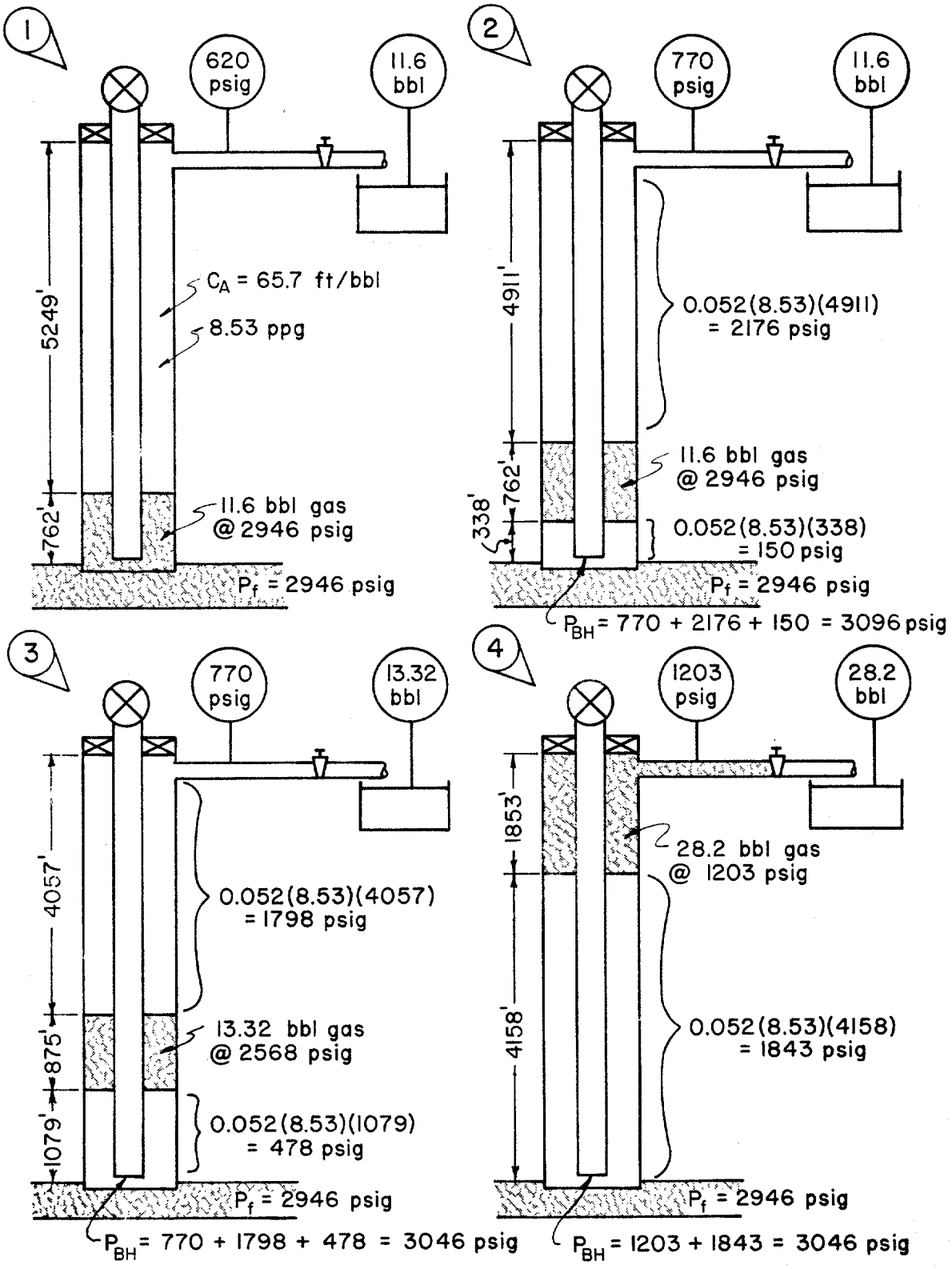

FIGURE 2.9 EXAMPLE ILLUSTRATING VOLUMETRIC METHOD OF WELL CONTROL

Once 1.7 bbls of mud have been bled (Figure 2.9, schematic 3), the gas pressure is given by equation (2.29):

$$P_2 = \frac{2961(11.6)}{(11.6 + 1.7)} - 15$$

$$= 2568 \text{ psig}$$

Since the bottomhole pressure is now 3096-50 = 3046 psig, the length of mud between the gas kick and formation is

$$h_B = \frac{3046 - 2568}{0.052(8.53)} = 1079 \text{ feet}$$

At this point the casing pressure is allowed to increase an additional 50 psi and the cycle is repeated. The casing pressure-pit volume schedule to be followed by this example is shown in Table 2.1 and Figure 2.10. Well conditions for the first cycle are also shown in Figure 2.9, schematics 2 and 3.

The final well conditions—when the gas reaches the surface—are shown in schematic 4 of Figure 2.9 and are the same conditions as those in schematic 4 of Figure 2.7. The calculation procedure was also discussed in section 2.2.1.

One complicating factor of the volumetric method concerns the treatment of an annulus having more than one annular capacity. If the annular capacity of the well varies at different depths, the calculations involved for the volumetric method can become very complex, especially if the kick zone lies opposite more than one annular capacity. One way this can be detected at the surface is by a change in the rate of casing pressure increase, since the gas will

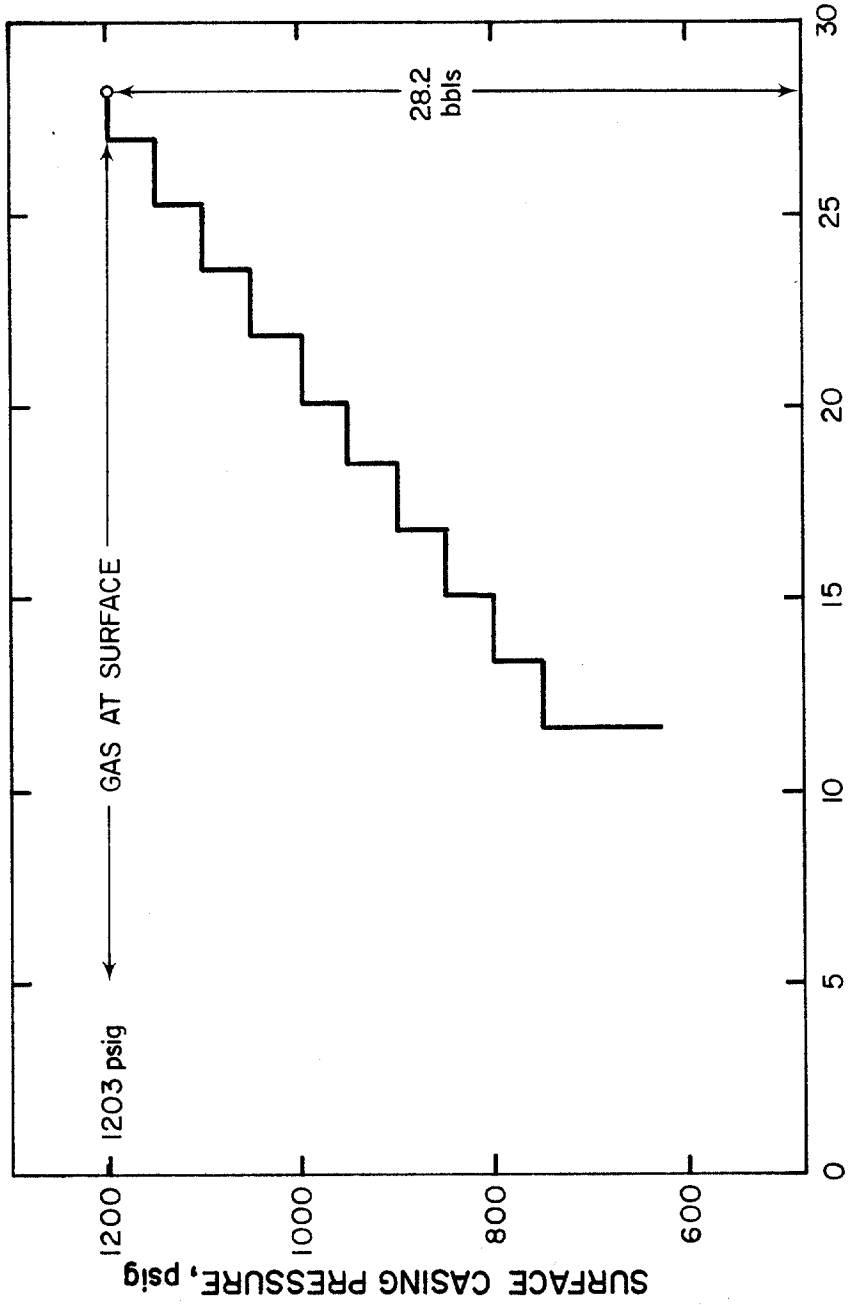

FIGURE 2.10 CASING PRESSURE – PIT GAIN SCHEDULE FOR EXAMPLE ILLUSTRATION OF VOLUMETRIC METHOD

change in velocity when it moves from one annular capacity to another.

The previous authors made several simplifying assumptions in their discussions of the volumetric method:

a) The gas remains as a continuous slug occupying the entire cross-sectional area of the annulus.

b) The gas has negligible density.

c) Once gas reaches the surface, no gas is to be produced.

CASING PRESSURE, psig	PIT GAIN, bbl	
720	11.6	
770	11.6	1.7
770	13.3	
820	13.3	1.7
820	15.0	
870	15.0	1.7
870	16.7	
920	16.7	1.7
920	18.4	
970	18.4	1.7
970	20.1	
1020	20.1	1.7
1020	21.8	
1070	21.8	1.7
1070	23.5	
1120	23.5	1.7
1120	25.2	
1170	25.2	1.7
1170	26.9	
1203	26.9	
1203	28.2	

Table 2.1
CASING PRESSURE-PIT GAIN RELATION FOR EXAMPLE ILLUSTRATING VOLUMETRIC PROCEDURE

These assumptions are inherent in the example calculations shown earlier and may cause considerable error in the calculated versus actual well behavior.

The major objectives of the present study were (1) to experimentally evaluate the proposed volumetric methods, (2) to determine the importance of the simplifying assumptions made by the authors and (3) to develop a mathematical model capable of accurately predicting well behavior.

CHAPTER III

EXPERIMENTAL STUDY

3.1 Training Well

In order to experimentally evaluate the volumetric method of well control, the L.S.U. "B" No. 7 well was utilized. This well is normally used to train industry personnel in the proper methods of well control. Figure 3.1 is a schematic of the training well, and the layout of the surface equipment at the well site is shown in Figure 3.2. The casing is 5-1/2 inch, 17 lb/ft, J-55 pipe cemented at 6140 feet. Simulating the drill pipe is 2-7/8 inch, 6.50 lb/ft, J-55 tubing, run to a depth of 6011 feet. A 1-inch nitrogen injection line, run inside the 2-7/8 inch tubing to a depth of 6029 feet, is used to place a nitrogen bubble on bottom to simulate a gas kick. A check valve, located at the bottom of the 1-inch string, serves to prevent mud from entering the string if bottomhole pressure increases too much during the runs.

The BOP stack consists of a Cameron Type U Preventer and Hydrill. The choke manifold contains one hand-adjustable choke (1) and three remote-operated chokes [Cameron high pressure (3), Patterson (4), Swaco Super (2)]. Also, the well is equipped with both ram and annular type blowout preventers and an accumulator. From the well, the mud flows through a choke, a mud-gas separator (13), and into one of two mud tanks. Mud conditioning equipment as well as a mixing pump are available if needed.

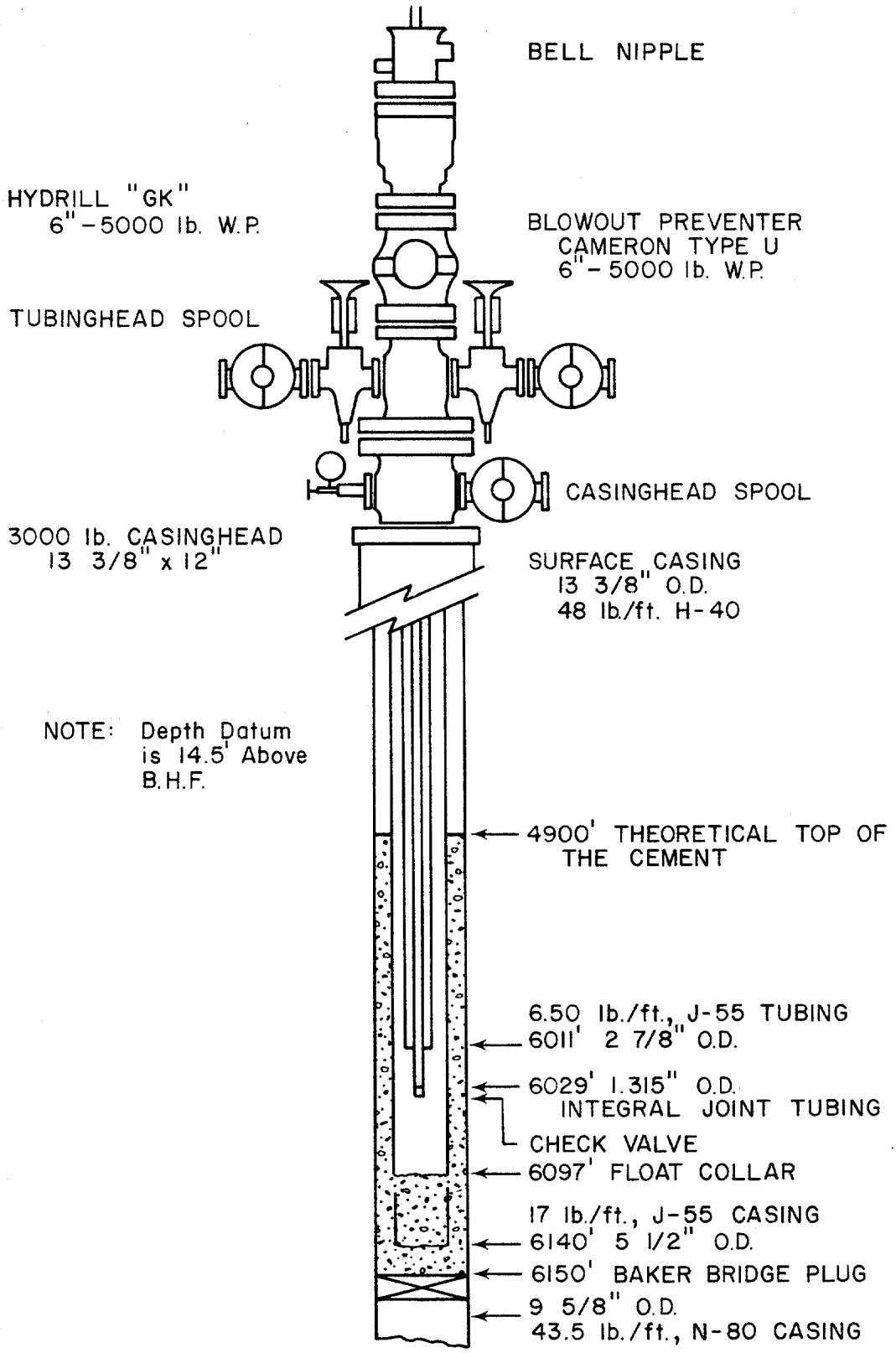

FIGURE 3.1 SCHEMATIC OF L.S.U. TRAINING WELL

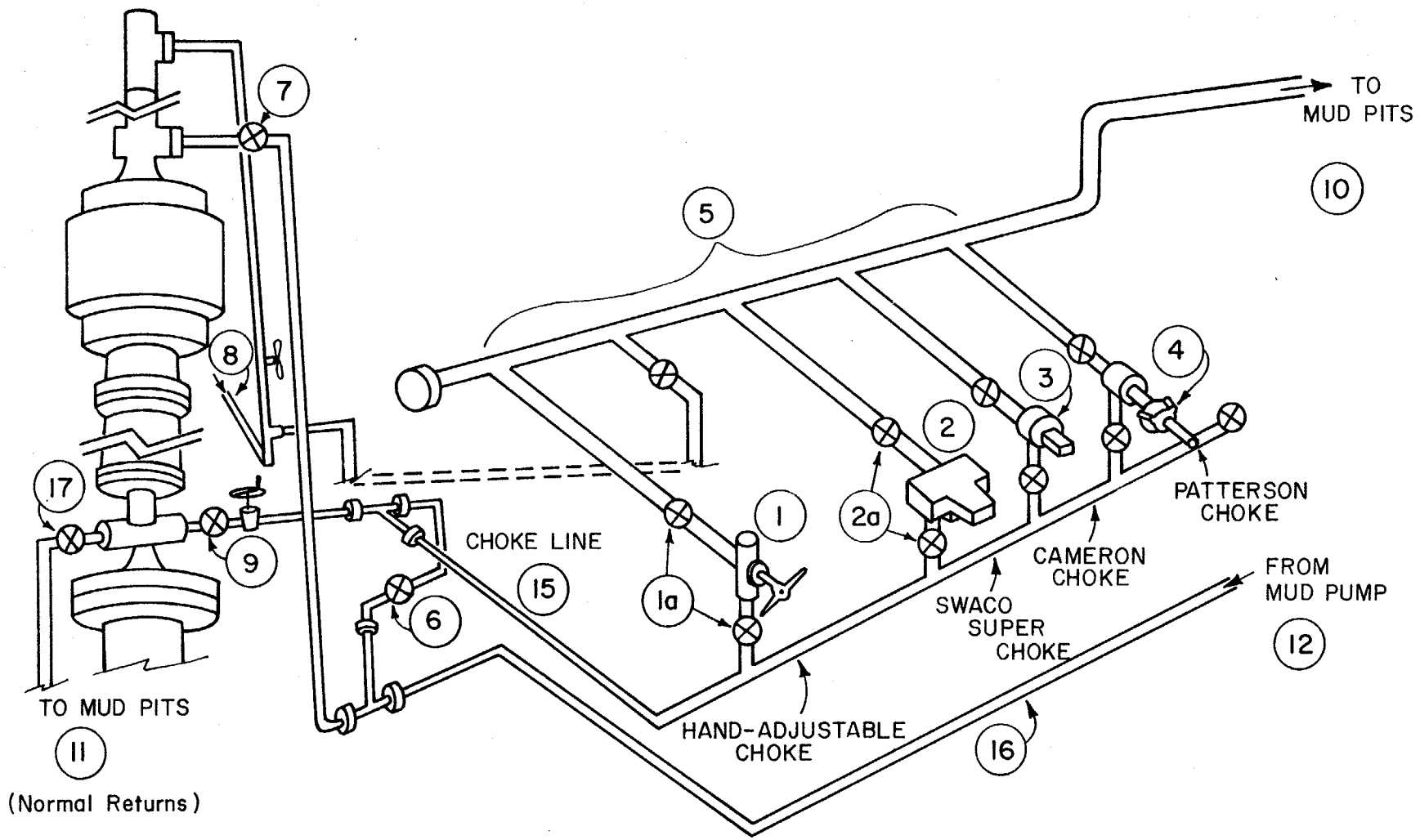

FIGURE 3.2 SURFACE LAYOUT OF L.S.U. TRAINING WELL

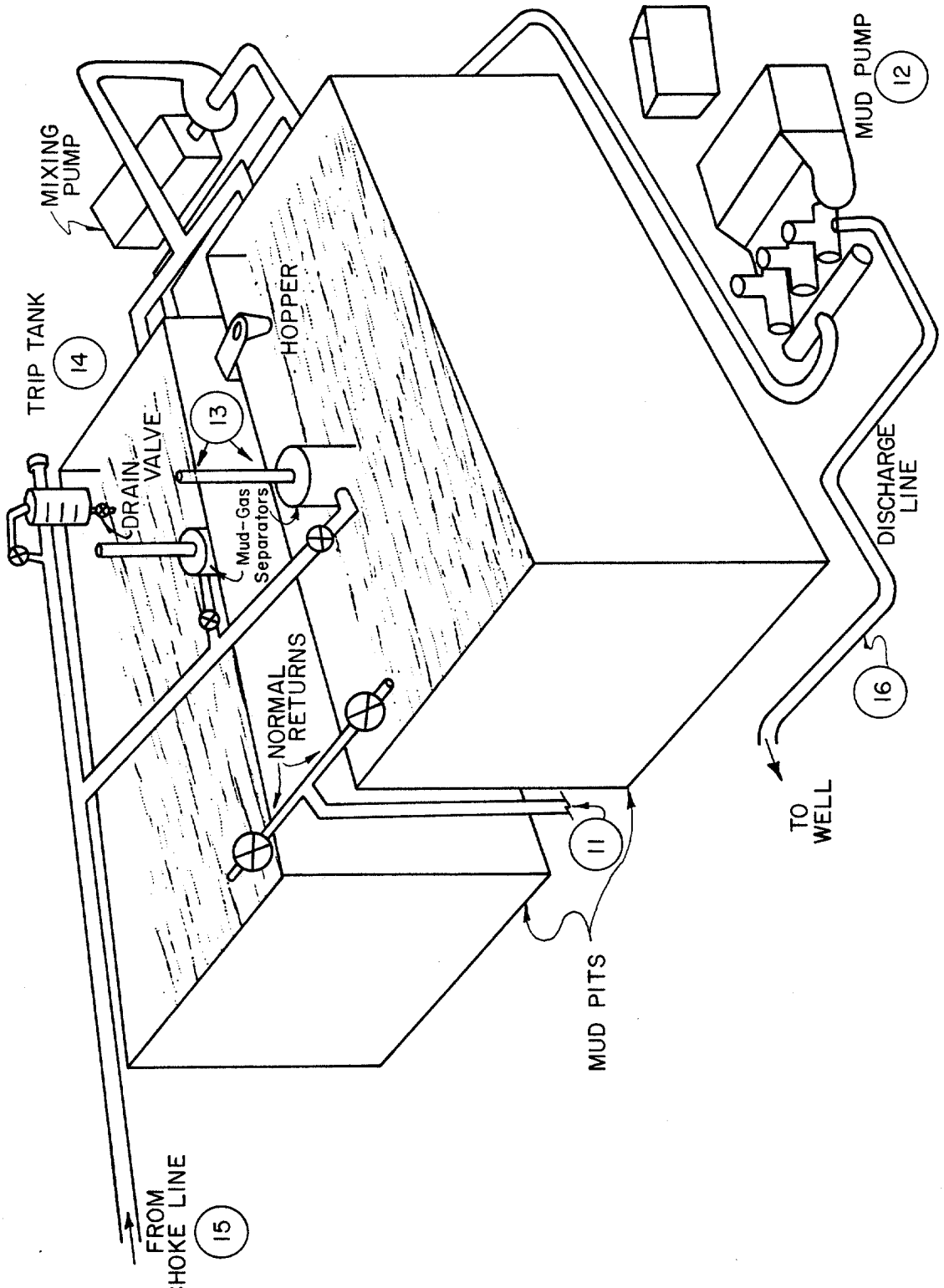

FIGURE 3.2 (Cont'd.)

A lightly-treated fresh water-bentonite mud is circulated in the well. Table 5.1 lists the mud properties for each experimental run. Plastic viscosity was varied from 4 to 57 cp and yield point from 1 to 59 lb/100 ft^2. This range of viscosities was accomplished by increasing the bentonite clay content or water content, as necessary, to the mud in the tanks.

The mud is circulated using a diesel-powered Halliburton Model T-10 pump (12). The 1x2-7/8-inch drill pipe annulus at the wellhead is connected to the pump discharge. An alternate path for the dynamic method is also shown in Figure 3.2, in which the mud is pumped directly into the choke line (15) from the discharge line (16) to simulate pumping across the top of the annulus. The pump has an output of 0.038 bbls/cycle at 60 CPM. The capacities of the 1-inch injection line, 1x2-7/8-inch drill pipe annulus, and 5-1/2x2-7/8-inch casing annulus are 6.4, 24.7, and 91.5 barrels respectively.

A high-pressure nitrogen pump truck injects the gas into the well through the 1-inch tubing (8).

3.2 Experimental Procedure

In evaluating the volumetric method of well control, two procedures were utilized:

a) the static method, in which no mud is circulated during the upward gas migration

b) the dynamic method, in which mud is pumped across the top of the annulus while the kick is migrating up the hole.

A total of 16 experimental runs were made, 13 runs for the static method and 3 runs for the dynamic method. Of the 13 static runs, twelve followed the volumetric method while one followed the conventional drill pipe pressure method.

Table 5.1 shows the range of fluid properties for the experimental runs and Table 5.2 compares well data such as initial pit gain and shut-in pressures which are used as correlating parameters among the runs.

Based on the annular capacity of the drill pipe-casing annulus (0.0152 bbl/ft) and the mud density, the volume of mud to bleed to have a 50 psi change in the mud hydrostatic head is approximately 1.7 bbls. This value is used in the volumetric procedures outlined in section 3.2.2.

3.2.1 Conventional Drill Pipe Pressure Method

A simplified schematic of the well layout for evaluating the conventional drill pipe pressure method is shown in Figure 3.3. The basic procedure is to maintain the drill pipe pressure at a constant pressure above the initial shut-in value. Due to considerations of the well, however, it was decided to bleed a certain amount of drill pipe pressure rather than holding it at one particular value.

The procedure for evaluation of the conventional drill pipe pressure method is outlined below.

(1) Circulate the entire well (3300 strokes) with the mud to be used in the run. Catch a mud sample and measure its properties.

(2) Close all valves in choke manifold (5 in Figure

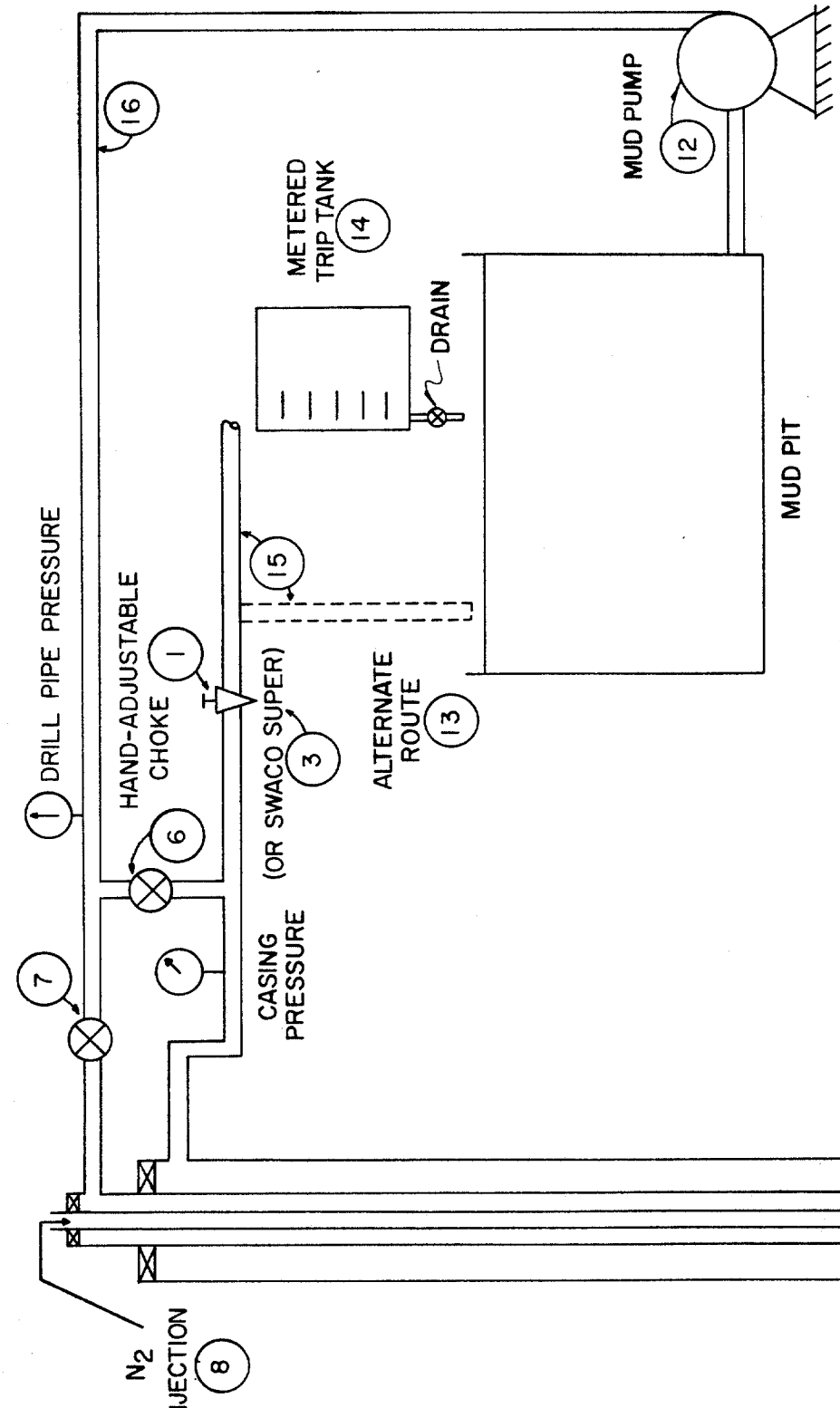

FIGURE 3.3 SIMPLIFIED WELL LAYOUT FOR EVALUATION OF PROPOSED METHODS

3.2) except those which route the flow through the hand-adjustable choke (1a). Close the hand-adjustable choke (1).

(3) Close remote-operated valve upstream of choke manifold (9) and open the bypass line (17) from the well to the pit (11).

(4) Zero pump stroke counters and check mud level in the pit using a metered stick.

(5) Inject nitrogen into well through 1.315-inch injection line (8) at approximately 1000 SCF/min.

(6) After mud level in pit has risen to the desired value, close the bypass line to the pit and open the remote-operated valve upstream of the choke manifold.

(7) Continue injecting nitrogen until desired casing pressure is reached. Then stop nitrogen injection and pump a few strokes with mud pump (12) to move gas kick away from drill pipe annulus.

(8) At the time this procedure was carried out, the check valve was not in the 1.315-inch line. So the line had to be filled with mud to prevent additional feed-in of the gas. So the line is opened at the surface and mud is pumped down the drill pipe annulus, keeping the casing pressure constant. Once mud is bled from the line at the surface, the pump is shut off and the line is closed.

(9) Note values of stabilized casing and drill pipe pressures at this time and record as initial

shut-in values.

(10) Recheck pit level to ascertain total gain. Record the value as initial pit gain.

(11) Allow drill pipe pressure to build by 100 psi above initial shut-in value. Then allow it to build about 20 psi more.

(12) Using hand-adjustable choke (1), slowly bleed down the drill pipe pressure until the pressure is 100 psi above the initial value.

(13) Close hand-adjustable choke and allow pressure to build up a little.

(14) Repeat steps 12 and 13 until the drill pipe pressure stabilizes to a final value (100 psi above the initial shut-in value).

(15) Record time, drill pipe and casing pressures, and incremental volumes of mud bled from the annulus during each cycle. The volume of mud bled into the pit is measured using a metered trip tank (14). Once the tank is filled with mud, the drain valve is opened to drain the mud into the pit.

3.2.2 Volumetric Methods

The procedures outlined below describe the experimental evaluation of the static and dynamic methods for handling upward gas migration when only casing pressure is available. The present well configuration is described in the procedures and variations in the procedure for the

earlier experimental runs are discussed afterwards.

It should also be pointed out that the volumetric methods state that bleeding should occur at constant casing pressure until the incremental volume of mud has been bled. Due to difficulties in monitoring the casing pressure and pit volume simultaneously while adjusting the choke setting, the procedure was modified so as to allow the periodic bleeding of a given pressure change in the casing rather than holding it constant.

Static Method

The procedure followed in evaluating the static method is as follows (see Figures 3.2 and 3.3):

(1) Follow steps 1 through 7 of the conventional drill pipe pressure method.

(2) Follow steps 9 and 10 of the conventional drill pipe pressure method.

(3) Allow casing pressure to build by 100-150 psi above initial shut-in value. Then allow it to build an additional 50 psi, the incremental pressure value used on all test runs.

(4) Using the hand-adjustable choke (1), bleed 50 psi off the casing pressure. Then close the choke and check the increase in pit level using the metered stick. If it is less than 1.7 barrels, allow the casing pressure to build by 50 psi. Continue to bleed mud and build the casing pressure until 1.7 barrels have been gained

in the surface pits. Record shut-in values of casing and drill pipe pressures, time, and incremental volumes of mud bled from the annulus.

(5) Allow the casing pressure to build to a value of 50 psi above the previous buildup value from step 3.

(6) Repeat steps 4 and 5 as required. Once gas reaches the surface and no more mud bleeds from the well, hold the casing pressure constant at the previous value. Continue bleeding gas periodically until the casing pressure no longer increases, signifying that all of the gas has migrated to the top of the annulus.

In the early experimental runs there was no check valve on the 1.315-inch injection line. For these runs step 8 of the conventional drill pipe pressure method is followed; namely, mud is pumped into the drill pipe annulus to displace the gas in the injection line. In addition, a trip tank (14) was used for measuring the volume of mud bled from the well. It was later noted that adequate volumetric accuracy could be obtained using the large mud pit and a metered stick to measure pit level changes.

Dynamic Method

The dynamic method is essentially the same as the static method, except that mud is pumped through the kill line, across the annulus, and back through the choke line into the mud pits. At the test well, however, the choke line and kill line were connected to a 4-foot length of pipe which

was joined to the spool on the well head. Thus, mud was not pumped across the top of the annulus, but rather at a point 4 feet from the annulus. This setup virtually reacts the same way that the recommended setup would prior to when gas reaches the surface. The main problem with this setup is that both the drill pipe and casing pressure gauges read casing pressure. In order to read the drill pipe pressure the well had to be entirely shut in and the pump discharge line (16) reconnected to the drill pipe annulus. Figures 3.2 and 3.3 show the setup for the procedure.

The procedure for the dynamic method is as follows:

(1) Follow steps 1 through 7 of the conventional drill pipe pressure method, except that the remote-operated Swaco Super Choke (2) is used rather than the hand-adjustable choke.

(2) Follow steps 9 and 10 of the conventional drill pipe pressure method.

(3) Valve number 7 connecting the drill pipe annulus to the pump is closed and valve number 6 between the choke line and pump is opened. By doing this the pump is flowing mud in a U-pattern across the line leading from the casing annulus.

(4) Allow the casing pressure to build to a value 100-150 psi above the initial shut-in value.

(5) Open Swaco choke to 1/4 open, and adjust pump speed to hold casing pressure constant at the buildup value.

(6) Monitor pit level. Once 1.7 barrels is returned, either increase pump speed or decrease choke setting until casing pressure has risen 50 psi.

(7) Repeat step 6 as necessary. Once gas reaches the surface, hold casing pressure constant (as long as no more pit gain is noticed).

(8) Record casing and drill pipe pressures, time, pit gain, and pump rate at different times during the run.

As with the static method, the early experimental runs using the dynamic method had no check valve on the injection line. However, once the nitrogen was displaced with mud in the line a drill pipe pressure was available. Also, a trip tank (14) was used initially for volume measurements but was later removed and a metered stick monitored level changes in the mud pit.

CHAPTER IV

COMPUTER MODEL DESCRIPTION

A valuable aid to the control of the upward migration of gas kicks in a shut-in well would be a means of predicting the kick's effect on wellbore pressures as a function of time and volume of mud bled at the surface. For example, if the fracture pressure of the formation at the casing seat is known to be low, it is important to predict if the volumetric method of well control would prevent excessive pressure buildup so as not to fracture the formation or if some other well control procedure would be advisable.

It was an objective of this study to develop a computer program capable of accurately predicting well behavior during the upward gas migration period such as surface and bottomhole pressures, kick location, and pit volume changes (for the volumetric method) as a function of time. This program would be especially valuable in stripping operations when it is important to keep track of the volume bled from the well. Presently the expansion of the gas is not taken into account when keeping track of the volume to bleed while stripping pipe into the hole. Initially the kick is located in open hole. As the stripping operations progress, the kick first lies opposite the drill collars and finally the drill pipe itself. The casing pressure increases due to the increase in the gas zone length at these locations. Thus if the program could predict these changes

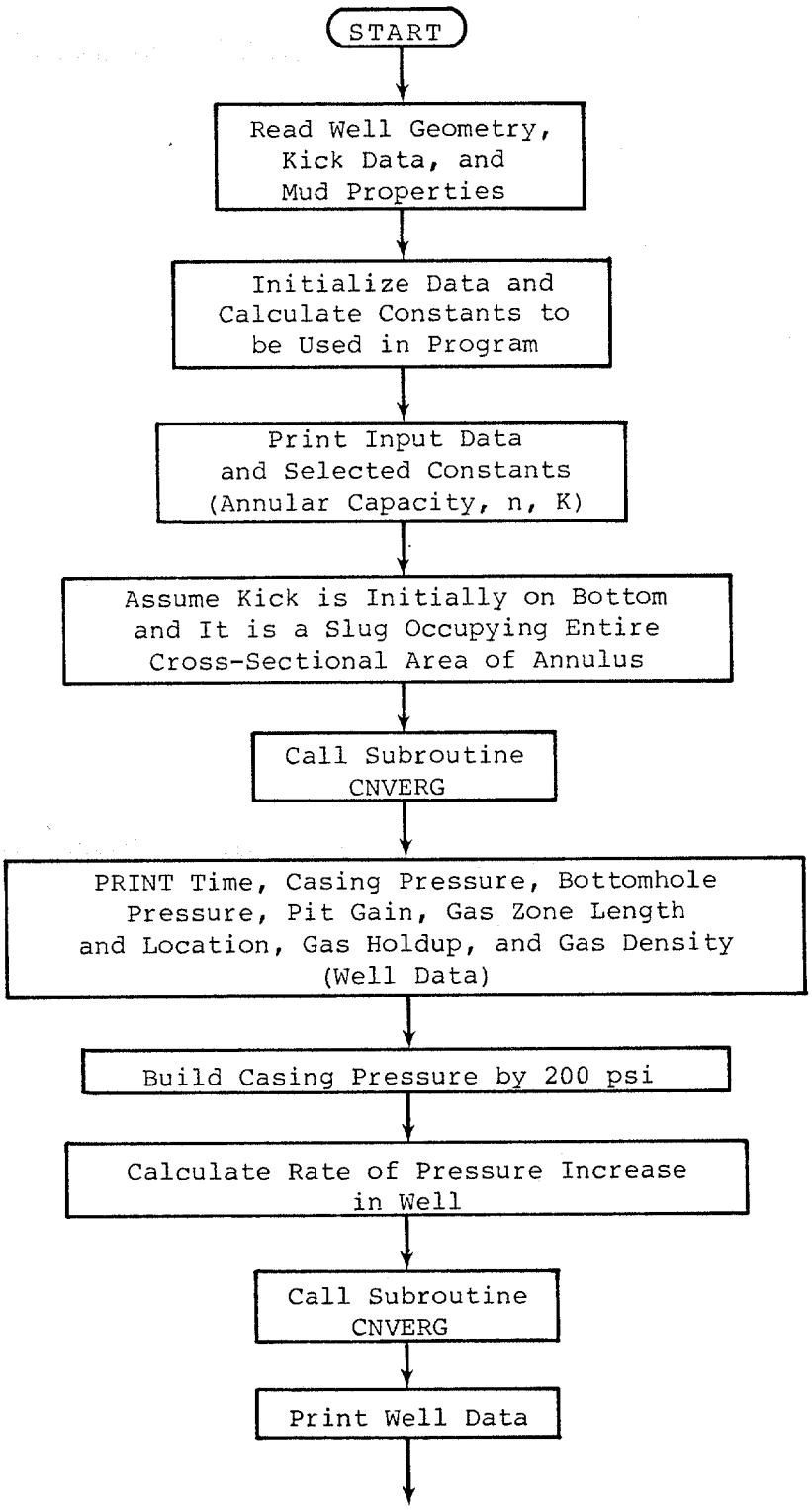

FIGURE 4.2

FLOW CHART OF COMPUTER MODEL

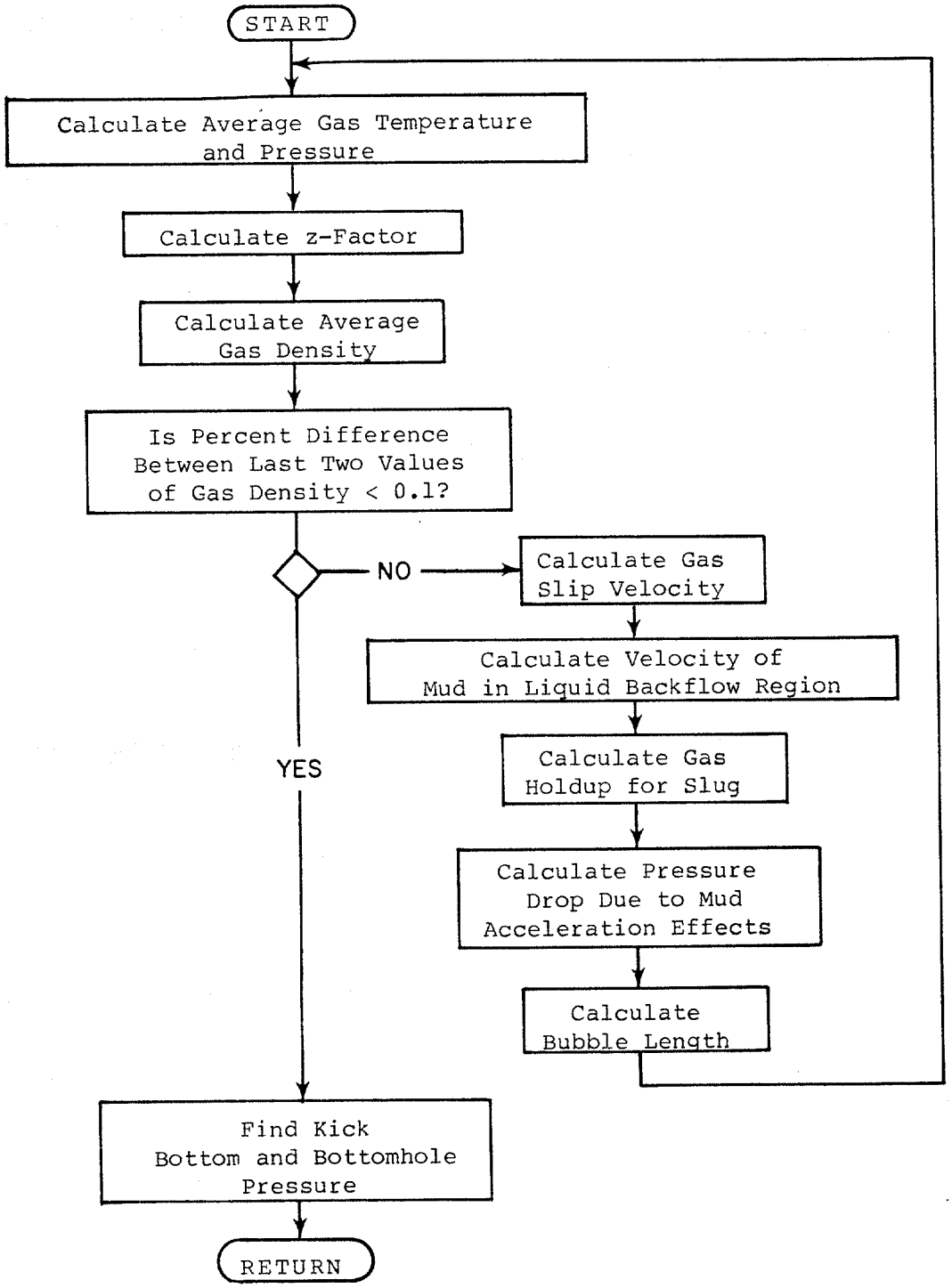

FIGURE 4.3

SUBROUTINE CNVERG

4.3.1 Gas Slip Velocity

The calculation of gas slip velocity is an iterative procedure and is taken care of in a subroutine of the program. Equations (2.13) and (2.14) are used in the calculations. The slip velocity is used to keep track of the location of the gas bubble as it migrates up the hole. In addition, it is used to calculate the fraction of the annulus cross-sectional area occupied by the gas and the rate of surface casing pressure increase.

4.3.2 Liquid Backflow Velocity and Gas Holdup

The derivation of the equations for the velocity of the mud in the backflow region opposite the gas bubble was covered in Chapter 2. The procedure used in the computer program is to calculate the velocity for both laminar and turbulent flow [equations (2.19a) and (2.19b)] and take the smaller value as correct. Combining this value and the value of slip velocity from equation (2.13) will give a value for the fractional cross-sectional area of the annulus occupied by the gas (equation 2.16). However, Figure 2.5 should be entered to correct the value of gas fraction for the viscous effects of the gas-liquid interface.

4.3.3 Pressure Changes Due to Acceleration Effects

The pressure drop which occurs immediately above the gas bubble due to the acceleration of the mud as it slips past the upper curved surface of the gas is calculated using equation (2.23). This pressure drop is required in the calculation of the average gas pressure which in turn is used

to calculate gas density. The pressure recovery as the mud decelerates once it has passed below the gas zone is calculated again using equation (2.23) and is necessary for the calculation of bottomhole pressure.

4.3.4 PVT Behavior of Gas

An average gas density is calculated from the real gas equation of state:

$$\bar{\rho}_g = \frac{\bar{p}M}{80.2\ \bar{z}\bar{T}} \quad \text{.....(4.1)}$$

where $\bar{p}$ = average gas pressure, psia

M = molecular weight of gas, lb/lb-mole

$\bar{z}$ = average gas compressibility factor

$\bar{T}$ = average gas temperature, ^0R

Since gas gravity is read into the program the molecular weight is given by

$$M = \gamma_g \times 28.964 \quad \text{.....(4.2)}$$

where γ_g = gas gravity (air = 1.0)

Using the gas gravity of the kick, the pseudoreduced temperature and pressure are computed, and these in turn are used to calculate the gas compressibility factor. The pseudocritical properties are calculated from

$$p_c = 708.75 - 57.5\gamma_g \quad \text{.....(4.3a)}$$

$$T_c = 169 + 314\gamma_g \quad \text{.....(4.3b)}$$

where p_c = pseudocritical pressure, psia

T_c = pseudocritical temperature, ^0R

With the pseudocritical properties known, the pseudo-reduced pressure and temperature are given by

$$p_r = \frac{\bar{p}}{p_c} \quad \text{.....(4.4a)}$$

$$T_r = \frac{\bar{T}}{T_c} \quad \text{.....(4.4b)}$$

where p_r = pseudoreduced pressure

T_r = pseudoreduced temperature

The gas compressibility factor is then estimated by use of a subroutine[17] which uses a hard-sphere equation as the basis for calculation and the Newton-Raphson method for rapid convergence. The subroutine allows extrapolation to values of reduced pressure above 15, the maximum reduced pressure data taken by Standing and Katz[13] for the formation of the z-factor chart shown in Figure 4.4. The agreement between the subroutine and the chart is excellent except for values of reduced temperature less than 1.10.

Based upon the previous location of the gas zone, the model performs an iterative procedure using gas density, slip velocity, gas fraction, and gas zone length as the variables. Once the new value of gas density is within 0.1 percent of the last computed value, convergence is complete. Bottomhole pressure as well as other parameters are then calculated. These calculations all take place in subroutine CNVERG.

4.3.5 Rate of Casing Pressure Change

The rate of change of the surface casing pressure is

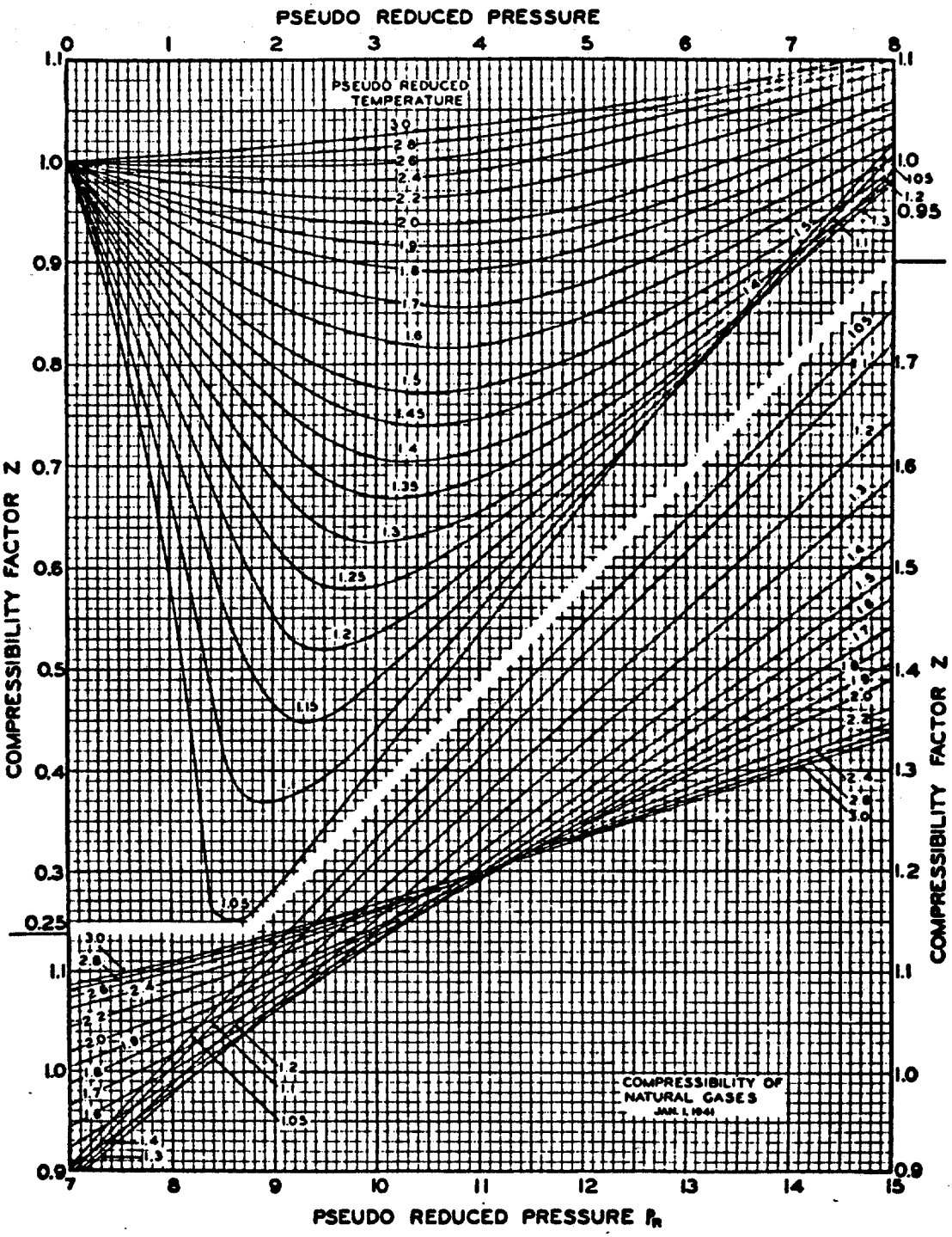

FIGURE 4.4 COMPRESSIBILITY FACTORS FOR NATURAL GASES
(Beggs and Brill[1]. After Standing and Katz[13])

directly related to the velocity of the leading edge of the gas slug. Thus equation (2.25) gives the rate of surface casing pressure increase as the gas migrates upward in a shut-in well. The computer calculates this value and uses it to compute the time required for a given casing pressure change to occur during the buildup periods.

CHAPTER V

DISCUSSION OF RESULTS

The major objectives of this study were:

(1) to experimentally evaluate the proposed methods for safe handling of gas kicks migrating upwards in a shut-in well

(2) to determine the relative importance of the simplifying assumptions made by previous investigators

(3) to develop a mathematical model to accurately predict upward gas migration.

As a consequence of the second objective above, the following parameters were also studied:

a) initial size of kick

b) viscosity of the mud

c) initial shut-in wellhead pressures

d) fragmentation of the gas

5.1 Experimental Evaluation of Proposed Techniques

The following subsections discuss the results obtained using the proposed methods for maintaining control of a well if a gas kick is taken and normal kill procedures cannot be implemented. These methods include:

1) Conventional drill pipe pressure method

2) Static Volumetric method

3) Dynamic Volumetric method

Table 5.1 lists the properties of the mud used for each experimental run and Table 5.2 presents other well parameters

RUN NO.	DATE	MUD PIT TEMP., °F	DENSITY, lb/gal	FANN VISCOMETER READINGS 600 rpm	300 rpm	200 rpm	100 rpm	6 rpm	3 rpm	10 sec gel, lb/100 ft^2	10 min gel, lb/100 ft^2	PLASTIC VISCOSITY cp	YIELD POINT lb/100 ft^2
1	3/15/79	--	8.52	9.0	5.0	3.5	2.0	0.5	0.2	--	--	4.0	1.0
2	3/22/79	--	8.53	14.5	8.5	6.5	4.0	1.5	1.0	--	--	6.0	2.5
3	6/12/79	--	--	13.5	7.5	5.5	4.5	1.0	0.5	1.5	--	6.0	1.5
4	8/28/79	--	--	--	--	--	--	--	--	--	--	--	--
5	10/02/79	--	--	--	--	--	--	--	--	--	--	--	--
6	10/09/79	70	8.5	10.0	6.0	4.5	3.0	1.0	0.5	0.0	--	4.0	2.0
7	11/06/79	60	8.48	75.0	49.0	37.5	24.5	8.0	6.5	7.0	29.0	26.0	23.0
8	11/13/79	50	8.54	55.0	33.5	25.5	16.0	5.0	3.5	2.0	14.5	21.5	12.0
9	1/15/80	60	8.53	36.0	21.0	15.0	9.0	0.5	0.0	3.0	4.0	15.0	6.0
10	1/22/80	84	8.75	173	116	92.0	61.5	21.5	18.0	31.0	48.5	57.0	59.0
11	1/29/80	64	8.6	90.0	57.0	43.5	27.5	8.5	5.5	24.0	--	33.0	24.0
12	2/05/80	74	8.67	68.0	42.0	31.0	19.0	3.5	2.0	12.0	15.0	26.0	16.0
13	2/12/80	56	8.75	140	92.0	72.0	48.5	16.5	13.0	31.0	45.0	48.0	44.0
14	3/04/80	70	8.6	22.0	13.0	9.0	6.0	2.5	2.0	1.5	1.5	9.0	4.0
15	3/11/80	84	8.6	26.0	15.0	11.0	6.5	1.0	0.5	2.0	1.0	11.0	4.0
16	4/15/80	84	--	62.0	39.0	30.0	19.0	3.5	2.5	8.0	12.0	23.0	16.0

Table 5.1
SUMMARY OF FLUID PROPERTIES FOR EXPERIMENTAL RUNS

RUN NO.	DATE	METHOD USED	KICK SIZE		INITIAL PRESSURES(psig)		TOTAL MUD BLED(bbl)	REMARKS
			INITIAL GAIN(BBL)	SCF N_2 inj.	DRILL PIPE	CASING		
1	3/15/79	Static	6.0	10,800	700	1000	2.2	Pumped ~20 spm while taking kick
2	3/22/79	Static	10.3	25,000	530	830	3.26	
3	6/12/79	Conventional	17.5	--	280	620	0.8	Monitored drill pipe pressure
4	8/28/79	Dynamic	--	--	--	--	--	Gas in drill pipe-data of questionable value
5	10/02/79	Dynamic	6.5	--	780	950	--	
6	10/09/79	Dynamic	9.75	23,800	490	890	0.35	
7	11/06/79	Static	5.1	17,000	480	790	3.51	Injection line had hole in it
8	11/13/79	Static	13.2	25,000	950	550	4.74	Injection line had hole in it
9	1/15/80	Static	11.6	--	315	620	7.2	Check valve now in inj. line
10	1/22/80	Static	9.5	--	450	930	7.36	High viscosity mud in annulus, low viscosity mud in drill pipe
11	1/29/80	Static	10.53	12,000	470	650	4.21	
12	2/05/80	Static	16.5	16,800	260	750	8.43	
13	2/12/80	Static	18.6	24,000	360	750	4.38	Difficult to monitor casing pressure due to viscosity of mud
14	3/04/80	Static	10.9	15,600	380	750	3.51	
15	3/11/80	Dynamic	10.9	14,200	340	755	4.9	} Comparison of volumetric procedure
16	4/15/80	Static	18.5	16,100	200	760	5.7	Shut-in after gas reached surface

Table 5.2
KICK PROPERTIES FOR EXPERIMENTAL RUNS

such as initial gain and shut-in pressures. Appendix A contains tabulated pressure-volume-time data for all the runs.

5.1.1 Conventional Drill Pipe Pressure Method

The conventional method of handling upward gas migration is through maintaining a constant drill pipe pressure and thus bottomhole pressure. As long as a meaningful drill pipe pressure is available, this method normally would be preferred.

Figure 5.1 is a plot of casing pressure and drill pipe pressure versus time for experimental run number 3. For this run, the drill pipe pressure was held constant through manipulation of a hand-adjustable choke. Variations in casing pressure as bleeding progressed were studied.

One interesting feature of Figure 5.1 is that prior to 8:28 p.m., the casing pressure continued to build although drill pipe pressure was relatively constant. After 8:28 p.m., casing pressure stabilized and began changing by the same amount the drill pipe pressure did. This stabilization is due to gas reaching the surface. After this time only gas was produced and thus the casing pressure did not need to increase due to loss of mud.

For this particular example, since drill pipe pressure remains constant, bottomhole pressure stays constant as well. The early increase in casing pressure is due to the loss of mud from the well and its hydrostatic pressure. This type of pressure profile is seen in normal well control

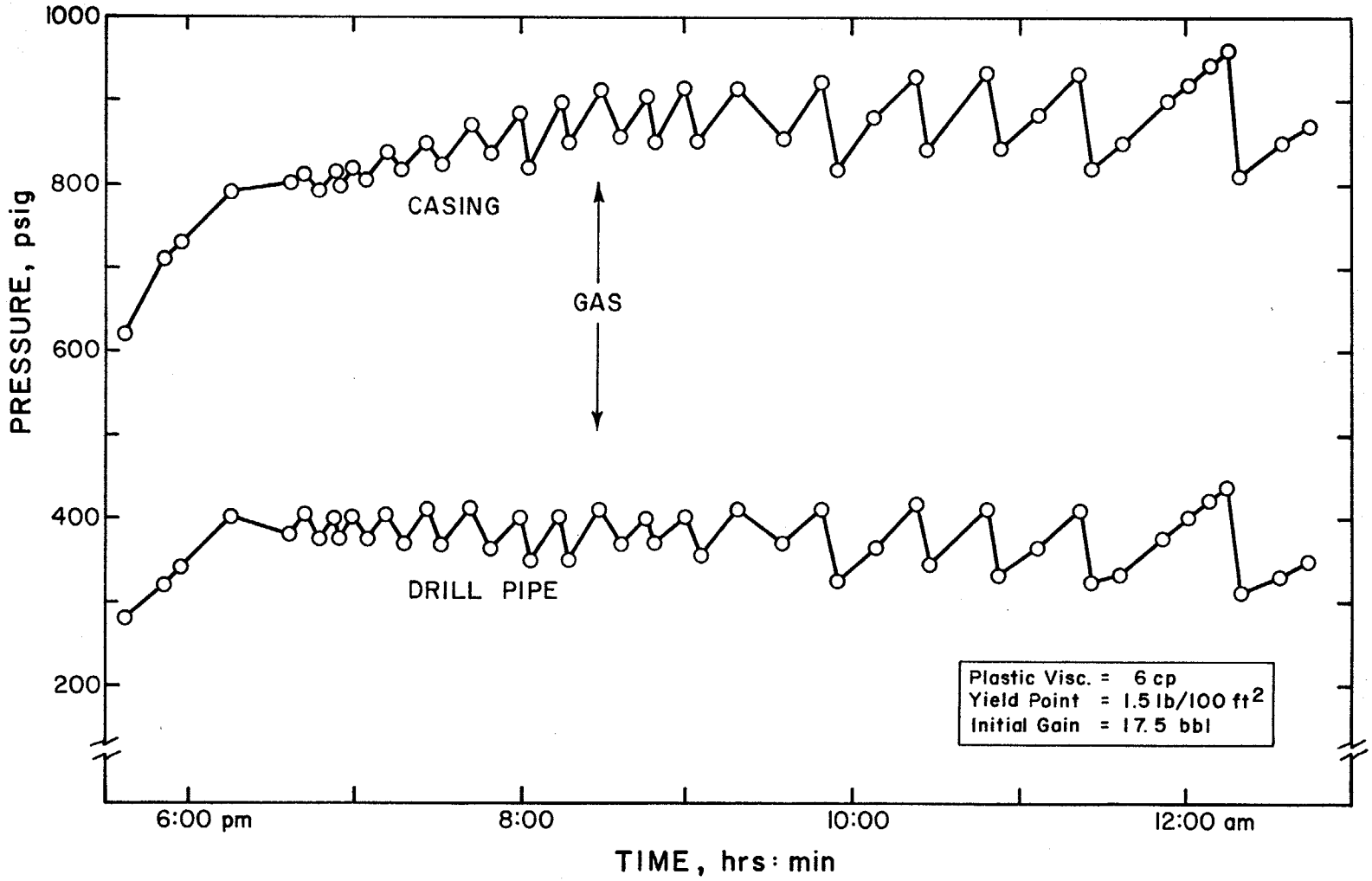

FIGURE 5.1 PRESSURE-TIME DATA FOR CONVENTIONAL DRILL PIPE PRESSURE METHOD--RUN NO. 3

operations, in that prior to gas reaching the surface, casing pressure builds although drill pipe pressure is held constant.

A second feature of Figure 5.1 is that once gas reaches the surface, a period of 4 hours is required for the pressures to stabilize. This period of continued pressure increase is due to gas fragmentation, to be discussed in a later section. The bubble, as it migrates upward, is continually being broken up at its trailing edge due to the turbulence created by mud slipping below the gas. Another cause of increased fragmentation, especially for this example, is that the lower the viscosity of the mud, the more the gas appears to fragment and string out in the well.

5.1.2 Static Volumetric Method

For the static volumetric method, casing pressure is monitored in combination with pit level changes for situations when a meaningful drill pipe pressure is not available. The experimental runs were conducted at the B-7 test well in such a manner as to monitor both casing and drill pipe pressure data to ascertain the feasibility of this method. The static method also was modified in that bleeding was continued after the gas had reached the surface, as long as casing pressure continued to increase.

Figure 5.2 is a pressure-volume-time plot for experimental run 12. A viscous mud was used in this particular run and a 16.5-bbl gain was taken. The initial shut-in casing pressure was allowed to build by 200 psi and then

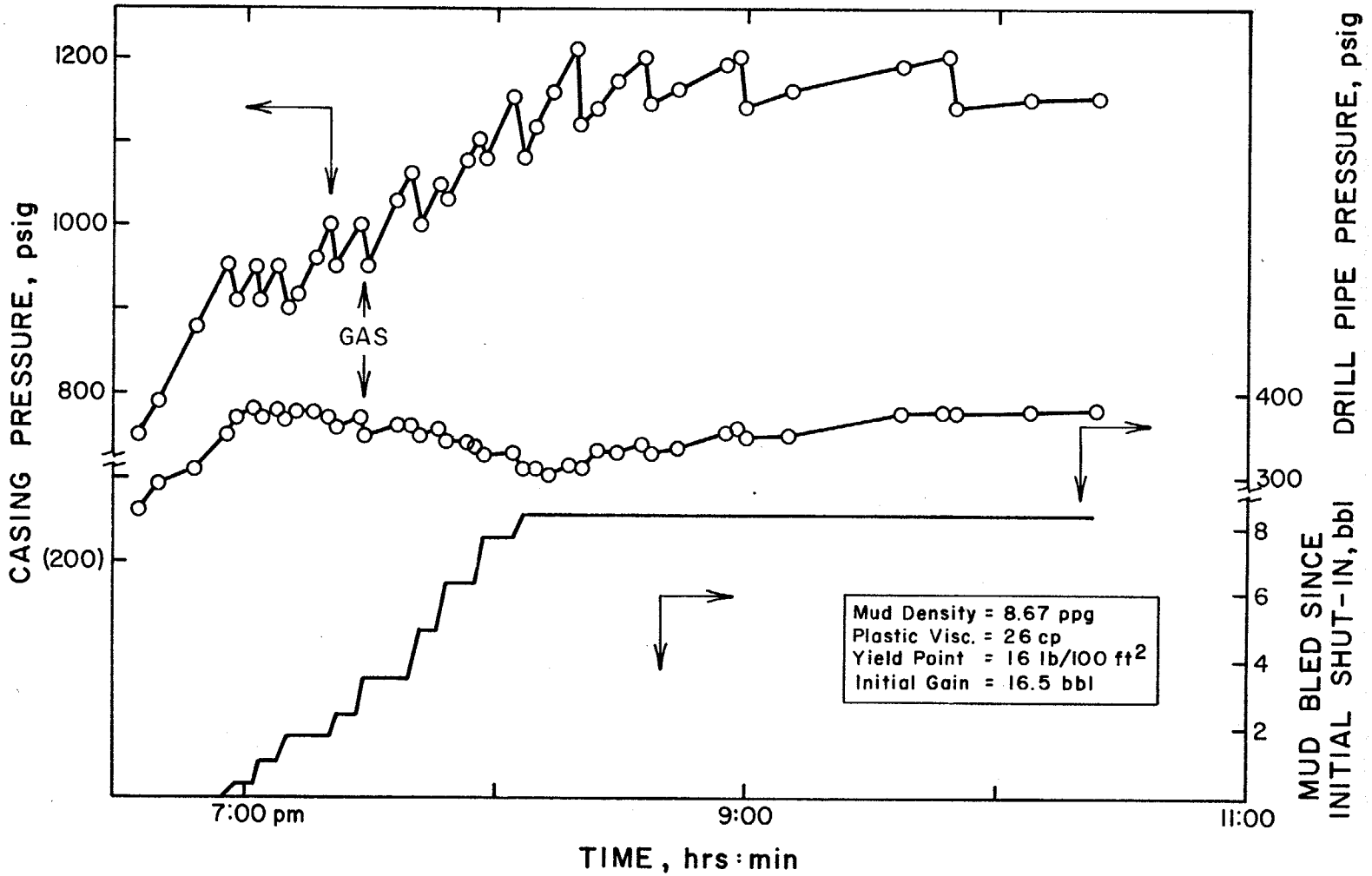

FIGURE 5.2 PRESSURE–VOLUME–TIME DATA FOR STATIC VOLUMETRIC METHOD -- RUN NO. 12

the static volumetric method was implemented.

The most important observation is that the drill pipe pressure never fell below the initial shut-in value during the run. Although the drill pipe pressure slowly decreased during the early portion of the bleeding, once gas reached the surface the pressure began to rebuild and approach the initial buildup value. Again, as in the conventional drill pipe pressure method, casing pressure continued building after gas had already reached the surface, signifying that fragmentation of the gas had occurred.

Figures 5.3, 5.4, and 5.5 graphically display the pressure-volume-time data for experimental run numbers 7, 9, and 11, respectively. Similar trends in the pressure behaviors can be seen, especially the fact that at no time did the drill pipe pressure fall below the initial shut-in value. Therefore the well would remain in control and no additional influx of formation fluids would occur. Therefore by including the modification that bleeding should continue even after the gas reaches the surface, the static volumetric method does maintain bottomhole pressure above initial formation pressure, thereby maintaining well control. The importance of this modification is shown in a later section.

5.1.3 Dynamic Volumetric Method

The dynamic method was suggested as an alternate procedure to the static volumetric method. This method allows continuous bleeding from the annulus by pumping

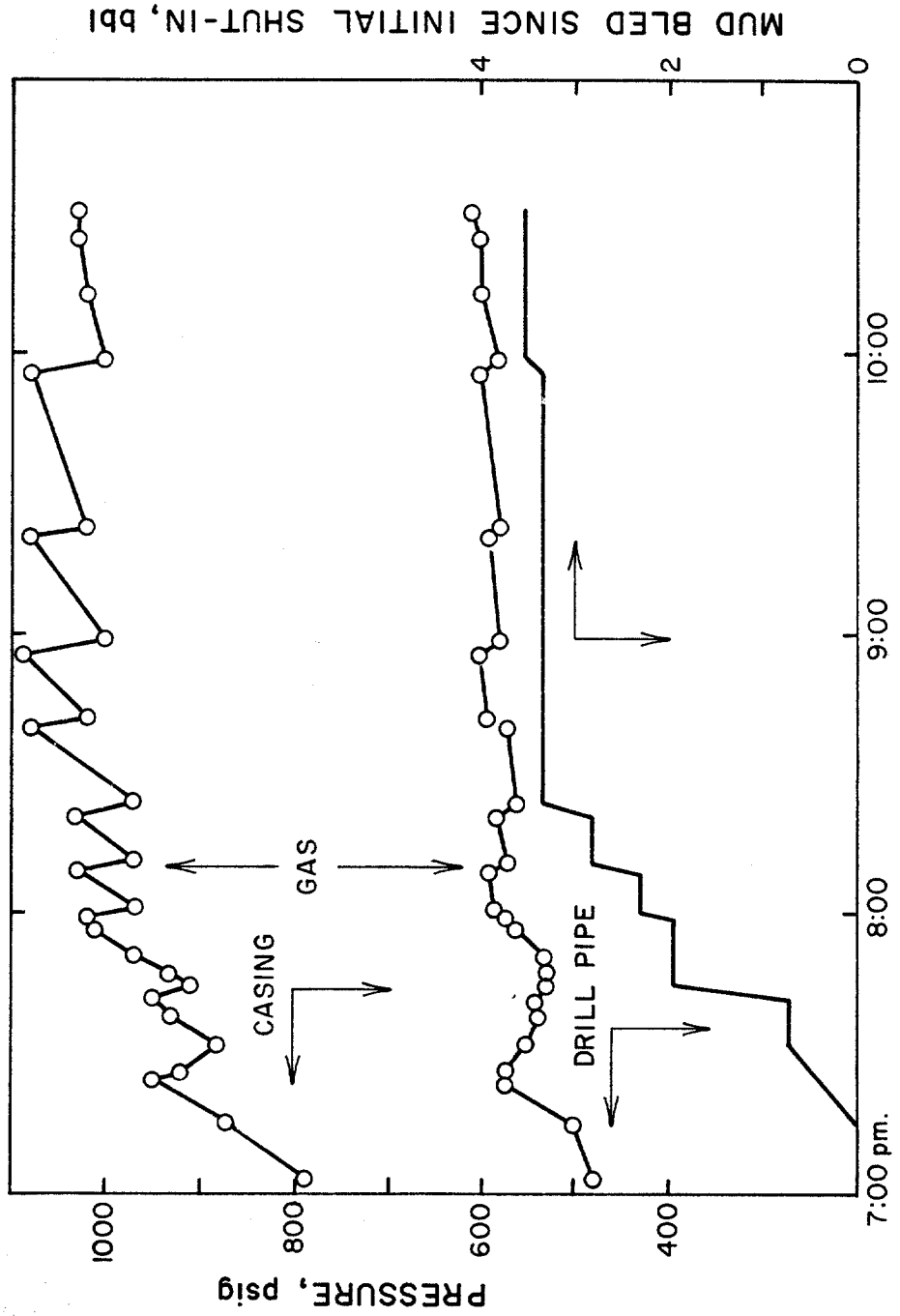

FIGURE 5.3 PRESSURE-VOLUME-TIME DATA FOR STATIC VOLUMETRIC METHOD -- RUN NO. 7

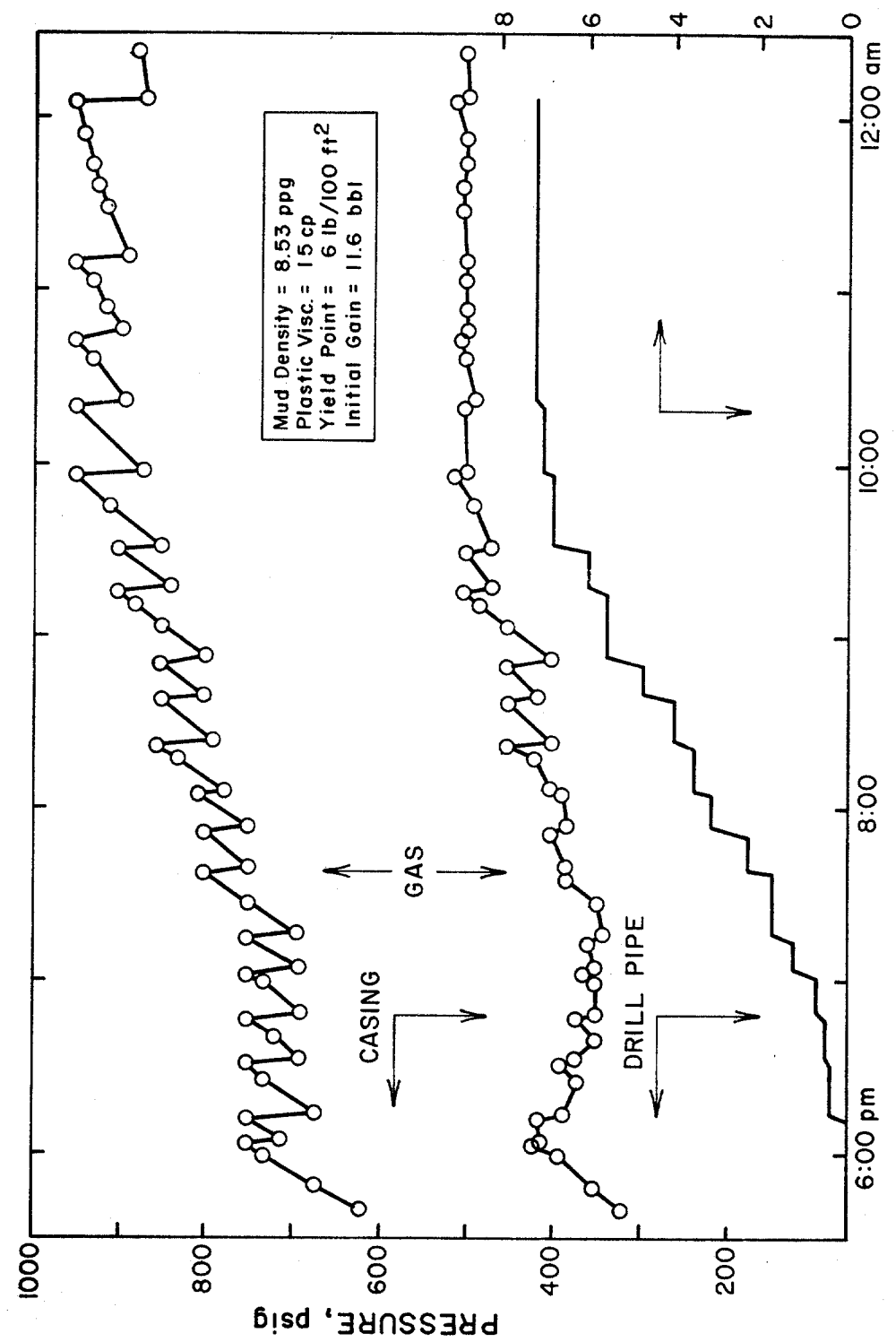

FIGURE 5.4 PRESSURE–VOLUME–TIME DATA FOR STATIC VOLUMETRIC METHOD -- RUN NO. 9

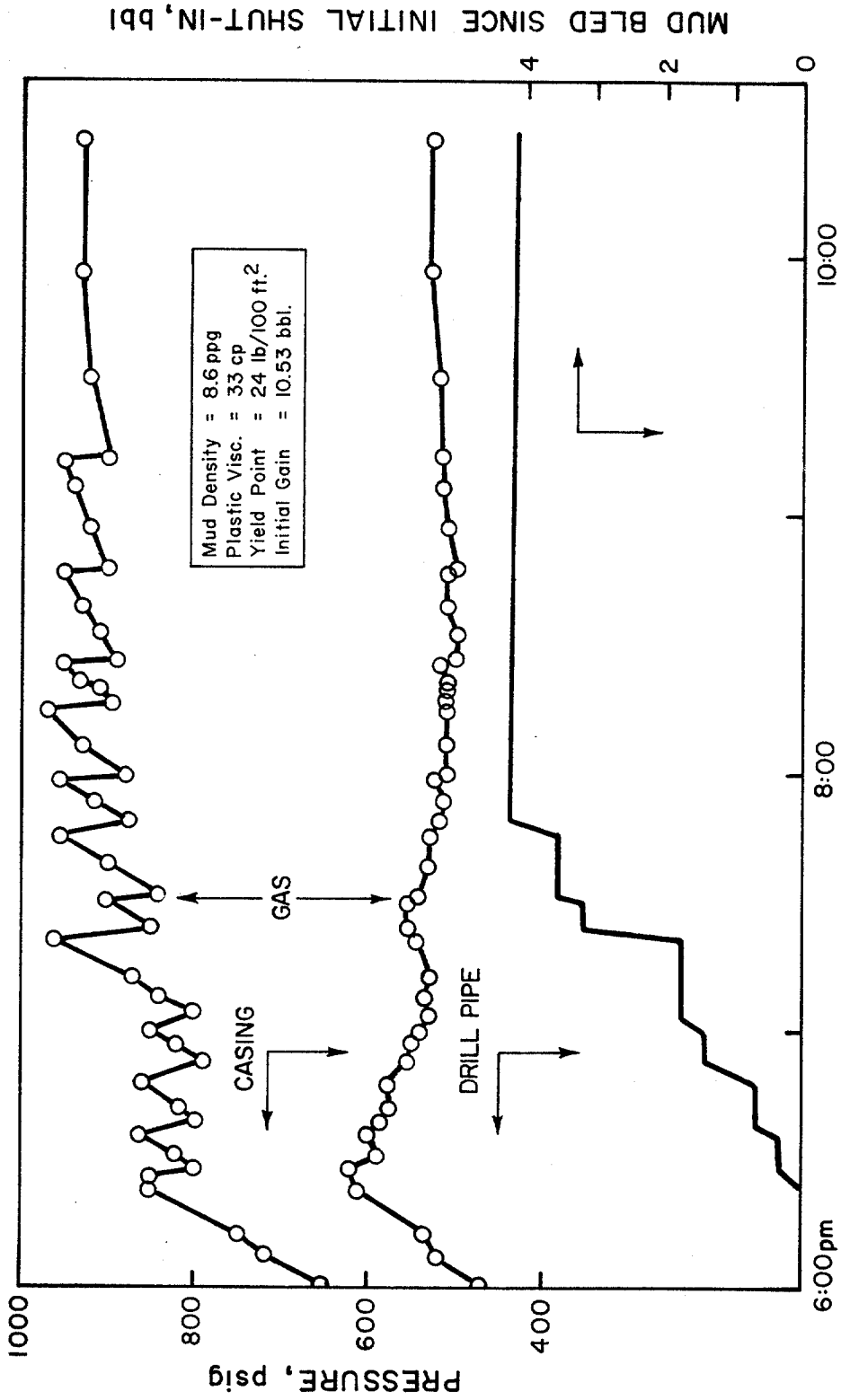

FIGURE 5.5 PRESSURE-VOLUME-TIME DATA FOR STATIC VOLUMETRIC METHOD--RUN NO. 11

across the top of the annulus and maintaining a constant backpressure. This backpressure is varied according to the volume of mud bled from the well in the same manner as the static method.

Run number 15 (Figure 5.6) is an experimental verification of the dynamic method. The choke was set at 1/4-open and initially pump rate was adjusted to hold the casing pressure at the desired value. As the figure shows, up to the point that gas reached the surface it was easy to hold the casing pressure relatively constant. However, after gas reached the surface it was difficult to maintain a constant pressure on the casing due to the high compressibility of the gas.

A physical problem of the well while evaluating the dynamic volumetric method is that drill pipe pressure cannot be monitored constantly during the run. By shutting the well in, however, and adjusting a few valves, drill pipe pressure can be read. This was done for run number 15 after gas had been at the surface for a short time. Note that the drill pipe pressure was 130 psi above the initial shut-in value. For an ideal run, the pressure should have been 100 psi above the initial value. Thus, the dynamic method can successfully maintain well control.

Another interesting result of this particular run is that at one point mud began being pumped back into the well due to having too great a backpressure on the annulus. Once the well was shut in again, the drill pipe pressure

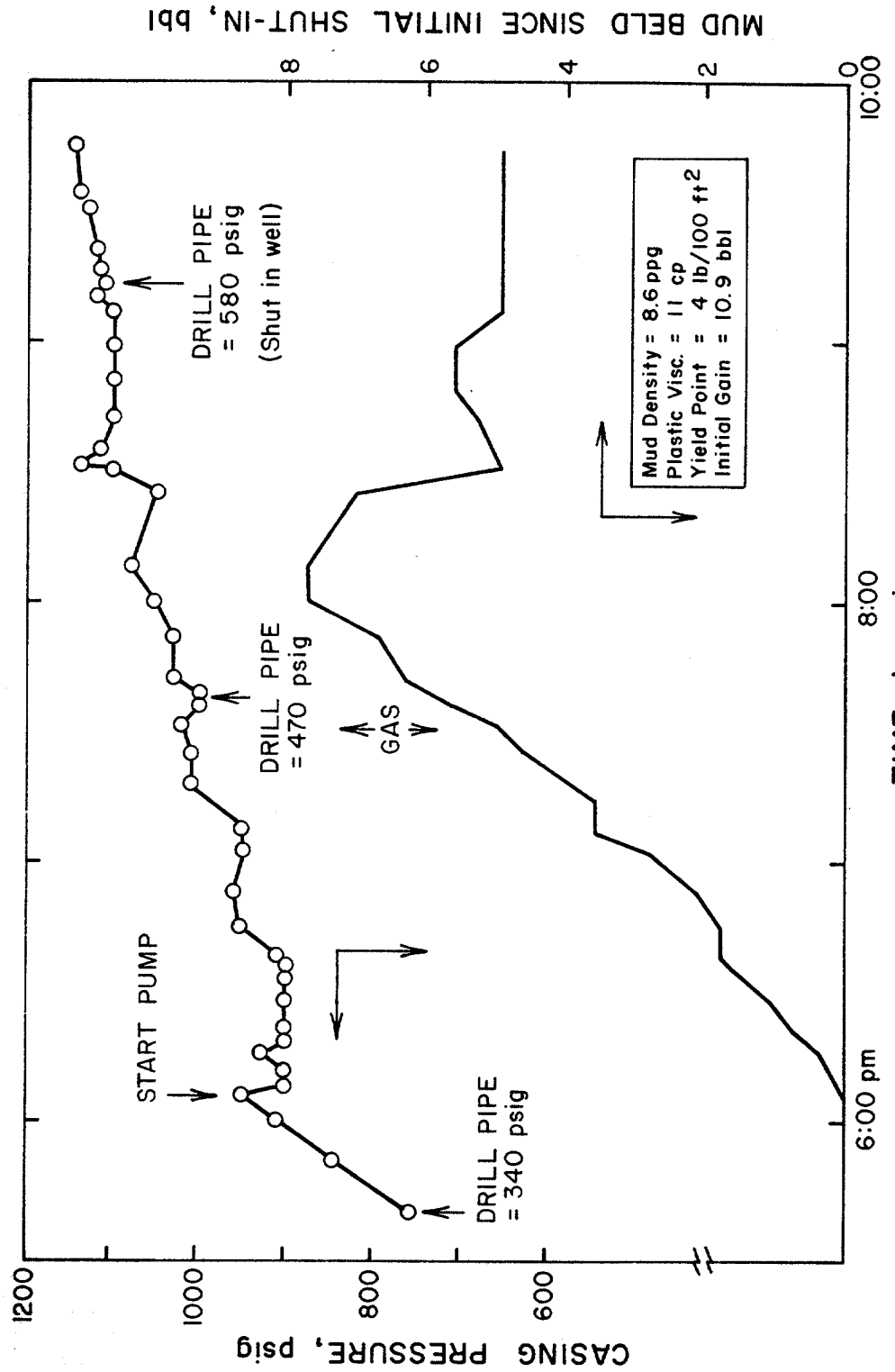

FIGURE 5.6 PRESSURE-VOLUME-TIME DATA FOR DYNAMIC VOLUMETRIC METHOD--RUN NO. 15

read 580 psig—90 psi above the value it would have been for an ideal run. However, at this point 1.9 barrels of mud had been pumped back into the well (equivalent to a hydrostatic head of 56 psi). Therefore, if mud is accidentally pumped into the well, the casing pressure should be decreased by the equivalent hydrostatic head the mud would exert in the annulus [equation (2.12)]. This could be an excellent way to remove the gas kick from the well and replace it with mud, making the well easier to control.

5.1.4 Comparison of Volumetric Procedures

As discussed in the previous sections, both the static and dynamic procedures of the volumetric method for handling upward migration of gas kicks will maintain well control. The question is how do the two procedures compare with each other under the same situations.

A comparison was carried out using the same kick size, initial shut-in pressures, and mud properties for experimental runs 14 (static) and 15 (dynamic). Figures 5.6 and 5.7 graphically illustrate run numbers 15 and 14, respectively, and selected results are shown in Table 5.3. It is interesting to note that more mud is bled from the well when utilizing the dynamic method, and in a much shorter time span, than the static procedure. Also, gas fragmentation seems to be less severe for the dynamic method since the period of time from first gas production to casing pressure stabilization is much less than for the static procedure (casing pressure stabilization is defined as that point

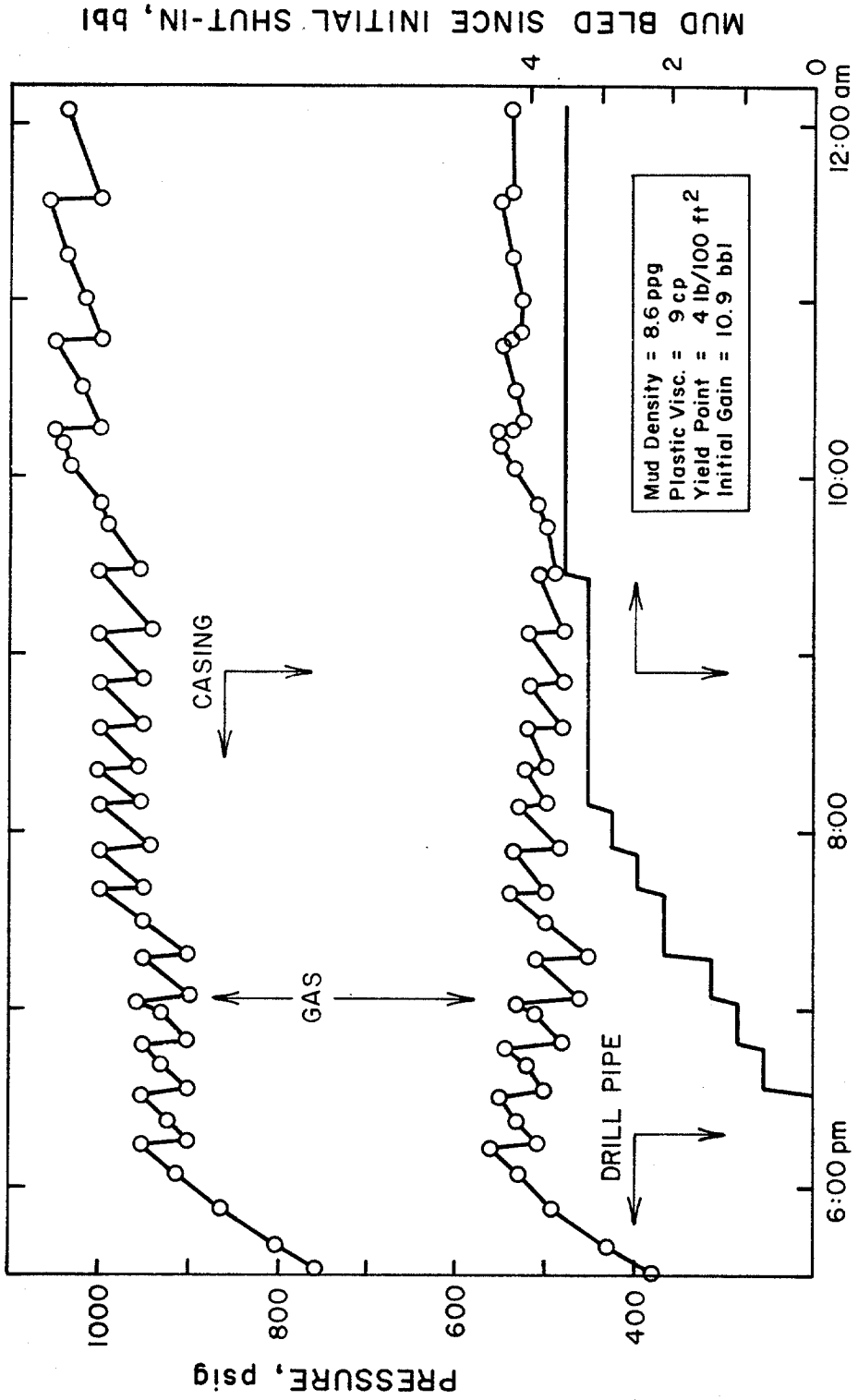

FIGURE 5.7 PRESSURE–VOLUME–TIME DATA FOR STATIC VOLUMETRIC METHOD -- RUN NO. 14

in the run when the rate of change of surface casing pressure is less than 1 psi/min). This difference could be due in part to the effects of the sudden pressure drops that occur when mud is bled using the static method. The gas would tend to have a more rapid and erratic expansion during these times, resulting in additional gas fragmentation. The gas would then be strung out over a larger portion of the well, hence the reason that the pressure stabilization for run number 14 takes a long time.

The volumetric procedures can also be compared based on the ease of operation. For the static method, manipulation of the choke and monitoring pit level are all that are necessary. For the dynamic method the pump stroke rate, choke setting, and pit level must be monitored. The problem of maintaining a constant casing pressure occurs after gas reaches the surface. Due to the high compressibility of the

DATA	RUN 14 (STATIC)	RUN 15 (DYNAMIC)
Time to Take Kick, min	17	18
Time to Bleed First Increment of Mud, min	108	59
Time for Gas to First Reach Surface, min	108	112
Time Until Only Gas Being Produced, min	187	149
Total Mud Bled from Well, bbl	3.51	4.9
Time for Casing Pressure to Stabilize, min	360	240

Table 5.3
COMPARISON OF VOLUMETRIC METHODS

gas, it is difficult to maintain the desired casing pressure. Both choke setting and pump rate must be adjusted simultaneously. Prior to gas reaching the surface, however, all that is necessary is to set a choke setting and adjust pump rate to keep the required casing pressure.

5.2 Effect of Various Parameters on Pressure Behavior During Volumetric Method

As was discussed in Chapter 1, the previous investigators of the volumetric method made several assumptions:

1) Gas density is negligible
2) The gas remains as a continuous slug occupying the entire cross-sectional area of the annulus
3) Once gas reaches the surface, no gas is to be produced since all gas is at the surface.

The assumption of negligible gas density is valid and does not introduce much error into the calculations. However, the second assumption of a continuous gas slug occupying the entire cross-section of the annular region is not valid. The result of using this assumption is to predict too many required bleeding cycles for gas to reach the surface as shown in Figure 5.8. Also, the gas does not remain continuous, but fragments into one large slug and a trailing edge of bubbles. This idea is carried over in the third assumption that once gas reaches the surface, no gas is to be produced. Due to bubble fragmentation, bubbles of gas are still rising in the well after the main slug has reached the surface. These smaller bubbles are at a higher pressure

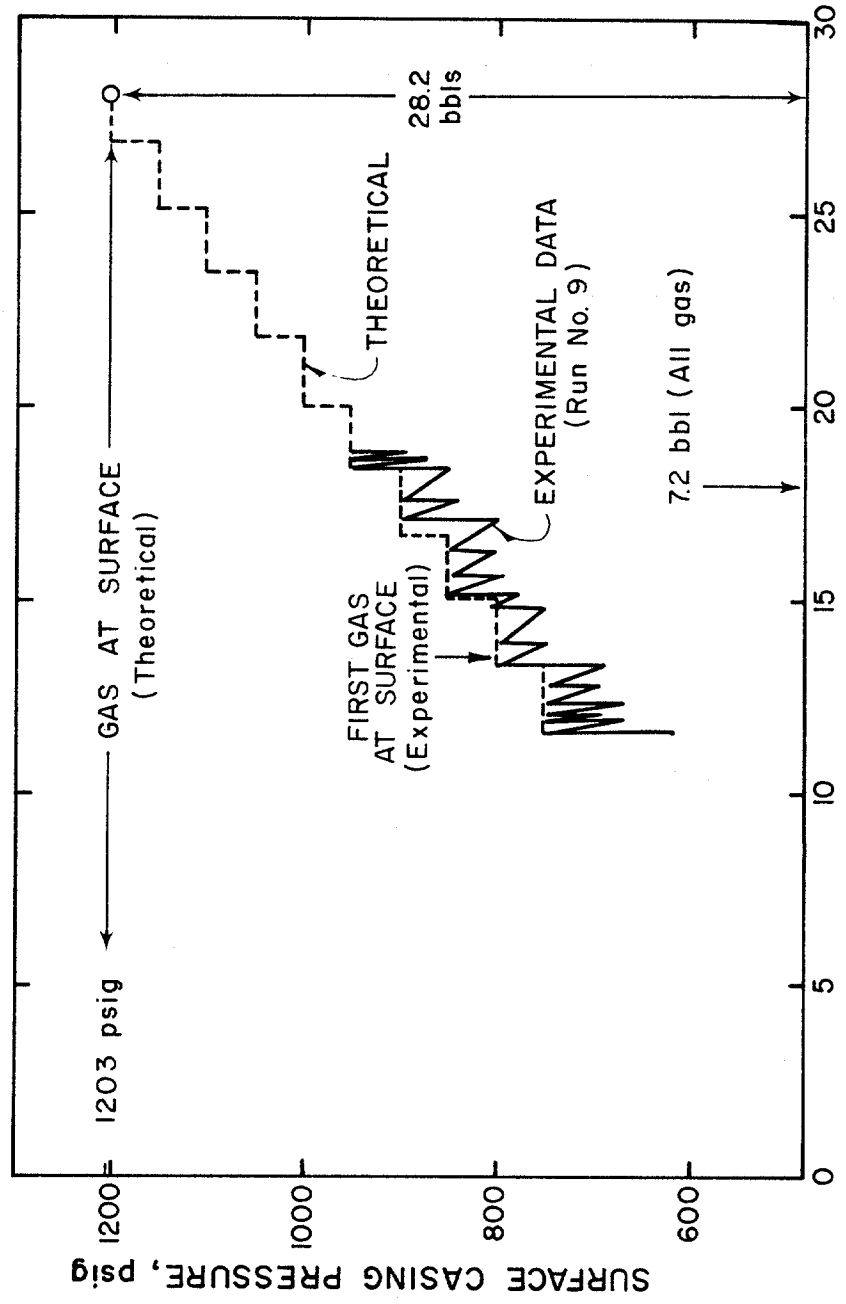

FIGURE 5.8 COMPARISON OF PIT CHANGES AND POINT WHEN GAS REACHES SURFACE--RUN NO. 9

and thus continue building up the casing pressure. A discussion of the pressure behavior of a well that is shut in once the kick first reaches the surface is presented later in this chapter.

The following sections discuss the phenomena of gas fragmentation in detail, the effect of initial kick volume, mud viscosity, and initial shut-in pressures.

5.2.1 Kick Size

A comparison of experimental run numbers 7, 11, and 12 is shown in Table 5.4. For these runs, the only parameter varied was initial gain taken. From this table, the following generalizations can be made concerning the effect of increasing the initial size of the kick:

(a) Less time will transpire from initial shut-in to the first gas produced.

(b) Less time will transpire from initial shut-in to bleeding only gas at the surface.

DATA	RUN 7	RUN 11	RUN 12
Initial Gain, bbl	5.1	10.53	16.5
Time for Gas to First Reach Surface, min	142	95	76
Time Until Only Gas is Produced, min	171	129	125
Initial dp_s/dt, psi/min	7.6	9.1	9.5
Time for Casing Pressure to Stabilize, min	276	222	204
Total Mud Bled From Well, bbl	3.51	4.21	8.43

Table 5.4
EFFECT OF KICK SIZE

(c) The rate of casing presure change increases for the shut-in periods.

(d) The casing pressure stabilizes sooner (essentially all gas is at the surface since dp_s/dt is about 1 psi/min).

(e) The total mud bled from the well increases.

It is also noticed that the size of the gain has no effect on the time elapsed from the first gas reaching the surface until all the gas is at the surface. A possible explanation for this effect is that the severity of bubble fragmentation is not dependent upon the size of the kick. Essentially the same volume of gas is fragmented for any size kick, since the table shows only a small decrease in time from when all gas is produced until all the gas is at the surface. On a percentage basis, the larger the initial gain, the smaller will be the portion that is fragmented and strung out below the first slug of gas.

An expected result that can be seen is that gas slip velocity increases as bubble size increases. Although it is partially masked by the increase in initial gain, the higher slip velocities are readily seen by the increase of the rate of change of casing pressure with bubble size. Both of these phenomena are created by less fragmentation of the gas at higher initial gains. Thus, the bubble migrates upward more as a unit. This is also the cause for the increase in mud bled from the well. The magnitude of the mud bled during run number 12 seems high compared to the other runs. However, theoretical calculations affirm

that the larger the initial gain, the larger will be the mud volume bled from the well.

5.2.2 Mud Viscosity

The effects of mud viscosity on the well behavior for the volumetric method are shown in Table 5.5. Although variables such as pit gain and initial shut-in pressure were not held constant for the experimental runs shown, the qualitative effects of increasing mud viscosity, holding all other variables constant, are as follows:

(a) The gas apparently reaches the surface sooner.

(b) The casing pressure stabilizes much sooner (all gas is at the surface).

(c) The rate of change of casing pressure during the shut-in periods increases.

(d) Total mud that is bled from the well does not seem

DATA	RUN 2	RUN 14	RUN 11	RUN 13
Plastic Viscosity, cp	6	9	33	48
Yield Point, lb/100 ft^2	2.5	4	24	44
Gel Strength, lb/100 ft^2	---	1.5	24	31
Time for Gas to First Reach Surface, min	140+	108	95	59
Time Until Only Gas is Produced, min	215+	187	129	73
Iintial dp_s/dt, psi/min	3.7	4.7	9.1	13.3
Time for Casing Pressure to Stabilize, min	>464	410	222	132
Total Mud Bled from Well, bbl	3.26	3.51	4.21	4.38

Table 5.5
EFFECT OF MUD VISCOSITY

to be affected except for maybe a slight increase with viscosity.

The gas reaches the surface sooner for the thicker muds because bubble fragmentation is not as severe. The viscous mud "holds" the bubble together and thus it migrates upward more as a unit. This is also evidenced by the tendency of the bleed time to decrease as mud viscosity increases, which says that very little fragmentation occurs with the higher-viscosity muds.

5.2.3 Initial Shut-In Pressures

Based on the available data from the experimental runs conducted, only certain correlations could be ascertained for the effect of the magnitude of initial shut-in pressures and are presented in Table 5.6. The effect of increased surface shut-in pressures seems to be a decrease in rate of change of surface casing pressure. This is to be expected since bubble rise velocity is proportional to the square root of the density difference between the gas and mud

DATA	RUN 2	RUN 14	RUN 9
Initial Shut-in Drill Pipe Pressure, psig	530	380	315
Initial Shut-in Casing Pressure, psig	830	750	620
Initial Gain, bbl	10.3	10.9	11.6
Total Mud Bled From Well, bbl	3.3	3.5	7.2
Initial dp_s/dt, psi/min	3.7	4.7	5.7

Table 5.6
EFFECT OF INITIAL SHUT-IN PRESSURES

[equation (2.13)]. Thus, as pressure increases gas density increases as well, resulting in a decrease in gas slip velocity; and for a large bubble of gas migrating upward in an annulus, the rate of casing pressure increase [equation (2.25)] is proportional to gas slip velocity.

The second trend in increasing the initial shut-in pressures is that more mud is bled at the surface. This effect, like the rate of change of surface casing pressure increase, may be partially masked by the slight increase in gain as shut-in pressures decrease for the examples shown. However, the trend of increasing mud bled with increasing rate of change of surface casing pressure has been seen already (Tables 5.4 and 5.5).

5.2.4 Gas Fragmentation

The purpose of this section is to present the effects of the various parameters in gas fragmentation in one table. Thus, Table 5.7 summarizes the effect of (1) using the static versus dynamic procedure of the volumetric method, (2) initial pit gain, (3) mud viscosity, and (4) initial shut-in pressures.

Previous authors advise for the volumetric procedure that once the gas reaches the surface no gas should be produced. The well is to be shut in and supposedly the casing pressure stabilizes at this time. Their assumption is that no fragmentation of the gas kick occurs. Thus, when the gas reaches the surface all the gas is at the surface.

The inaccuracy of the above recommendation is shown in

1. Dynamic versus Static Method

   Bubble fragmentation is less for the dynamic method due to more uniform changes in well pressures with time.

2. Initial Pit Gain

   Bubble fragmentation seems to be essentially independent of bubble size.

3. Mud Viscosity

   Bubble fragmentation is inversely proportional to the viscosity of the mud. As viscosity of the mud increases, the bubble tends to stay together more as a slug, resulting in shorter bleeding times with gas at the surface.

4. Initial Shut-In Pressures

   No real trend could be seen.

Table 5.7
SUMMARY OF EFFECT OF VARIOUS
PARAMETERS ON GAS FRAGMENTATION

Figure 5.9 for run number 16. A viscous mud was used in the study and an 18.5 bbl gain was taken. After ascertaining that the gas had reached the surface the well was shut in. The 270 psi increase in surface casing pressure after this point shows that not all the gas had yet reached the surface but was still migrating upwards. The drill pipe pressure also increases by 250 psi, signifying an increase in bottomhole pressure by the same amount [equation (2.1)].

Although this pressure increase due to shutting in the well when the gas first reaches the surface may not be severe for some instances, in other cases it may be sufficient to cause a breakdown of a low-strength formation in the uncased portion of the well, resulting in an underground

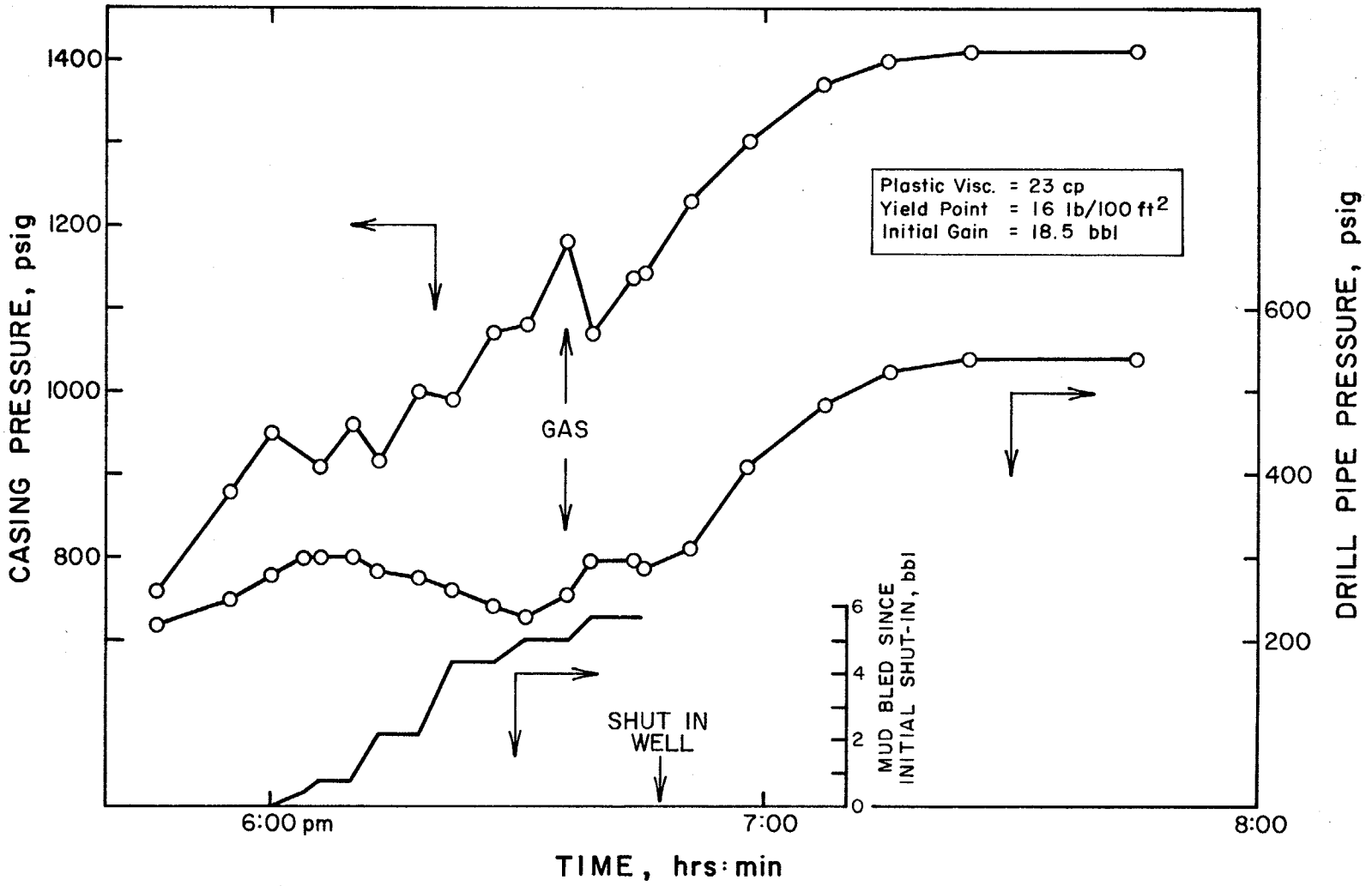

FIGURE 5.9 PRESSURE-VOLUME-TIME DATA FOR STATIC VOLUMETRIC METHOD-- RUN NO. 16

blowout. In addition, this run was conducted using a viscous mud. Therefore, the fragmentation was not as severe as it would be for thinner muds. Thus, thinner muds would result in even larger pressure increases after shut-in.

5.3 Computer Model

An early version of the computer model was designed to read in the various changes in surface casing pressure that occurred for a particular run. In this manner the model could be verified by comparing bottomhole pressure calculated versus pit gain for the experimental run and the computer model.

An example verification is shown in Figure 5.10 in which experimental run number 9 is plotted along with the computer program results. It can be seen that the computer model overpredicts the volume of mud that is bled at the surface which is the main reason that the bottomhole pressures calculated steadily decreases. The reason for this overprediction is that gas fragmentation is not taken into account in the program. Thus, during the bleeding periods the entire bubble is expanded. With fragmentation taken into account, only the main slug of gas highest in the well would expand significantly.

In addition, the calculated rate of change of casing pressure during the shut-in periods was far in excess of the field data. Again the reason is that gas fragmentation is not allowed for in the program. Fragmentation would result in much slower changes in the surface casing pressure

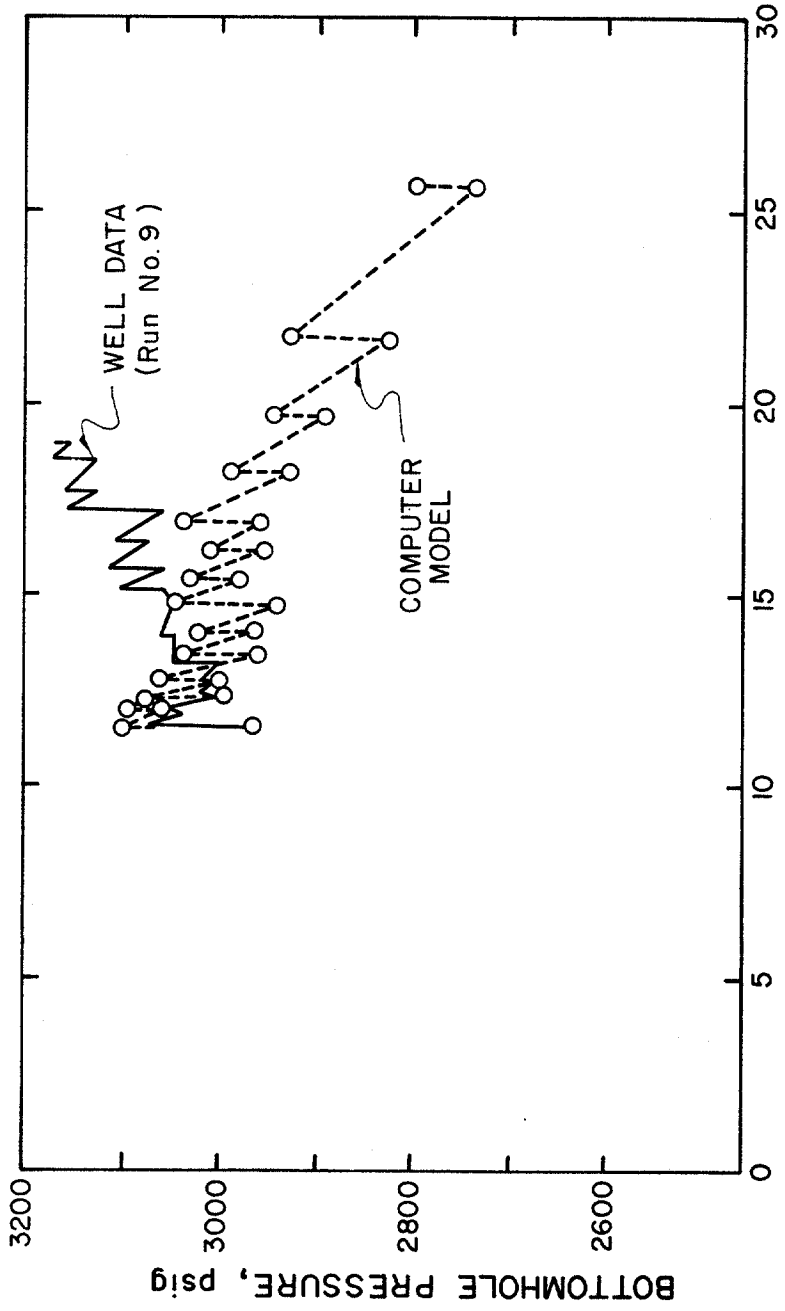

FIGURE 5.10 COMPARISON OF COMPUTER MODEL TO EXPERIMENTAL DATA

and consequently the gas would migrate upwards more during the shut-in periods.

An interesting feature of Figure 5.10 is that initially the model matches the field data. This is believed to be due to the gas remaining essentially as a slug when it is injected into the well (see Appendix B). Therefore, as it migrates upward the bubble begins to fragment and create the divergence between the experimental and computer results.

CONCLUSIONS

As a result of the study of the upward migration of gas kicks in a shut-in well, the following conclusions can be drawn:

1) The assumption made by early authors that the gas kick remains as a continuous slug during upward gas migration was found to be invalid.
2) The following factors were found to significantly affect gas fragmentation:
   (a) viscosity of the mud
   (b) the manner in which pressure is bled from the well (i.e., static versus dynamic volumetric method)
3) The following factors affect the rate at which the first gas bubbles reach the surface:
   (a) initial pit gain
   (b) viscosity of the mud
4) Pressure buildup in the annulus of a shut-in well containing a gas kick is affected by
   (a) initial pit gain
   (b) viscosity of the mud
   (c) initial shut-in pressures
5) In spite of a portion of the gas reaching the surface prematurely due to fragmentation, the modified volumetric method of handling upward gas migration is a valid and practical technique.
6) Contrary to previously accepted practices, the

venting of gas that reaches the surface prematurely does not cause any problems in maintaining well control, as long as a portion of the gas is still rising in the well. This is indicated by a continuous increase in the shut-in casing pressure.

7) With the proper modifications, both the static and dynamic volumetric methods can be used with success. The choice depends on individual and mechanical considerations.

RECOMMENDATIONS

As a result of this study the following recommendations are suggested:

1) Additional studies on the effect of various well parameters on bubble fragmentation should be taken into account and incorporated into the computer model.
2) A drill pipe pressure tap should be installed at the test well in the flow line to the drill pipe annulus such that the drill pipe pressure is available for any valve configuration (i.e., for the dynamic method).
3) A better procedure should be incorporated to monitor changes in the surface pit level. If possible, a critical flow prover should be installed upstream of the mud-gas separator to monitor the volume of gas being bled.
4) A pressure recorder should be installed at the test well to provide a continuous pressure-time plot for both the casing and drill pipe pressures during the experimental runs.
5) A means of monitoring bottomhole pressure directly during experimental runs at the test well should be implemented to ascertain the cause for the reduction of drill pipe pressure during the early portion of the static volumetric method.

REFERENCES

1. Beggs, H. D. and J. P. Brill, Two-Phase Flow in Pipes, The University of Tulsa (1978).

2. Bourgoyne, A. T., Jr. and F. S. Young, Jr., Applied Drilling Engineering, Louisiana State University, Petroleum Engineering Department (1975).

3. Brown, G. G., et al., Natural Gasoline and the Volatile Hydrocarbons, N.G.A.A. (1948).

4. Chevron U.S.A., Incorporated, Personal Communication.

5. Hawthorne, J. W., "Hole Conditions Govern Gas Kick Circulating Method," World Oil (September 1978) 67.

6. Hise, Bill R., ed., Blowout Prevention, Louisiana State University Petroleum Engineering Department (October 1978).

7. Koederitz, W. L., "The Mechanics of Large Bubbles Rising in an Annulus," M.S. Thesis, Louisiana State University, Baton Rouge (1976).

8. Rader, D. W., "Movement of Gas Slugs Through Newtonian and Non-Newtonian Liquids in Vertical Annuli," M.S. Thesis, Louisiana State University, Baton Rouge (1973).

9. Rader, D. W., et al., "Factors Affecting Bubble-Rise Velocity of Gas Kicks," Journal of Petroleum Technology (May 1975) 571.

10. Rehm, B., Pressure Control in Drilling, Tulsa, Oklahoma: The Petroleum Publishing Company (1970).

11. Reid, C. A., "Determining Hydrostatic Loss Caused by Gas Cut Mud," World Oil (July 1968) 132.

12. Shell Oil Company, Personal Communications.

13. Standing, M. B. and D. L. Katz, "Density of Natural Gases," Trans. AIME (1942) 140.

14. Strong, M. W., "Mud Technique in Iran," Trans. AIME, Vol. 132 (1939) 11.

15. Ward, R. H., "Movement of Gas Slugs Through Static Liquids in Large Diameter Annuli," M.S. Thesis, Louisiana State University, Baton Rouge (1974).

16. White, R. J., "Bottomhole Pressure Reduction Due to Gas Cut Mud," Trans. AIME, Vol. 210 (1957) 382.

17. Yarborough, L. and K. R. Hall, "How to Solve Equations of State for Z-factors," Oil and Gas Journal (February 18, 1974) 86.

APPENDIX A

EXPERIMENTAL DATA

APPENDIX A

LISTING OF DATA FROM EXPERIMENTAL RUNS

The following statements are to be referred to when reading the "comments" column in the Tables.

a. Begin kick injection.

b. Shut annular preventer and open HCR valve, making sure all chokes are closed. Build pressure of gas kick by continuing N_2 injection.

c. Stop N_2 injection. Build casing pressure to desired value using pump.

d. Bleed 1-inch injection line clean of gas, holding casing pressure constant with pump.

e. Begin buildup period.

f. Switch valves on choke line to allow mud to flow from pump to choke line (essentially pumping across the top of the annulus).

g. Start pump and hold casing pressure at the desired value.

h. Build casing pressure to 50 psi above previous buildup value (one increment of mud has been bled).

B. Begin bleeding.

SI. Shut well in.

* First gas produced at surface.

TIME, p.m. (hrs:min)	P_{CSG} (psig)	P_{DP} (psig)	GAIN(bbl) Inc.	GAIN(bbl) Total	dp_s/dt (psi/min)	COMMENTS
6:38		535				a
:50		645				b,c
7:00		695				d
:15	1000	700		6.0		e
:25	1030	730			↑	
:36	1100	790			4.9	
:48	1150	840	0.06	6.06		
:56	1200	880			↓	B
:58	1160	850	0.42	6.48	20.0	SI
8:00	1200					B
:01	1080	730	0.43	6.91	↑	SI
:07	1105	765				
:20	1190	850			5.2	
:21					↓	B
:24	1200	860	0.28	7.19		SI*
:25						B
:33	1130	770	0.55	7.74	↑	SI,h
:41	1190	830			6.3	
:52	1250	890			↓	B
:53	1210	850	0.40	8.14	5.0	SI
9:01	1250	880				B
:04	1200	830	0.02	8.16	5.6	SI
:13	1250	880				B
:19	1220	870				
:32	1190	825	0.04	8.2	5.8	SI
:44	1260	900				B
:50	1185	820			7.5	SI
10:00	1260	890				B
:09	1190	820			5.0	SI
:22	1255	890				B
:30	1195	820			4.6	SI
:42	1250	880				B
:51	1180	810			4.1	SI
11:08	1250	880				B
:19	1205	830			3.4	SI
:38	1270	900				B
:49	1195	830			2.8	SI
12:09am	1250	880				B
:24	1140	760				SI
7:20	1140	780			0.0	

Mud Weight: 8.52 ppg
Plastic Visc.: 4.0 cp
Yield Point: 1.0 lbs/100 ft^2

Table A-1
RUN NO. 1
(Static Method)

TIME, p.m. (hrs:min)	P_{CSG} (psig)	P_{DP} (psig)	GAIN(bbl) Inc.	GAIN(bbl) Total	dp_s/dt (psi/min)	COMMENTS
4:52	660	350				a,b,c
5:11	705	400				d
:26	830	530		10.3		e
6:06	970	650			3.7	
:12	1000	670				B
:18	825	480	0.75	11.05		SI
:43	930	580			4.2	
7:00	1000	650				B
:03	1000	650	0.47	11.52	5.0	SI
:12	1045	690				B
:21	1010	640	0.48	12.0	5.8	SI,h*
:27	1045	665				B
:37	1005	615	0.59	12.59	6.1	SI
:46	1060	660				B
:52	1070	680	0.24	12.83	6.7	SI
:55	1090	700				B
8:05	1005	600	0.43	13.26	5.6	SI
:13	1050	640				B
:19	1000	595	0.16	13.42	6.2	SI
:27	1050	640				B
:33	1000	590			4.6	SI
:46	1060	650				B
:56	980	570			3.9	SI
9:12	1050	640				B
:28	1000	590			4.6	SI
:40	1055	640				B
:46	1030	625	0.02	13.44		SI
:48						B
:55	1000	585	0.02	13.46	3.7	SI
10:10	1055	640				B
:19	975	560			3.2	SI
:46	1060	650				B
:56	980	570	0.04	13.50	2.5	SI
11:39	1090	675				B
:46	950	540	0.06	13.56	2.1	SI
12:12am	1005	590				B
:17	920	515			1.6	SI
:36	950	540				

Mud Weight: 8.53 ppg
Plastic visc.: 6.0 cp
Yield Point: 2.5 lbs/100 ft^2

Table A-2
RUN NO. 2
(Static Method)

TIME, p.m. (hrs:min)	P_{CSG} (psig)	P_{DP} (psig)	GAIN(bbl) Inc.	GAIN(bbl) Total	dp_s/dt (psi/min)	COMMENTS
4:57						a
5:12						b
:23	720	360		17.5		c
:37	620	280			↑	e
:51	710	320			4.5	
:57	730	340			↓	
6:15	790	400	no useful data			B
:37	800	380			2.0	SI
:42	810	405		available		B
:47	790	375			4.2	SI
:53	815	400				B
:54	800	375			4.0	SI
:59	820	400				B
7:04	805	375			3.8	SI
:12	835	405				B
:17	815	370			3.9	SI
:26	850	410				B
:32	825	365			4.5	SI
:42	870	410				B
:49	835	365			5.0	SI
:59	885	400				B
8:03	820	350			6.8	SI
:14	895	400				B
:17	850	350			5.4	SI
:28	910	410				B
:36	855	370			5.6	SI*
:45	905	400				B
:48	850	370			5.9	SI
:59	915	400				B
9:04	850	355			4.6	SI
:18	915	410				B
:34	850	370			5.0	SI
:48	920	410				B
:54	815	325			4.8	SI
10:08	880	365				
:21	930	415				B
:26	840	345			4.7	SI
:47	930	410				B
:52	845	330			↑	SI
11:06	885	365			2.9	
:21	930	410			↓	B
:25	820	325			↑	SI
:37	850	330				
:52	900	375			2.9	
12:00am	920	400				
:08	940	420				
:14	960	435			↓	B

:19	810	310		SI
:33	850	330	2.9	
:43	870	350	2.0	

Mud Weight: 8.5 ppg
Plastic visc.: 6.0 cp
Yield Point: 1.5 lbs/100 ft^2

Table A-3
RUN NO. 3
(Conventional Drill Pipe Pressure Method)

TIME, p.m. (hrs:min)	P_{CSG} (psig)	P_{DP} (psig)	GAIN(bbl) Inc.	GAIN(bbl) Total	dp_s/dt (psi/min)	COMMENTS
5:43						a
:52						b
6:19	690	540		13(?)	N/A	c
:20	720	560	no data			d
7:13	820	650				
7:21	815		available			
:33	850					e
:54	950					
8:01	1050					f,g
:36	1150					
	1170					
	1200					
	1250	∿750				

No data for mud -- assume same as Run No. 3

Table A-4
RUN NO. 4
(Dynamic Method)

TIME, p.m. (hrs:min)	P_{CSG} (psig)	P_{DP} (psig)	GAIN(bbl) Inc.	GAIN(bbl) Total	dp_s/dt (psi/min)	COMMENTS
4:57						a
5:05					N/A	b
:08	330	600		6.5		c
:11	620	830				
:17			no data			d
:56	880	750				
6:18	950	780	available			e,f
:26	1000	800				
:29	1000	820				
:45	1050	870				
:53	1070	900				
:58	1100	930				
7:03	1120	950				
:07	1140	950				g
:08	1080	900				
:10	1100	930				
:26	1080	920				
:28	1120	950				2276 strokes
:38	1100	920				
:55	1110	920				(total)

No data for mud -- assume same as Run No. 3

Table A-5
RUN NO. 5
(Dynamic Method)

TIME, p.m. (hrs:min)	P_{CSG} (psig)	P_{DP} (psig)	GAIN(bbl) Inc.	GAIN(bbl) Total	dp_s/dt (psi/min)	COMMENTS
5:21						a
:33		420			N/A	
:38		450				
:40		450				b
:43	340	680				c
:49						
:54	910	770				d
6:05	910	630				
:24	890	490(475=1")		9.75		f
:35	810	375				
:57	915	475				
7:09	975	530				
:23	1050	600				e,g
:50	1050	600	0.35	10.10		
8:08	1050	580				
:26	1050	560				
:52	1060	570				*
9:09	1050	550				

Mud Weight: 8.5 ppg
Plastic visc.: 4.0 cp
Yield Point: 2.0 lbs/100 ft^2

Table A-6
RUN NO. 6
(Dynamic Method)

TIME, p.m. (hrs:min)	P_{CSG} (psig)	P_{DP} (psig)	GAIN(bbl) Inc.	GAIN(bbl) Total	dp_s/dt (psi/min)	COMMENTS
5:49						a
6:04						b
:06	500	830				c
:13						d
:28						
:36	1100					
:53	1200					
7:03	790	480		5.1	↑	e
:15	870	500			7.6	
:24	950	570			↓	B
:26	920	570				
:32	880	550	0.70	5.80	↑	SI
:38	930	540			7.0	
:42	950	540			↓	B
:45	910	530	1.23	7.03	↑	SI,h
:47	930	530				
:51	970	530			7.9	
:57	1010	565				
:59	1020	570			↓	B
8:01	970	580	0.35	7.38	7.5	SI
:09	1030	590				B
:11	970	570	0.53	7.91	6.0	SI*
:21	1030	580				B
:24	970	560	0.53	8.44	6.9	SI,h
:40	1080	570				B
:42	1020	590			5.0	SI
:56	1090	600				B
:59	1000	580			3.6	SI
9:21	1080	590				B
:23	1020	580			1.8	SI
:56	1080	600				B
:59	1000	580	0.17	8.61		SI
10:13	1020	600			1.4	
:25	1030	600			0.8	
:31	1030	610			0.0	

Mud Weight: 8:48 ppg
Plastic visc.: 26 cp
Yield Point: 23 lbs/100 ft^2

Table A-7
RUN NO. 7
(Static Method)

TIME, p.m. (hrs:min)	P_{CSG} (psig)	P_{DP} (psig)	GAIN(bbl) Inc.	GAIN(bbl) Total	dp_s/dt (psi/min)	COMMENTS
5:50						a
6:13						b
:17	550	950		13.2		c,e
:34	620	1000			↑	
:45	670	1030			4.6	
:52	710	1030			↓	B
:55	680	1040			3.6	SI
7:06	720	1010				B
:08	670	1000			4.6	SI
:19	720	980				B
:21	660	980			4.6	SI
:34	720	960				B
:36	690	990	1.58	14.78	4.7	SI,h
:53	770	1010				B
:54	730	1010	0.18	14.96	5.7	SI
8:01	770	1010				B
:03	710	1010	0.35	15.31	6.0	SI
:13	770	1000				B
:15	720	990	0.70	16.01	5.8	SI*
:27	790	980				B
:28	720	980	0.70	16.71	7.1	SI,h
:42	820	975				B
:44	750	970	0.53	17.24	7.0	SI
:54	820	980				B
:56	770	980	0.70	17.94	6.3	SI
9:04	820	980				B
:06	750	970			6.2	SI
:19	830	975				B
:21	700	965			5.9	SI
:43	830	960				B
:45	750	950			2.9	SI
10:13	830	950				B
:15	710	935				SI
:26	740	960			2.7	
:34	760	960			2.5	
:47	780	960			1.5	
11:06	795	960			0.8	

Mud Weight: 8.54 ppg
Plastic visc.: 21.5 cp
Yield Point: 12.0 lbs/100 ft^2

Table A-8
RUN NO. 8
(Static Method)

TIME, p.m. (hrs:min)	P_{CSG} (psig)	P_{DP} (psig)	GAIN(bbl) Inc.	GAIN(bbl) Total	dp_s/dt (psi/min)	COMMENTS
5:21						a
:32						b
:33	500	200		11.6		c
:40	620	315			↑	e
:48	670	350			5.6	
:59	730	390			↓	
6:03	750	420				B
:04	710	410			5.0	SI
:12	750	410				B
:14	670	385	0.35	11.95	↑	SI
:25	730	370			4.7	
:31	750	390			↓	B
:33	690	370	0.18	12.13	↑	SI
:40	715	350			4.3	
:47	750	370			↓	B
:49	670	350	0.17	12.3	↑	SI
:59	730	350			6.2	
7:02	750	360			↓	B
:04	690	350	0.52	12.82	6.0	SI
:14	750	355				B
:16	690	340	0.48	13.30	↑	SI,h
:27	750	345			5.2	
:37	800	385			↓	B
:39	750	385	0.58	13.88	4.2	SI*
:51	800	400				B
:54	750	385	0.88	14.76	5.0	SI
8:05	805	390				B
:06	775	400	0.35	15.11	↑	SI,h
:17	830	420			5.3	
:21	855	450			↓	B
:23	790	400	0.52	15.63	4.2	SI
:37	850	450				B
:39	800	415	0.70	16.33	4.5	SI
:50	850	450				B
:52	800	400	0.80	17.13	↑	SI,h
9:03	850	450			4.4	
:11	880	485				
:15	900	500			↓	B
:17	840	470	0.44	17.57	5.0	SI
:29	900	500				B
:31	850	470	0.87	18.44	↑	SI,h
:45	910	490			4.0	
:56	950	510			↓	B
:57	870	500	0.19	18.63	3.5	SI
10:20	950	500				B
:22	890	495	0.17	18.8	↑	SI
:36	930	500			2.9	
:43	950	505			↓	B

:46	895	500		SI
:54	915	500		
11:03	930	500	2.2	
:10	950	500		B
:12	890	500		SI
:28	915	505		
:36	925	505		
:44	930	500	1.1	
:55	940	500		
12:05am	950	510		B
:07	870	500		SI
:25	880	500	0.6	

Mud Weight: 8.53 ppg
Plastic visc.: 15 cp
Yield Point: 6 lbs/100 ft^2

Table A-9
RUN NO. 9
(Static Method)

TIME, p.m. (hrs:min)	P_{CSG} (psig)	P_{DP} (psig)	GAIN(bbl) Inc.	GAIN(bbl) Total	dp_s/dt (psi/min)	COMMENTS
7:25						a
:37						b
:41	940	960		9.5		c
:45	930	970				e
:51	900	990				
8:03	870	1010				
:16	850	1000				
:32	830	980				
:47	820	990				
9:00	880	990				
:12	870	980				
:35	860	980				
:50	840	990				
Problems with well due to having thin mud in drill pipe and thick mud in annulus. So bled casing down to 300 psi. Pumped 250 strokes of thin mud at d.p. pressure of 1400 psi. Then shut-in well again.						
			4.9	14.4		
10:25	930	450			↑	e
:31	1000	470			13.3	
:34	1050	475			↓	B
:37	1000	475				*
:41	1000	500	2.46	16.86		SI,h
:51	1110	510				B
:53	1030	500			↑	SI
:59	1075	510			7.0	
11:03	1100	520			↓	B
:04	1050	510				SI
:09	1060	520			2.0	
:15	1060	520				Probably
:25	1040	530			-2.0(?)	Mud is
:36	1040	540			0.0	Gelling up
:56	1030	540			-0.5(?)	in hole

Mud Weight: 8.75 ppg
Plastic visc.: 57 cp
Yield Point: 59 lbs/100 ft^2

Table A-10
RUN NO. 10
(Static Method)

TIME, p.m. (hrs:min)	P_{CSG} (psig)	P_{DP} (psig)	GAIN(bbl) Inc.	GAIN(bbl) Total	dp_s/dt (psi/min)	COMMENTS
5:49						a
:58						b
:59	530	330				c
6:01	650	470		10.53		e
:08	715	520			↑	
:13	750	535			9.1	
:23	850	610			↓	B
:25						SI
:26	850					B
:28	800	620	0.35	10.88		SI
:31	820	590			↑	
:36	860	600			7.5	
:39	795	585	0.35	11.23	↓	B
:42	815	575			↑	SI
:48	860	575			7.2	
:53	790	555	0.70	11.93	↓	B
:57	820	550			↑	SI
7:00	850	540			8.6	
:04	800	530	0.35	12.28	↓	B
:08	840	535			↑	SI,h
:12	870	530			7.6	
:21	960	545			↓	B
:24	850	555	1.41	13.69		SI
:30	900	555			8.3	B
:32	840	545	0.35	14.04	↑	SI
:38	900	530			8.8	
:45	955	530			↓	B
:49	875	520	0.70	14.74	↑	SI
:54	915	515			8.9	
:58	955	525			↓	B
:59	880	510			↑	SI
8:06	930	510			6.0	
:14	970	510			↓	B
:16	895	510			↑	SI
:19	910	510			6.1	
:21	930	510			↓	
:25	950	515				B
:26	890	500			↑	SI
:32	910	500			3.0	
:38	930	510			↓	
:46	950	510				B
:47	900	500			↑	SI
:57	920	510			2.0	
9:06	940	515			↓	
:12	950	515				B
:13	900	515				SI

:31	920	520	1.1
:56	930	530	0.4
10:26	930	530	0.0

Mud Weight: 8.6 ppg
Plastic visc.: 33 cp
Yield Point: 24 lbs/100 ft^2

Table A-11
RUN NO. 11
(Static Method)

TIME, p.m. (hrs:min)	P_{CSG} (psig)	P_{DP} (psig)	GAIN(bbl) Inc.	GAIN(bbl) Total	dp_s/dt (psi/min)	COMMENTS
6:13						a
:28						b
:30	480					c
:34	750	260		16.5		e
:39	790	290			9.5	
:48	880	310				
:55	950	350				B
:58	910	370	0.35	16.85	10.0	SI
7:02	950	380				B
:04	910	370	0.70	17.55	10.0	SI
:08	950	375				B
:10	900	370	0.70	18.25		SI,h
:12	915	375			10.0	
:16	960	375				
:20	1000	370				B
:23	950	360	0.70	18.95	10.0	SI
:27	1000	370				B
:28	950	350	0.06	20.01		SI,h*
:36	1030	360			10.0	
:39	1060	360				B
:42	1000	350	1.40	21.41	11.1	SI
:46	1050	355				B
:48	1030	345	1.41	22.82		SI,h
:53	1075	340			10.0	
:55	1100	335				B
:57	1080	330	1.40	24.22	10.0	SI,h
8:04	1150	330				B
:06	1080	310	0.71	24.93		SI,h
:09	1115	310			11.4	
:13	1160	305				
:18	1210	310				B
:20	1120	310				SI
:24	1140	330			5.3	
:29	1170	330				
:35	1200	335				B
:36	1145	330			2.5	SI
:58	1200	355				B
:59	1140	350			1.2	SI
9:48	1200	375				B
:50	1140	375				SI
10:08	1150	380			0.6	

Mud Weight: 8.67 ppg
Plastic visc.: 26 cp
Yield Point: 16 lbs/100 ft^2

Table A-12
RUN NO. 12
(Static Method)

TIME, p.m. (hrs:min)	P_{CSG} (psig)	P_{DP} (psig)	GAIN(bbl) Inc.	GAIN(bbl) Total	dp_s/dt (psi/min)	COMMENTS
5:51						a
6:14						b
:16	550					c
:19	750	360		18.6	↑	e
:26	835	360			13.3	
:30	900	370			↓	
:34	950	370				B
:40	910	360	1.05	19.65	11.4	SI
:43	950	360				B
:46	920	360	0.35	20.0	12.0	SI
:48	950	360				B
:50	910	360	2.8	22.8	↑	SI,h
:54	970	355			15.6	
:59	1050	355			↓	B
7:01	1015	350	0.18	22.98	14.0	SI
:04	1050	350				B
:06	1000	350			15.0	SI
:10	1060	350				B
:11	1000	350			17.5	SI
:15	1070	340				B
:17	990	330			↑	SI
:21	1035	315			9.2	
:23	1050	310			↓	B
:24	995	310			9.2	SI
:31	1055	310				B
:32	1010	310			8.9	SI
:36	1050	300				B
:37	970	290				SI
:43	1000	280			5.0	
:50	1030	290			4.3	
8:04	1045	290			1.1	
:25	1045	295			0.0	

Mud Weight: 8.75 ppg
Plastic visc.: 48.0 cp
Yield Point: 44.0 lbs/100 ft^2

Table A-13
RUN NO. 13
(Static Method)

TIME, p.m. (hrs:min)	P_{CSG} (psig)	P_{DP} (psig)	GAIN(bbl) Inc.	GAIN(bbl) Total	dp_s/dt (psi/min)	COMMENTS
5:14						a
:25						b
:28	560	200		10.9		c
:31	750	380			↑	e
:40	800	430				
:53	860	490			4.7	
6:04	910	530			↓	
:14	950	560				B
:15	900	510			↑	SI
:22	920	530			3.1	
:31	950	550			↓	B
:38	900	500	0.70	11.6	↑	SI
:41	930	520			3.4	
:48	950	545			↓	B
:49	900	480	0.35	11.95	↑	SI
:58	930	510			4.1	
7:03	955	530			↓	B
:04	895	460	0.35	12.3	4.2	SI*
:17	950	510				B
:19	900	450	0.70	13.0		SI,h
:30	950	500			4.7	
:40	1000	540				B
:41	950	500	0.36	13.36	4.2	SI
:53	1000	535				B
:55	945	485	0.35	13.71	4.1	SI
8:08	1000	530				B
:10	955	495	0.35	14.06	3.8	SI
:22	1000	525				B
:23	955	500			3.6	SI
:35	1000	525				B
:36	950	485			3.6	SI
:50	1000	515				B
:51	950	480			3.1	SI
9:07	1000	520				B
:08	940	480			3.1	SI
:28	1000	510				B
:29	955	490	0.35	14.41	↑	SI
:44	990	500				
:51	1000	510			2.0	
10:03	1030	535				
:11	1040	550			↓	
:16	1050	555				B
:17	1000	540			↑	SI
:30	1020	535			1.8	
:45	1050	550			↓	B
:46	995	545			↑	SI

11:00	1015	530		
:15	1035	540	1.3	
:34	1055	550	↓	B
:35	1000	550		SI
12:05am	1035	540	1.2	

Mud Weight: 8.6 ppg
Plastic visc.: 9.0 cp
Yield Point: 4.0 lbs/100 ft^2

Table A-14
RUN NO. 14
(Static Method)

TIME, p.m. (hrs:min)	P_{CSG} (psig)	P_{DP} (psig)	GAIN(bbl) Inc.	GAIN(bbl) Total	Pump Rate, SPM	COMMENTS
5:21						a
:33						b
:36	530					c
:39	755	340		10.9		e,f
:51	845					
6:00	910					
:06	950					
:08	900				37	
:12	900				40	
:16	930		0.35	11.25	51	
:18	900				63	
:21	900		0.35	11.6	61	
:28	900		0.35	11.95	63	
:33	900				58	
:36	900		0.53	12.48	63	
:38	910		0.17	12.65	63	h
:45	950				62	
:53	960		0.35	13.0	62	
7:03	950		0.70	13.7	61	
:07	950		0.70	14.4	61	h
:18	1010				59	
:25	1010		1.05	15.45	56	
:31	1020		0.35	15.8	57	*
:36	1000		0.7	16.5		SI
:38	1000	470				check d.p.
:42	1030		0.7	17.2		f,g,h
:52	1030		0.35	17.55	40	
8:00	1050		1.05	18.6	75	
:08	1080				45	
:25	1050		-0.7	17.9	76	Lost mud
:30	1100				74	to well
:31	1140		-2.1	15.8	73	
:35	1115				70	
:42	1100		0.35	16.15	65	
:49	1100		0.35	16.5	57	
:59	1100		-0.70	15.8	61	
9:07	1100				67	
:10	1120				66	SI well
:13	1110	580				
:30	1130	590				
:45	1145	610				

Mud Weight: 8.6 ppg
Plastic visc.: 11.0 cp
Yield Point: 4.0 lbs/100 ft^2

Table A-15
RUN NO. 15
(Dynamic Method)

TIME, p.m. (hrs:min)	P_{CSG} (psig)	P_{DP} (psig)	GAIN(bbl) Inc.	GAIN(bbl) Total	dp_s/dt (psi/min)	COMMENTS
5:27						a
:41						b
:43	560					c
:46	760	220		18.5		e
:55	880	250			13.6	
6:00	950	280				B
:04		300	0.45	18.95		
:06	910	300	0.35	19.3	12.5	SI
:10	960	300				B
:13	915	285	1.4	20.7	17.0	SI,h
:18	1000	275				B
:22	990	260	2.1	22.8	16.0	SI,h
:27	1070	240				B
:31	1080	230	0.7	23.5	20.0	SI,h
:36	1180	255				B
:39	1070	295	0.7	24.2	13.0	SI*
:44	1135	295				B
:45	1140	290				SI
:51	1230	310			15.0	
:58	1300	410			10.0	
7:07	1370	485			3.75	
:15	1400	525			1.0	
:25	1410	540			0.0	

Mud Weight: 8.2 ppg (gas-cut)
Plastic Visc.: 23.0 cp
Yield Point: 16.0 lb/100 ft^2

Table A-16
RUN NO. 16
(Static Method)

APPENDIX B

ANALYSIS OF BUBBLE FRAGMENTATION DURING KICK FEED-IN

APPENDIX B

ANALYSIS OF BUBBLE FRAGMENTATION DURING KICK FEED-IN

An important consideration in modeling the upward gas migration occurring during the volumetric method was whether the gas stayed as a slug while it was injected into the well or if it broke into a series of bubbles. To ascertain the form in which the gas first enters the well, the following parameters must be known:

a) Terminal slip velocity of gas

b) Injection rate of gas into well

c) Slip velocity versus bubble size

d) Annular geometry.

The terminal gas slip velocity is discussed in Chapter 2, section 1.4. This velocity is important in establishing a plot of slip velocity versus bubble volume in order to predict the point at which the bubble begins to rise faster than the gas being injected into the well. At that instant in time the bubble would break away from the injecting gas and migrate upwards, and a new bubble would begin forming below it. Knowing the terminal velocity and that gas slippage is proportional to the square root of the radius of curvature of the bubble[9], a relationship could be prepared that would relate bubble volume to radius of curvature and thus to gas slip velocity.

The terminal slip velocity is calculated assuming that the well is open to flow; and, since the injection gas is

pushing mud upward, the mud is in effect flowing. To correct for this flow of mud, an additional coefficient is multiplied to the slip velocity calculated assuming static conditions. The example problem at the end of this section shows the means of estimating this coefficient from a graph shown in Figure B.1.

Gas injection rate into the well is easily calculated from the known pit gain and time during which the gain is taken. Since the annular capacity of the well, in addition to the maximum cross-sectional area occupied by the bubble (from Chapter 2, section 1.4) is known, the average injection velocity can be calculated.

However, as the gas bubble first comes out of the injection line, its velocity is equal to the rate of change of its radius of curvature, assuming a hemispherical bubble. Thus the injection velocity can be very large at first and then rapidly decrease until the terminal (average) injection velocity is achieved. This terminal velocity of

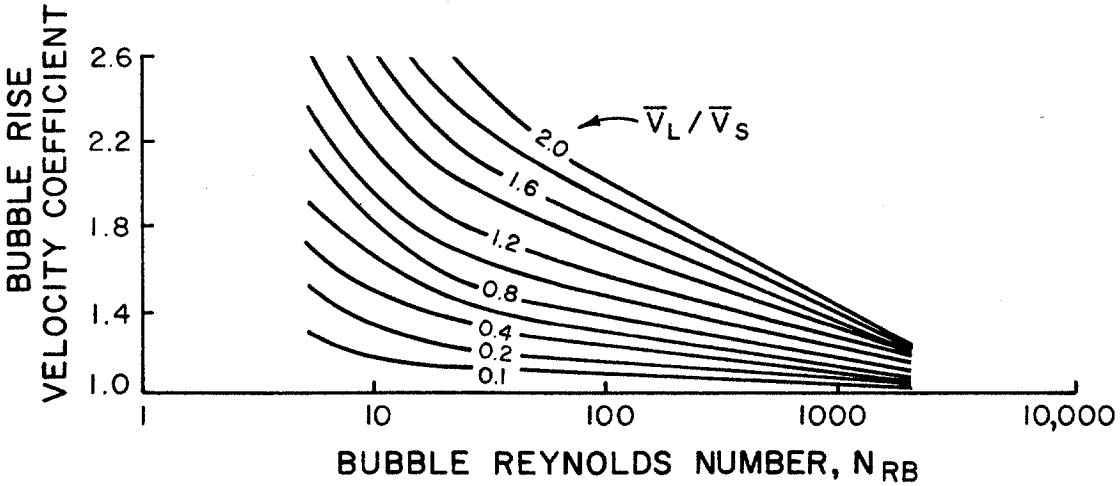

FIGURE B.1 BUBBLE RISE VELOCITY COEFFICIENT C_2 FOR AN ANNULUS (after Rader et al.[9])

injection occurs once the bubble has achieved a volume sufficient to take up the maximum cross-sectional area available to it, as is the case for the terminal gas slip velocity.

The following sections perform the necessary derivations to come up with values of radius of curvature of the bubble and the associated fraction of the annular cross-sectional area as well as the bubble volume. These are then used to come up with relationships of injection velocity and gas slip velocity versus bubble volume.

B.1 Outer and Inner Annular Radii

Consider the annular geometry shown in Figure B.2, in which the drill pipe is not centered inside the casing (or hole). Assuming a vertical hole, a gas bubble would tend to occupy the portion of the annulus cross-section having largest casing-pipe separation. The radius of curvature of the gas bubble, R_c, is defined as half the distance from one edge of the bubble to the other. A circle of radius r_c with center at the origin defines the location of the radius of curvature.

To get a relationship between R_c and the subsequent annular cross-sectional area occupied by the gas as well as bubble volume, the distance between the inner and outer radii must be known at all points. A geometric analysis is shown in Figures B.3 and B.4, and the important parameters include the following:

r_o = distance to inside surface of casing (outer

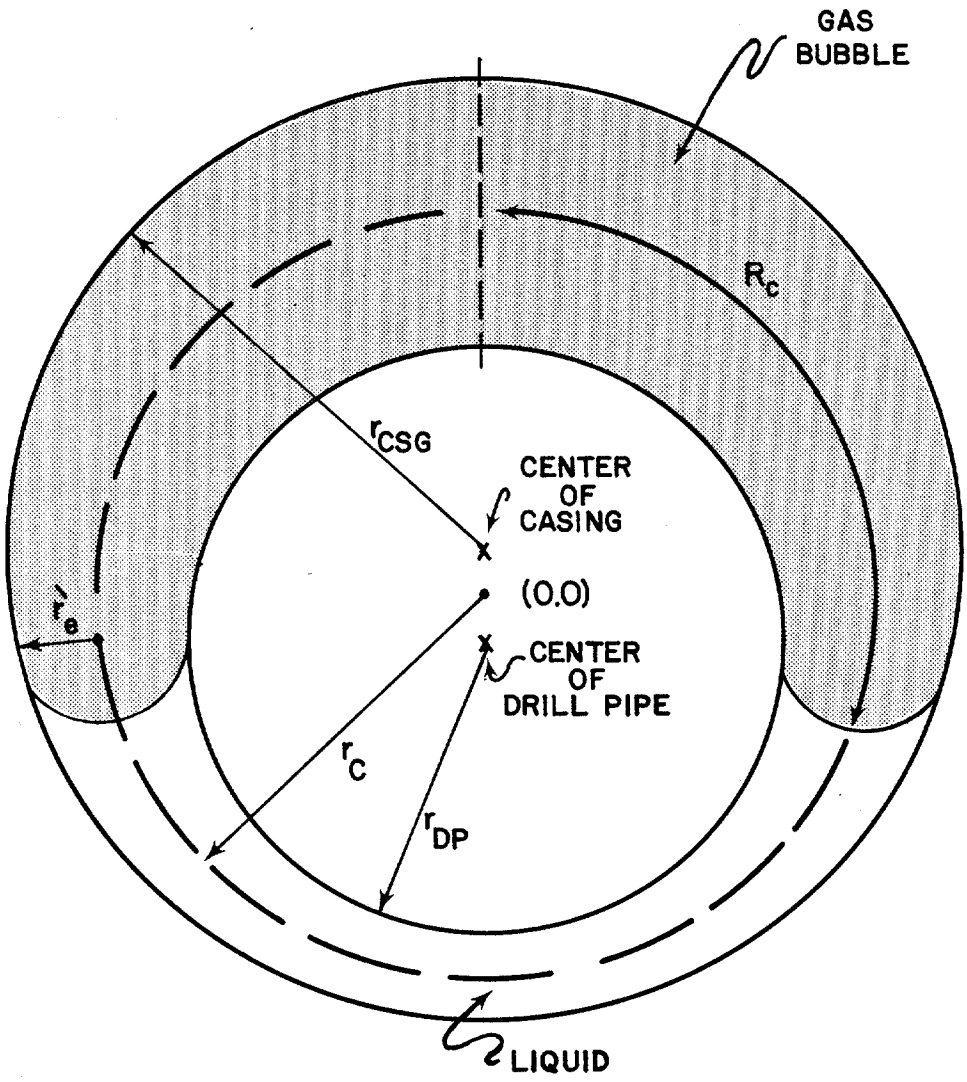

FIGURE B.2 ANNULAR GEOMETRY FOR
BUBBLE FRAGMENTATION STUDY

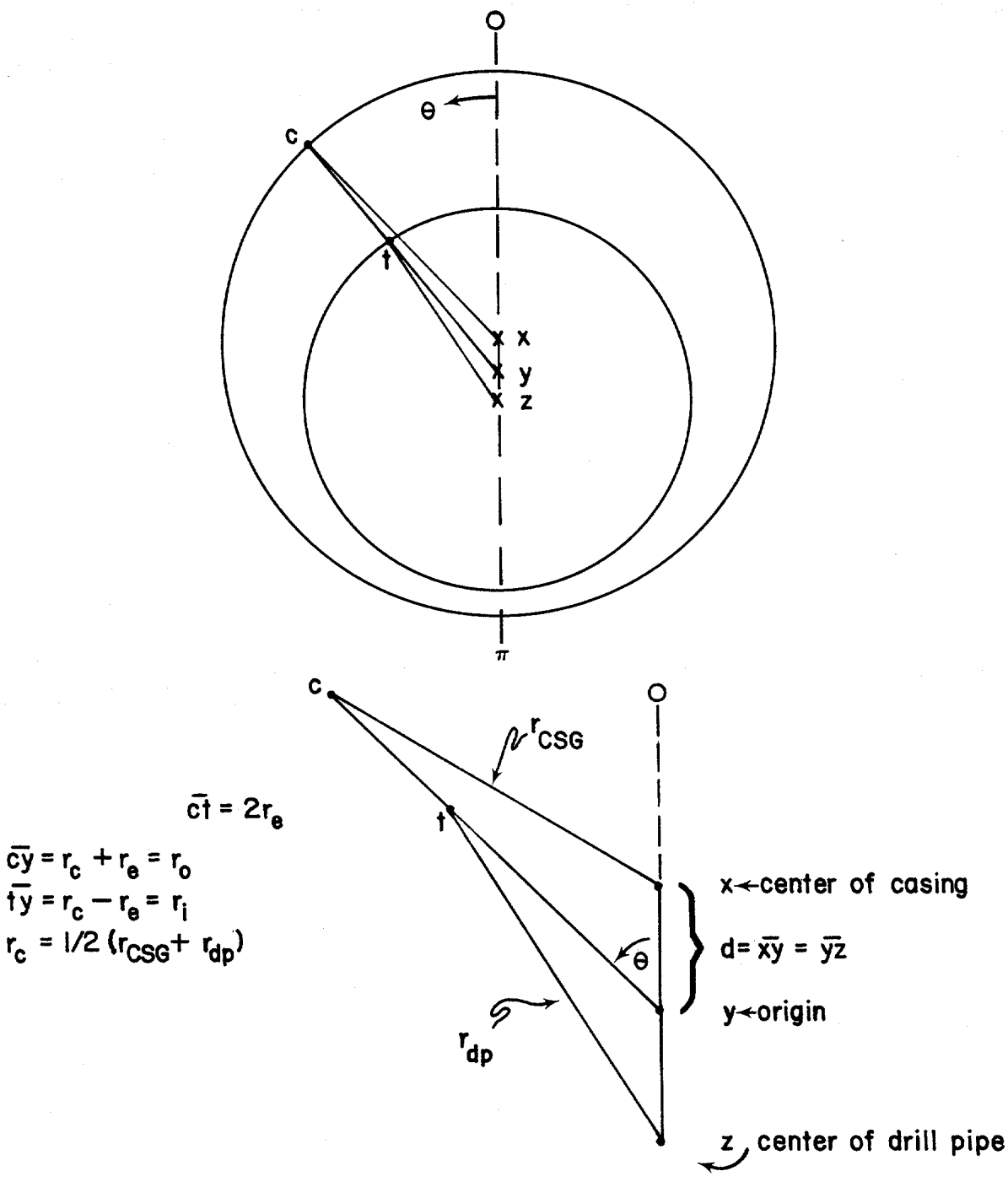

FIGURE B.3 GEOMETRIC RELATIONSHIP OF r_o AND r_i FOR DETERMINATION OF V_B, F_G, AND R_C.

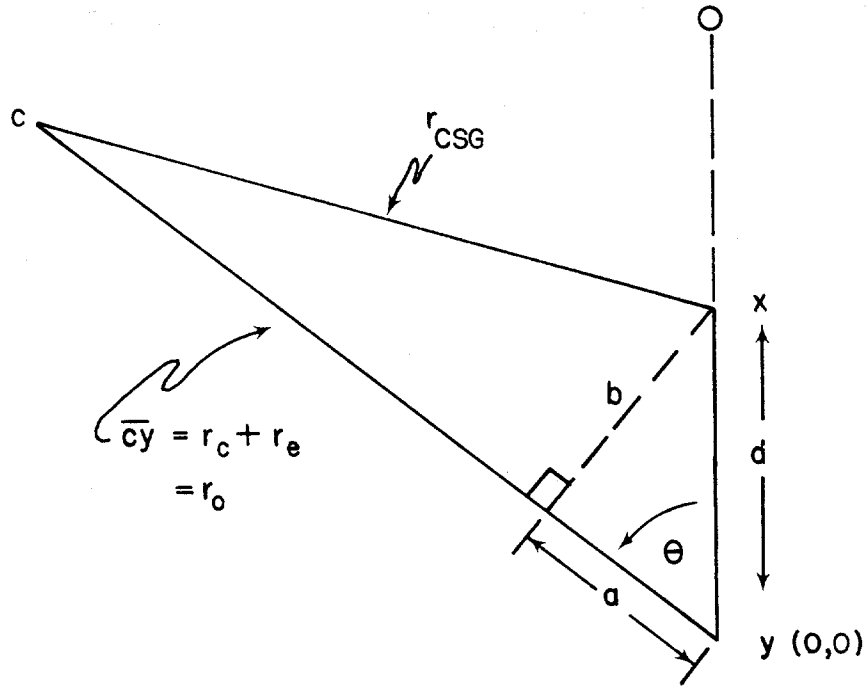

FIGURE B.4 ENLARGED VIEW OF GEOMETRIC ANALYSIS OF OUTER ANNULAR RADIUS

annular dimension), measured from origin, inches

r_i = distance to outer surface of drill pipe (inner annular dimension), measured from origin, inches

r_{CSG} = inside radius of casing, inches

r_{DP} = outer radius of drill pipe, inches

d = distance from origin to either the center of the casing or the drill pipe, inches

r_e = one-half the distance between the inner casing and outer drill pipe surfaces, measured along a line which passes through the origin, inches

r_c = the average value of the casing and drill pipe

radii, the circle formed from which has its center at the origin, inches.

Since the annulus possesses a symmetry as shown by the dashed line in Figure B.3, one side of the annulus will be studied. It is only necessary to double the values calculated for area and volume to give the required relationship with bubble radius of curvature (R_c).

The geometric considerations utilized to derive an equation for the outer annular radius (r_o) as a function of the sweep angle θ is illustrated in Figure B.4. Using basic laws of geometry,

$$a = d \cos\theta \quad \text{.....(B.1)}$$

$$b = d \sin\theta \quad \text{.....(B.2)}$$

Then,

$$(r_o - a)^2 + b^2 = r_{CSG}^2 \quad \text{.....(B.3)}$$

$$r_o^2 - 2ar_o + (a^2 + b^2) = r_{CSG}^2$$

$$r_o^2 - 2ar_o + (d^2 - r_{CSG}^2) = 0$$

Using the quadratic equation and solving for the positive root yields

$$r_o = d \cos\theta + \sqrt{r_{CSG}^2 - d^2 \sin^2\theta} \quad \text{.....(B.4)}$$

The inner radius of the annulus is given by

$$r_i = r_o - 2r_e \quad \text{.....(B.5)}$$

But $$r_o = r_c + r_e \quad \text{.....(B.6)}$$

Therefore,

$$r_e = r_o - r_c$$
$$= d\cos\Theta + \sqrt{r_{CSG}^2 - d^2\sin^2\Theta} - r_c \quad \ldots\ldots(B.7)$$

Combining equations B.5, B.6, and B.7 and simplifying gives

$$r_i = 2r_c - d\cos\Theta - \sqrt{r_{CSG}^2 - d^2\sin^2\Theta} \quad \ldots\ldots(B.8)$$

It is interesting to note that when d equals zero, equations B.4 and B.8 simplify to the case of drill pipe centered in the casing.

B.2 Area

The next step is to find cross-sectional area in the annulus as a function of gas bubble radius of curvature. Referring to Figure B.5, the differential element of area is given by

$$dA = 1/2\ (r_o^2 - r_i^2)d\Theta \quad \ldots\ldots(B.9)$$

Integrating equation B.8 and doubling the value of area results in

$$A = \int_o^{\Theta} (r_o^2 - r_i^2)d\Theta + \pi\hat{r}_e^2 \quad \ldots\ldots(B.10)$$

where $\hat{r}_e$ is given by equation B.7 using the value of Θ. This additional area is due to the curved ends of the bubble. Evaluation of equation B.10 results in

$$A = 4r_c\ (d\sin\Theta - r_c\Theta + \int_o^{\Theta} \sqrt{r_{CSG}^2 - d^2\sin^2\Theta}\ d\Theta)$$
$$+ \pi\hat{r}_e^2$$
$$\simeq 4r_c\ (d\sin\Theta - r_c\Theta + r_{CSG}\Theta) + \pi\hat{r}_e^2 \quad \ldots\ldots(B.11)$$
$$0<\Theta<\pi$$

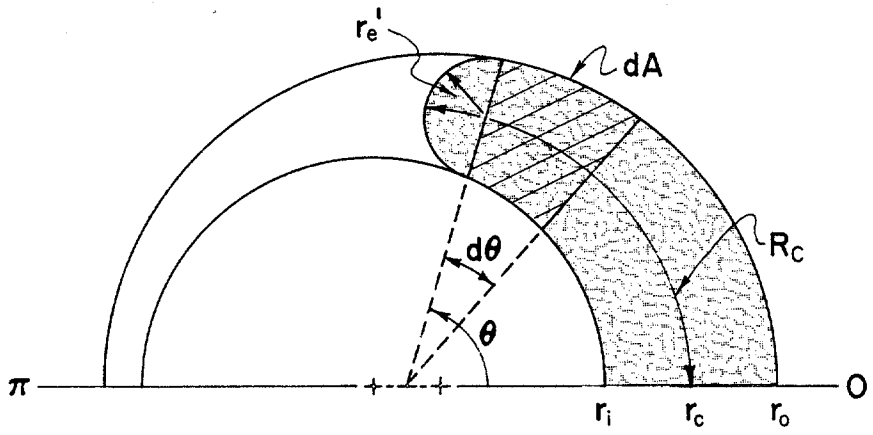

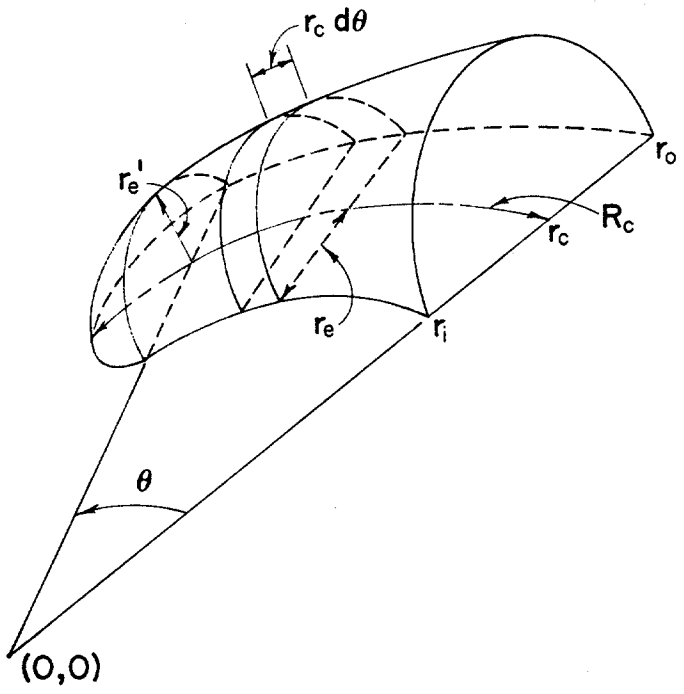

FIGURE B.5 MATHEMATICAL REPRESENTATION OF ANNULAR CROSS-SECTIONAL AREA AND BUBBLE VOLUME

The approximation allowing integration of the equation above B.11 results in a maximum error of less than 0.07%.

The total cross-sectional area of the annulus is

$$A_{ann} = \pi(r_{CSG}^2 - r_{DP}^2) \quad \text{.....(B.12)}$$

Thus, the gas fraction is given by

$$F_g = \frac{A}{A_{ann}} \quad \text{.....(B.13)}$$

B.3 Volume

Referring to the lower illustration in Figure B.5, the volume occupied by the gas bubble, including the curved ends, is given by

$$V = \int dV = \int_o^\Theta \pi r_e^2 \, r_c \, d\Theta + \frac{2}{3} \pi \hat{r}_e^3 \quad \text{.....(B.14)}$$

Evaluation of this integral yields

$$\begin{aligned} V &= \pi r_c \left[\frac{d^2}{2} \sin 2\Theta - 2 r_c \, d \sin\Theta + (r_{CSG}^2 + r_c^2)\Theta \right. \\ &\quad \left. + 2 \int_o^\Theta (d\cos\Theta - r_c)\sqrt{r_{CSG}^2 - d^2 \sin\Theta}\, d\Theta \right] \\ &\quad + \frac{2}{3} \pi \hat{r}_e^3 \\ &\simeq \pi r_c \left[\frac{d^2}{2} \sin 2\Theta - 2 r_c \, d \sin\Theta + (r_{CSG}^2 + r_c^2)\Theta \right. \\ &\quad \left. + 2 r_{CSG} (d \sin\Theta - r_c\Theta)\right] + \frac{2}{3} \pi \hat{r}_e^3 \quad \text{....(B.15)} \\ &\qquad\qquad\qquad\qquad\qquad\qquad\qquad\qquad\qquad\qquad 0<\Theta<\pi \end{aligned}$$

Use of the approximation that $d^2 \sin^2\Theta << r_{CSG}^2$, as was done for equation B.11, results in a maximum error of 0.07%.

B.4 Radius of Curvature of Bubble

The bubble radius of curvature for an annulus is given by

$$R_c = r_c\Theta + \grave{r}_e \quad \text{.....(B.16)}$$

The physical relationship of R_c and $\grave{r}_e$ to Θ is shown in Figure B.5. It should be noted that $\grave{r}_e$ is given by equation B.7 using the value of Θ.

B.5 Data Tabulation

Table B.1 was compiled using the equations from the previous sections. The geometry of the L.S.U. B-7 test well was included, and it was assumed that the tubing was one-half inch off-center from the casing (d = 0.25 inches).

B.6 Example Calculations

The example described here illustrates the use of Table B.1 to give a relationship between bubble volume and the velocity of both the gas bubbles slipping up the annulus and the gas being injected.

1. Using well data from Run number 9 (see Table 5.1), the bottomhole pressure prior to shut-in is given by

$$p = 0.052(8.53)\ 6029 + 14.7$$
$$= 2689 \text{ psia}$$

2. Nitrogen is the injection gas and assuming a bottomhole temperature of 120^0F (Z = 1.035), from equation (4.1):

$$\bar{\rho}_g = \frac{2689(28)}{80.2\ (1.035)580} = 1.56 \text{ lb/gal}$$

Θ	AREA, IN^2	VOLUME, IN^2	R_c	F_g
--	0.196	0.033	0.250	0.016
--	0.785	0.262	0.500	0.064
--	1.131	0.452	0.600	0.092
--	1.767	0.884	0.750	0.144
*0	1.787	0.899	0.754	0.145
10	2.788	1.487	1.089	0.227
20	3.741	2.031	1.415	0.304
30	4.639	2.520	1.734	0.377
40	5.480	2.949	2.046	0.445
50	6.263	3.315	2.352	0.509
60	6.989	3.620	2.653	0.568
70	7.661	3.868	2.951	0.623
80	8.281	4.067	3.246	0.673
90	8.853	4.223	3.542	0.719
100	9.380	4.345	3.837	0.762
110	9.865	4.442	4.135	0.802
120	10.314	4.521	4.436	0.838
125.75	10.556	4.561	4.611	0.858
130	10.729	4.589	4.742	0.872
140	11.115	4.652	5.052	0.903
150	11.479	4.713	5.368	0.933
160	11.826	4.775	5.690	0.961
170	12.166	4.840	6.019	0.989
174.06	12.304	4.873	6.100	1.000

*For all points above $\Theta = 0$, bubble is a hemisphere.

Data: Casing $r_i = 2.446$ inches

Tubing $r_o = 1.4375$ inches

Tubing center is 0.5 inches from casing center (d = 0.25 inches)

Table B.1
RELATIONSHIP BETWEEN VARIOUS BUBBLE PARAMETERS
FOR GAS FRAGMENTATION STUDY

3. Flow behavior index and consistency index of mud:

$$n = 3.322 \log_{10} \left(\frac{\Theta_{600}}{\Theta_{300}}\right) \quad \text{.....(B.17)}$$

$$K = \frac{510\Theta_{300}}{511^n} \quad \text{.....(B.18)}$$

where n = flow behavior index

K = consistency index, eq. cp.

Θ_{600}, Θ_{300} = Fann viscometer dial readings at 600 and 300 rpm, respectively

Therefore,

$$n = 3.322 \log_{10} \left(\frac{36}{21}\right) = 0.7776$$

$$K = \frac{510(21)}{510^{0.7776}} = 83.88 \text{ eq. cp.}$$

4. Bubble Reynolds number (equation 2.14):

$$N_{RB} = \frac{133,632(8.53)\bar{v}_s^{1.2224}}{83.88} \times \left[\frac{0.0208}{2 + \frac{1}{0.7776}} (4.892 - 2.875)\right]^{0.7776}$$

$$= 457.62\bar{v}_s^{1.224}$$

5. Terminal gas slip velocity, static fluid (equation 2.13):

$$\bar{v}_s = (0.16 + 0.092 \log_{10} N_{RB}) \sqrt{(4.892+2.875)\frac{(8.53-1.56)}{8.53}}$$

$$= (0.16 + 0.092 \log_{10} N_{RB}) 2.519$$

Simultaneous solution of N_{RB} and $\bar{v}_s$ gives

$$N_{RB} = 470.3$$

$$\bar{v}_s = 1.023 \text{ ft/sec}$$

6. Velocity of mud in backflow region (equations 2.22a and 2.22b):

$$(\bar{V}_{LB})_{Lam} = \frac{52(8.53 - 1.56)(4.892 - 2.875)^2}{15} - \frac{5(6)(4.892 - 2.875)}{15}$$

$$= 94.3 \text{ ft/sec}$$

$$(\bar{V}_{LB})_{Turb} = 11.564 \left[\frac{(8.53 - 1.56)^4 (4.892 - 2.875)^5}{(8.53)^3 (15)}\right]^{1/7}$$

$$= 15.690 \text{ ft/sec}$$

Therefore, $\bar{V}_{LB} = 15.690$ ft/sec.

7. Gas Fraction (equation 2.16):

$$F_g = \frac{15.690}{15.690 + 1.023} = 0.939$$

From Figure 2.5, $(F_g)_{corr} = 0.858$

8. Gas injection velocity:

$$\bar{q}_i = \frac{\text{Total Gain}}{\text{Injection Time}} = \frac{11.6 \text{ bbls}}{11 \text{ min}} \times \frac{1 \text{ min}}{60 \text{ sec}}$$

$$= 0.0176 \frac{\text{bbl}}{\text{sec}} = 170.5 \frac{\text{in}^3}{\text{sec}}$$

$$\bar{V}_i = \frac{\bar{q}_i}{C_A F_g} = \frac{0.0176 \text{ bbl/sec}}{0.858} \times \frac{1000 \text{ ft/bbl}}{0.97135(4.892^2 - 2.875^2)}$$

$$= 1.346 \text{ ft/sec}$$

9. Assume mud velocity ($\bar{V}_m$) = injection velocity ($\bar{V}_i$).

$$\frac{\bar{V}_m}{\bar{V}_s} = \frac{1.346}{1.023} = 1.316$$

From Figure B.1, $C_2 = 1.42$. The corrected slip velocity is

$$\bar{V}_s = 1.42(1.023) = 1.452 \text{ ft/sec}$$

10. Knowing that $\bar{V}_s = k\sqrt{R_c}$ and assuming it remains constant over the range of values of R_c, for a gas fraction of 0.858, R_c is 4.611 inches. Thus, using the corrected

terminal gas slip velocity,

$$k = \frac{1.452}{\sqrt{4.611}} = 0.6762 \text{ ft/sec-inch}^{1/2}$$

Table B.2 shows the values of R_c, V_B and F_g which correspond to values of slip velocity calculated from

$$\bar{V}_s(R_c) = 0.6762 \sqrt{R_c}$$

11. Injection velocity profile:

Assuming bubbles form in a hemispherical shape,

$$\bar{q} = \frac{d(V_B)}{dt} = \frac{d}{dt}\left(\frac{2}{3}\pi r^3\right) = 2\pi r^2 \frac{dr}{dt} = 170.5 \frac{in^3}{sec}$$

Thus,

$$V_i = \frac{dr}{dt} = \frac{170.5}{2\pi r^2} \times \frac{1}{12}\left(\frac{ft}{sec}\right) = \frac{2.2616}{r^2} \frac{ft}{sec}$$

where r = bubble radius, inches

Bubble volume is calculated assuming the bubble is hemispherical as in the above derivation. As a result, a relationship of gas injection velocity versus bubble volume is formed. Once the gas bubble touches both the casing and tubing walls and begins to deform, the injection velocity is actually zero due to the bubble wrapping itself around the annulus until it achieves a gas fraction of 0.858. However, the bubble is still moving upward, so it is assumed that the velocity is based on the radius of a hemisphere having the same bubble volume.

Table B.2 compares the value of injection velocity versus bubble volume with gas slip velocity. Figure B.6 is a plot of velocity, both slip and injection, versus bubble

F_g	R_c (in.)	V_B (in.^{3})	V_s (ft/sec)	r (for V_i)	V_i (ft/sec)
0.	0.	0.	0.	0.	∞
0.064	0.500	0.262	0.478	0.500	9.046
0.145	0.754	0.899	0.587	0.754	3.978
0.304	1.415	2.031	0.804	0.990	2.308
0.445	2.046	2.949	0.967	1.121	1.800
0.568	2.653	3.620	1.101	1.200	1.571
0.673	3.246	4.067	1.218	1.248	1.452
0.802	4.135	4.442	1.375	1.285	1.370
$\geq$0.858	4.611	4.561	1.452	1.296	1.346

Table B.2
RELATIONSHIP BETWEEN BUBBLE VOLUME AND GAS VELOCITY FOR FRAGMENTATION STUDY

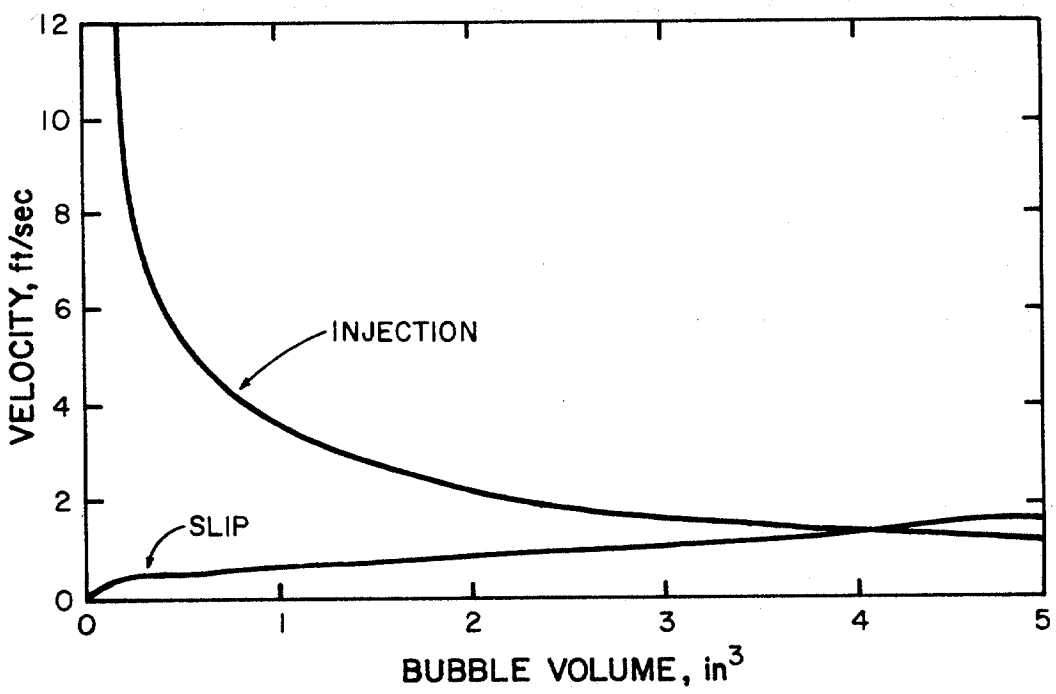

FIGURE B.6 GAS VELOCITY PROFILES VERSUS BUBBLE VOLUME FOR FRAGMENTATION PROBLEM

volume.

B.7 Discussion

Referring to Figure B.6, the gas slip velocity exceeds the injection velocity at a bubble volume of 4.4 in^3. Therefore, the bubble will break free and begin migrating upward, and a new bubble would begin to form beneath it. However, the new injection bubble has a much greater velocity than the bubble above it. Thus, the new bubble actually catches the bubble above it and the net result is a continuous column of gas is injected into the hole. Based upon this it can be assumed that the injected gas remains as a continuous slug while the kick is being taken.

VITA

Jeffrey Lawrence Mathews, the son of Mr. and Mrs. Thomas J. Mathews, Sr., was born December 15, 1957 in Alexandria, Louisiana and has lived there all his life.

A three year letterman in football and All-District in both football and track my senior year, I graduated from Bolton High School in 1975, ranked fourth out of 250 seniors. In the Fall of 1975 I enrolled at Louisiana State University.

During my undergraduate years I maintained a perfect 4.0 average and was the College of Engineering Senior of the Year and Phi Kappa Phi Alternate Senior of the Year in 1978. I graduated summa cum laude in Petroleum Engineering in May 1979, and began working towards my Master's degree that summer.

In addition to my studies, I gained valuable field experience from three summers of work with Gulf, Marathon, and Mobil Oil companies. I also taught the Drilling Fluids Lab at L.S.U. for 2-1/2 years.

I have accepted a job with Mobil Oil as a Drilling Engineer and will be married on May 31, 1980 to Diane Marcotte.